Autofluorescence-Based Assessment of Chlorine Dioxide Disinfection in Industrial Water Systems

BERGISCHE UNIVERSITÄT WUPPERTAL

Bergische Universität Wuppertal

Fakultät Mathematik und Naturwissenschaften

Dissertation zur Erlangung der Doktorwürde

– Doktor der Naturwissenschaften –

(Dr. rer. nat.)

Vorgelegt von

Sebastian Wilfried Birr

Wuppertal, 17.04.2025

Table of Contents

Acknowledgements

I would like to express my gratitude to Prof. Dr. Hans-Willi Kling for his invaluable support and for fostering a positive and tranquil work environment.

I would also like to express my gratitude to Dr. Bernd Jakob, who was always willing to listen to and address any issues that arose.

Furthermore, I would like to express my gratitude to the entire working group "Management of Chemical Processes and Analytical Chemistry" at the University of Wuppertal, who extended me a cordial welcome.

I would like to express my gratitude to the physical chemistry working group, particularly Ferdinand Wachter for the valuable scientific exchange and Walter Wißdorf for his efforts in programming the prototype.

I also extend my thanks to the food chemistry working group, especially Prof. Dr. Julia Bornhorst for her guidance on microbiology.

Additionally, I would like to thank my master's student, Max Menzel, for his collaboration and for providing me with important research results.

I would like to express my gratitude to the company a.p.f Aqua System AG, which provided me with financial and chemical support. I would like to express my gratitude to Professor Dr. Hans-Josef Altenbach, Dr. Helmut Uhlmann, Dr. Jochen Sturhan, Felix Dahlhaus, Harald Hömstreit and the entire team at a.p.f Aqua System AG for their invaluable guidance and technical support.

I would also like to express my gratitude to my family and friends, who have consistently provided me with unwavering support and stability. I would also like to express my gratitude to my partner, who has consistently supported me.

I would also like to thank Mr. Cavallaro from the mechanical workshop at the University of Wuppertal for his advice and the production of the housing. I would also like to thank Mr. Brüning from the glassblowing workshop at the University of Wuppertal for the great and expert cooperation.

I would also like to thank all of the doctoral students' table, which always kept me up-to-date. Of course, I would also like to thank you for the fun evenings together, which were very special.

Abstract

This paper presents a method for inhibiting microbial load in water-containing systems with the oxidation agent chlorine dioxide, utilising an autofluorescence-based measurement setup. The fundamental premise of this process is that oxidising agents, particularly chlorine dioxide, can damage cells, leading to death. The proteins within the cell membrane are significantly damaged, which is the reason for chlorine dioxide's extensive spectrum of action. This oxidising agent can eliminate bacteria, fungi, viruses, and even spores that are considered very resistant.

This study demonstrates that bacterial fluorescence can be used to observe bacterial growth and thereby make semi-quantitative assessments of the overall bacterial count. This method measures a few hundred CFU/ml range and is suitable for various water-bearing processes. In addition, fluorescence can be used to evaluate the effectiveness of a disinfection process. This approach optimises water disinfection, whereby the required quantity can be precisely dosed and adjusted. One possible field of application could be metalworking fluids. These are highly complex solutions with many components, providing a suitable habitat for various microorganisms. Some of these components are highly reactive to chlorine dioxide, but as it turns out, some alternatives make the application possible. These are optically challenging solutions in which no measurements are feasible and can also be remedied with an optimised structure. Therefore, the setup suits clear process water or rinsing water and cooling lubricants. Based on the method developed here, a prototype will be further developed and tested during a field study, facilitating its application in industry.

List of Abbreviations

MWF	Metalworking fluid
NAD	Nicotinamide adenine dinucleotide
NADPH	Nicotinamide adenine dinucleotide phosphate
THM	Trihalogenmethane
US	United States
CFU	Colony forming unit
DNA	Deoxyribonucleic acid
RNA	Ribonucleic acid
Phe	Phenylalanine
Tyr	Tyrosine
Trp	Tryptophan
W	Watt
E. coli	Escherichia coli
ATP	Adenosine triphosphate
UV	Ultraviolet
Vis	Visible
PAO	Poly alfa olefine
QS	Quorum sensing
HPLC	High-performance liquid chromatography
PAG	Polyalkylenglycol
OD600	Optical density at 600 nm
EP	Extreme pressure
AW	Antiwear
AD	analogue-to-digital

1. Introduction

Bacteria and fungi pose significant challenges in all aquatic systems, including those found in various industry sectors. This is largely due to the omnipresence of microorganisms. The contamination of the fluid is generally from the water itself or airborne sources and is hard to prevent. Furthermore, water used in industrial applications often creates optimal conditions for their growth, with temperatures ranging between 20 and 40 degrees Celsius and in the presence of organic substances that act as nutrients. Industrial water often contains bacteria and fungi, which can pose health risks to workers (*1*), cause damage to machinery and products, and inhibit cooling properties (*2*). Biocides are used to inhibit the growth of microorganisms, and they work through various mechanisms. For example, some biocides denature proteins, disrupting their function. Others, such as formaldehyde-forming products, react with proteins and nucleic acids, leading to a similar disruption. Thiazoles have an inhibitory effect on proteins, while cationic surfactants destabilise the cell membrane. (*3*) However, as biocides are often harmful to health, they are subject to strict regulations, which means that many substances are banned.

The use of the oxidation agent chlorine dioxide in disinfection holds excellent promise. Chlorine dioxide is required in small amounts, posing no harm to humans while effectively exhibiting antimicrobial properties. (*4*) An example of this is the chlorine dioxide from the company a.p.f Aqua System AG, which is stable for months. In addition, other chlorine dioxide is reduced over time and often converted into compounds like free available chlorine (FAC), chlorite, and chloride, where chlorite and FAC can act as secondary oxidising agents. (*5*) Organic impurities can be reduced to carboxylic acids, aldehydes, quinones, etc. The formation of halogenated oxidation by-products is often a problem with strong oxidising agents like chlorine. In the case of chlorine dioxide, the formation is negligible in the normal dosed range. (*6*)(*7*)(*8*) Compared to other oxidation agents such as ozone or hydrogen peroxide, chlorine dioxide offers several advantages. It possesses superior disinfection properties, requiring lower concentrations, without producing trihalomethanes (THMs) or bromine oxidation by-products. While chlorine dioxide is commonly used in water disinfection, many unknown mechanisms remain.

Antibacterial agents are essential in the fight against bacterial contamination, but they do have their limitations. Over time, residues are formed, and the biocides used degrade. As a result,

additional dosing of biocides is often necessary. This can create a cycle in which an increasing number of resistant germs develop. Eventually, the solution is discarded, and a new one is used after a varying period of use. If discarded too late, significant financial and image damage can occur. Waste disposal too early is also problematic as cost efficiency and sustainability requirements must be met. The management of bacterial contamination is crucial for marketability. A clear understanding of contamination levels is necessary to implement on-point hygienization. Various methods have been developed to assess bacterial contamination, with culture-based techniques being the preferred choice. However, these methods cannot provide real-time results and often fail to capture the complete microbial diversity. There are also alternatives, such as flow cytometry, which is technically unsuitable due to its complexity and costs. Therefore, further options are needed to close this gap. (*9*)

It is essential to consider the economical use of resources, as quantification of chlorine dioxide is possible at levels as low as several hundred micrograms per litre. (*10*) This means that even when no measurable chlorine dioxide is present, there may still be an unnecessary excess. Multiple studies have shown the effectiveness of chlorine dioxide at low concentrations, and research has demonstrated that bacteria can be killed while still consuming chlorine dioxide. (*11*) (*12*) (*13*) Therefore, measuring bacteria's dead/alive status may be more accurate than focusing solely on the chlorine dioxide concentration. By understanding bacterial contamination and growth rates, chlorine dioxide dosage can be accurately adjusted, optimising its potential. A fast, accurate, and user-friendly analytical method, such as a microbiology sensor, is needed to address this challenge.

2.Objective

This study aims to establish a method for quantifying bacterial contamination in aqueous systems and demonstrate a correlation between the presence of living organisms and the measurement signal. The potential for developing a simple, automated measuring device is also explored. If feasible, the study will also examine how to effectively combat contamination through the controlled application of a sanitizing agent.

3. Theory

3.1 Microbiology

Microorganisms encompass a diverse range of species that have evolved to thrive in various environments. This group includes both pathogenic and non-pathogenic bacteria and fungi. Some species develop resistance to biocides, while others can adapt to challenging conditions. However, the most favourable circumstances for microorganisms often involve warm temperatures and the presence of organic material, which is why they can be found in nearly every habitat. (*14*) The cell is considered the smallest building block of life regardless of the living organism. Cells consist of DNA, RNA, proteins, lipids, and carbohydrates, and the chemistry behind reproduction, cell respiration, and synthesis is complex. Cells are measured in micrometres and have a large surface-to-volume ratio; this facilitates rapid interaction between the interior and exterior of the cell, maintaining short distances. The diameter of bacteria is ten times smaller than that of fungi, such as yeast. This significantly impacts the amount of surface proteins relevant for interacting with the environment. (*15*) Microorganisms are ubiquitous on Earth; unsurprisingly, they play a role in industrial processes. For instance, yeast ferments beer, while acetic acid bacteria contribute to vinegar production. Additionally, microorganisms are used in wastewater treatment. (*15*) However, they can also inadvertently contaminate pure water and cooling lubricants, leading to various issues that require management. Despite their differences, microorganisms share features that can be leveraged for multiple applications.

Escherichia coli, commonly known as *E. coli*, has been the subject of extensive microbiology research since the field's early days. Its widespread use in research can be traced back to the 1930s when scientists sought an organism that was readily available, relatively non-virulent, and easily cultured on defined media. (*16*) The cellular structure of *E. coli*, including its shape, proteins, and reproduction, has been a focal point of study. Research on *E. coli* has also contributed significantly to our understanding of biosynthetic pathways and the genetic code. These factors have made *E. coli* an ideal model organism for studying bacterial behaviour.

E. coli is a rod-shaped bacterium, approximately 2-4 µm in length and 1 µm in width, belonging to the gram-negative family. It possesses a thick cell membrane measuring 200nm. (*16*)

Even if they are small, the microscopic image allows for the observation of bacteria and fungi. However, more precise examination methods are necessary for studying bacteria in greater detail, like electron microscopy for structure and flow cytometry for the living-dead status. A closer inspection is required to gain a better understanding of the behaviour.

Analytical sensor technologies encompass a wide variety of measurement methods. A specific area within this field is biosensor technology, which primarily aims to identify biological targets using small sensors. These sensors can be categorised based on their measurement principles, including optical, electrical, gravimetric, and acoustic.

Optical methods in this context include UV/Vis, fluorescence, and phosphorescence spectroscopy. These techniques can be generalised to focus on a single molecule, which is unique to living cells, or they can be tailored to detect specific pathogenic species. (*17*)

Instrumental analytics devices play a crucial role in both quantitative and qualitative detection of microorganisms. Among them, flow cytometry stands out as the most significant, as it allows for the counting of both living and dead organisms. The fundamental principle behind this technique involves the use of fluorophores to stain living organisms. Depending on the organism's status, the fluorophore can be either on or within the cell. The sample is then directed through a capillary, where focused laser light is applied. This light not only induces fluorescence at specific wavelengths for analysis but is also utilized to count microorganisms. (*18*)

The bacterium comprises various components within the cell, including DNA, metabolism enzymes, and the cell membrane (see Figure 1). These components include freely located DNA in the cytoplasm, which serves as a target for antimicrobial substances. Furthermore, the energy balance involving ATP and NADPH is crucial in living organisms. Several methods focus on ATP detection. (*19*), as the absence of ATP in cells renders the cell incapable of sustaining life. Lastly, the protective cell membrane comprises a phospholipid double membrane safeguarding the interior. The membrane contains various proteins that create passages from the cell's exterior to the interior. These membrane proteins contain amino acids like tryptophan, which is sensitive to oxidation and exhibits fluorescence activity. This fluorescence, also known as autofluorescence or intrinsic fluorescence, is present in all fungi and bacteria. (*20*) (*21*) (*22*)

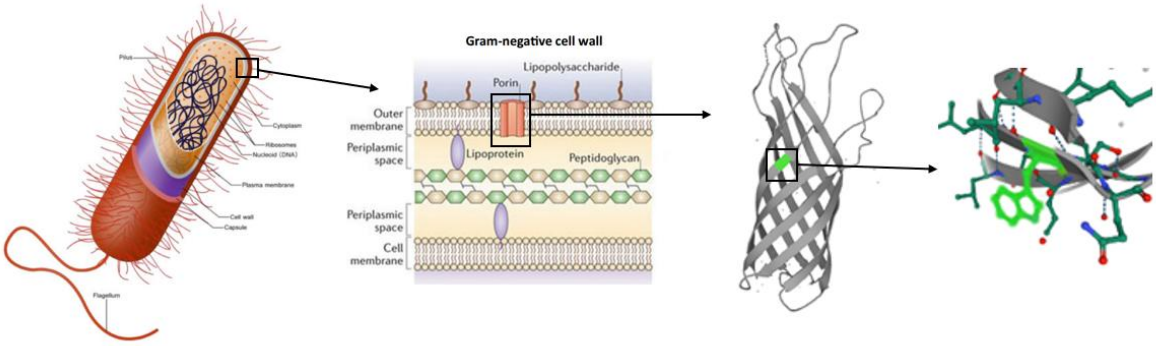

Figure 1: The cell wall of bacteria consists of a peptidoglycan double layer, saccharides, and proteins. Those proteins have a critical role, like the pores that are channels between the inner and outer cells. Like several others, those proteins contain amino acids like tryptophan, which is fluorescence active. The tryptophan is highlighted in green in the protein channel. Adapted from (22)

However, autofluorescence has limitations, such as low intensity, making quantification challenging. Moreover, the substances of interest are not always fluorescent, or their fluorescence may be overshadowed by other factors, such as metabolism. Specific analytical fluorophores known as extrinsic fluorophores are employed to address this issue. (*20*) (*23*)

3.2 Theory of Fluorescence Spectroscopy

Fluorescence spectroscopy belongs to the optical methods, and the phenomena of fluorescence describe the absorption of light with a short wavelength and the emission of light with a longer wavelength. More precisely, the absorption of energy lifts the molecule from the ground state to the excited state without changing the electron spin. The molecule reaches the first excited state through intermolecular effects and loses energy without emitting light. From here, it falls back to the ground state, and the remaining energy is released as light, perceived as fluorescence (Figure 2). (*24*)

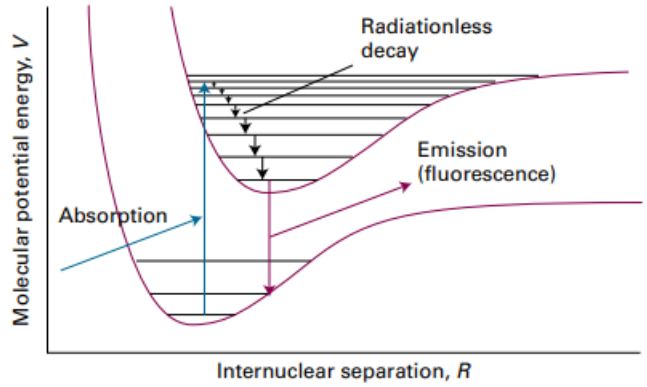

Figure 2: A schematic picture of fluorescence. A fluorescence-active molecule that absorbs light enters a higher vibrational state and undergoes radiationless decay. In this way, it gives up its energy to the surrounding molecules. Then, it falls from a lower vibrational state to a higher electronic state by emitting fluorescence light. (25)

In the phenomenon of fluorescence, there is a loss of energy, which is important for the change in wavelength. Another important point is that not every photon causes fluorescence. To describe this, there is the quantum yield Φ. This consists of the fluorescence of the analyte divided by the theoretical fluorescence. The value of the yield takes a number between 0-1. The other phenomena need a correction, like intersystem crossing leading to the equation below.

$$\boldsymbol{\Phi = \frac{\Phi_{korr} I_{fluorescence}}{I_0}} \qquad (1)$$

Then, there is also a relation to Lambert-Beer law (2), which describes how the absorption of a solution depends on the molar extinction coefficient, concentration, layer, and fluorescence.

$$\boldsymbol{E = \varepsilon_\lambda c d} \qquad (2)$$

With the quantum yield and the absorption, the following formulation can be written:

$$\boldsymbol{\Phi = \frac{I_{fluorescence}}{I_0} = \Phi \frac{I_{Absorbtion}}{I_0} = \Phi * 1 - \left(10^{\varepsilon_\lambda c d}\right)} \qquad (3)$$

Formulating that in the form of fluorescence produces an equation similar to the Lambert-Beer law (2) that describes the relation between concentration and fluorescence light.

$$I_{fluorescence} = I_0 * \Phi * 1 - 10^{\varepsilon_\lambda cd} \quad (4)$$

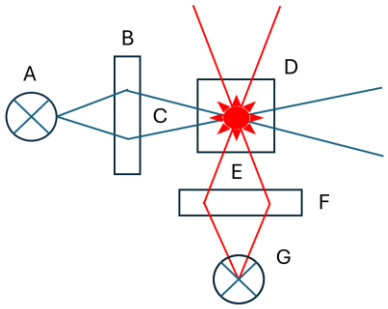

Figure 3: Schematic setup of a fluorescence spectrometer. A light source (A) emits light that passes through a monochromator (B), which leads to the excitation wavelength (C) that interacts with the probe (D). The emitted fluorescent light (E) passes the monochromator and ends in the photosensitive detection unit (G).

The principles of the theory led to a spectrometer, which is shown in Figure 3. There are many variations in the light source, monochromator, and detection units. The fluorescence light is significantly lower than that of the source, resulting in a 90° angle; however, other angles can also be achieved. The important thing here is to minimise the source light.

3.3 NADPH Fluorescence

NADPH is a fundamental compound in all living cells. It serves as an electron donor and plays a critical role in various biological processes, including biosynthesis, gene expression, cell death, and energy transfer. (*26*) Additionally, NADPH acts as a cofactor in photosynthesis, contributes to antioxidant defence, and is involved in the biosynthesis of lipids and DNA. Its significance renders NADPH an essential indicator of the presence of living cells. (*15*)

Various analytical methods have been developed for the detection of NADPH, such as HPLC (*27*), electrochemical analysis (*28*), enzymatic cycling assay (*29*), and spectroscopic methods. (*23*) While HPLC has limitations in cost, robustness, and sample preparation requirements,

spectroscopic methods offer excellent selectivity, do not necessitate sample preparation, and are user-friendly. (*26*)

Numerous studies have highlighted the feasibility of spectroscopic analysis of NADPH. UV-Vis spectroscopy reveals two maxima at 266 and 340, and research has shown that distinguishing between the oxidised and reduced forms of NADPH is possible with UV/Vis spectroscopy (Figure 4).

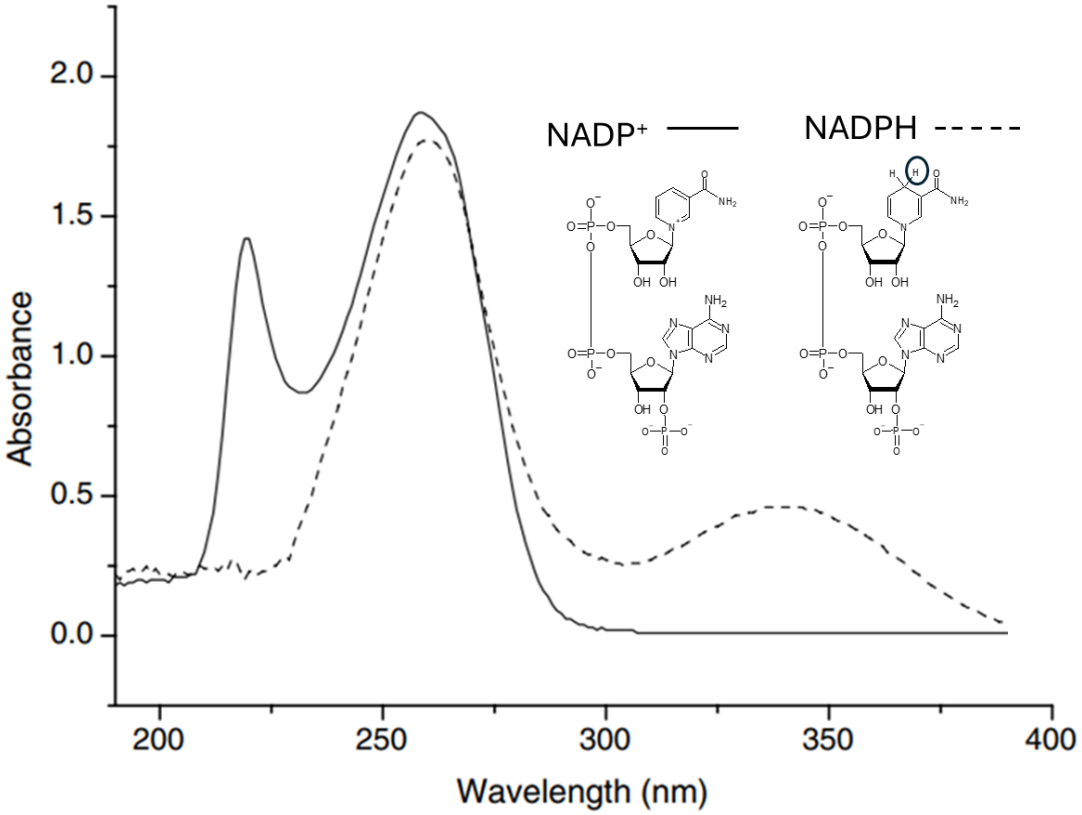

Figure 4: UV/Vis spectra of NADPH and NADP⁺ in the common metabolic forms. (30)

Another approach to quantification is fluorescence measurement. NADPH produces a blue fluorescence with a maximum wavelength of 460 nm. The measurement of fluorescence shows promise in detecting autofluorescence in living cells, and it presents various research possibilities (Figure 5). (*31*) It is well-documented that NADPH absorbs light at 340 nm and emits at 460 nm. In the UV/Vis spectroscopy image, the oxidised form does not absorb at 340 nm, making it a reliable indicator of oxidative attack. Additionally, it is known that bound

NADPH can enhance fluorescence. Hence, the fluorescence in living organisms is expected to be stronger than in the pure substance. (*20*)

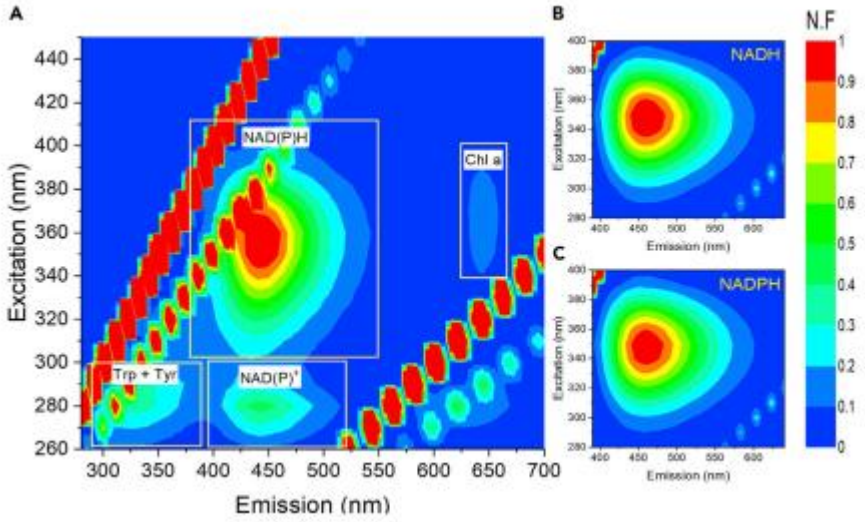

Figure 5: Fluorescence of NADPH in extracellular matrix from cyanobacteria. (32)

The study of Shlosberg et al. showed that cyanobacteria produce NADPH, which is transported to the cell surface. In doing so, they generate an electric current that can be used as an energy source. This shows that bacteria that can photosynthesise can also be measured using NADPH. NADPH is present in all organisms, but it is only known from the literature that NADPH is visible in organisms capable of photosynthesis. (*32*)

3.4 Amino Acid Fluorescence

Amino acids are the main building blocks of all living organisms. At present, almost 500 naturally occurring amino acids are known. Of these, 20 are essential, which means that they cannot be produced by heterotrophic but only by autotrophic organisms. (*33*) (*34*) Proteins are formed via peptide bonds between the carboxy and amino groups. The protein itself has additional bonds, such as disulphide and hydrogen bonds, which is how the proteins form their characteristic folded structures. The 20 amino acids are presented in Figure 6.

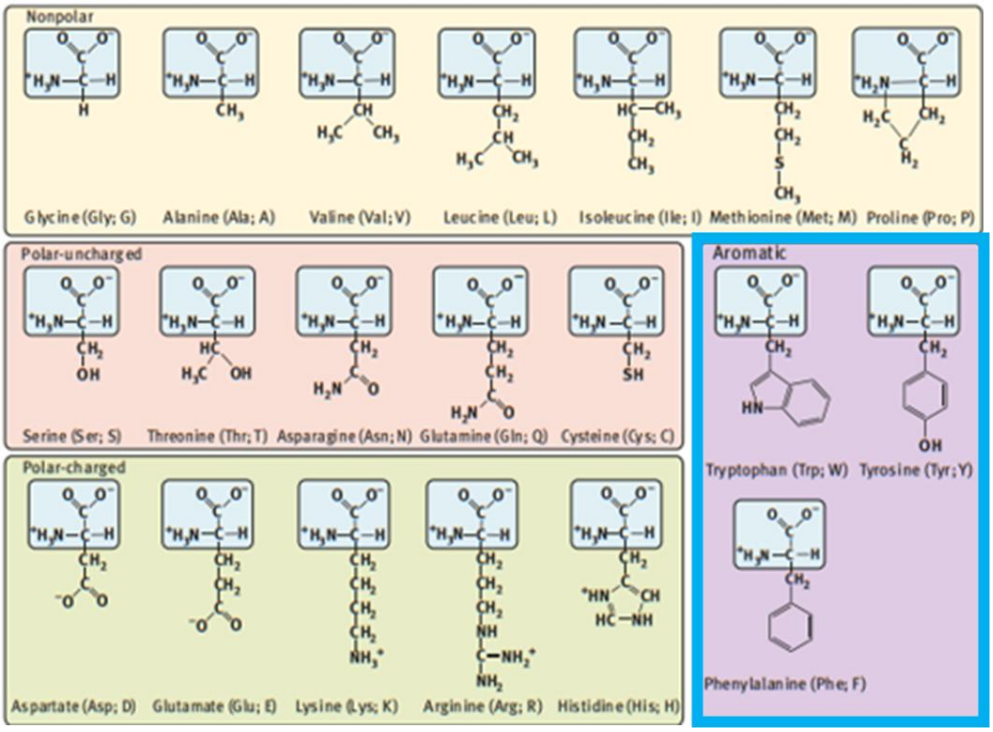

Figure 6: The 20 essential amino acids are divided into groups according to their structure. The relevant amino acids for the fluorescence are the aromatic ones. (34)

This creates a significant potential for the formation of proteins that are present in all cell areas and perform regulatory and catalytic functions. Many proteins are also present in the membrane, making up half of the total membrane mass. The structure of the proteins varies greatly, and the abundance of the proteins depends strongly on the external conditions. This is why a clear indication of the protein amount is invalid. (*15*)

The fluorescence of essential amino acids can be reduced to three aromatic amino acids. First, the strongest fluorescence activity is from tryptophan, the second strongest from tyrosine, and the third strongest from phenylalanine. The fluorescence of the rest is too small to be detected. In the case of microorganisms, the fluorescence of tryptophan dominates the spectra, indicating that all other fluorescence active substances are not detectable.

The fluorescence of peptides can usually be attributed to the fluorescence of tryptophan. However, the maximum absorption of peptides is not in the same place as that of tryptophan. It differs from peptide to peptide in a range of 40 nm. (*35*) (*36*) Tryptophan is highly sensitive to the change in a chemical environment. The study of Vivian et al. shows that the fluorescence shift in proteins is mainly affected by the electric potential difference across the long axis of the indole ring. Specifically, positive charges create a red shift on the benzene ring end and a blue shift on the pyrrole ring end. Negative differences have the opposite effect. The size of

the shift is inversely proportional to the distance of the indole ring centre, which makes it possible to calculate protein shifts. (*36*) The peptide binding in proteins affects not only the position but also the quantum yield, which makes it a good indicator of chances in the molecule. (*37*) Additionally, the pH value and temperature change the intensity of tryptophan fluorescence, which decreases rapidly in alkaline pH. (*38*) As already described, tryptophan is easily influenced by its environment, which includes ammonium and acidic groups. The fluorescence lifetime is also subject to fluctuations and can vary from 1-6 ns. The intensity of tyrosine in similar concentrations is often higher than that of tryptophan, as seen in the spectrum (Figure 21). This is mistakenly associated with a higher quantum yield, which is not true. The spectrum of tryptophan is slightly broader, but the quantum yield is similar (Figure 7).

Species[a]	λ_{ex} (nm)	λ_{ex} (nm)	Bandwidth (nm)	Quantum yield	Lifetime (ns)
Phenylalanine	260	282	–	0.02	6.8
Tyrosine	275	304	34	0.14	3.6
Tryptophan	295	353	60	0.13	3.1 (mean)

Figure 7: Excitation and emission bandwidths, quantum yield, and lifetime of the essential aromatic amino acids(20)

In proteins, this looks different; tyrosine is quenched here, and the energy is either lost or transferred to tryptophan. In the case of phenylalanine, fluorescence is also not visible when tryptophan or tyrosine is present. Because tryptophan dominates the spectra, it is an excellent target for fluorescence spectroscopy on the cell surface. (*20*)

3.5 Chlorine Dioxide

The first synthesis of chlorine dioxide was carried out in 1811. (*39*) At that time, Humphry Davy was working in the field of electrochemistry and succeeded in producing chlorine dioxide from chloric acid and sulphuric acid. (*40*) More than 100 years after the first synthesis, in 1921, Erich Schmidt and Erich Graumann found an application for chlorine dioxide as a bleaching agent. They found that chlorine dioxide destroys the dark lignin component from the wood, but the cellulose is not attached. Until this time, the bleaching method with sulphuric acid was slow and attacked lignin and the cellulose fibres; the other way was chlorine gas with its toxicity

and stability problems. The upcoming chlorine dioxide solves those problems. (*41*) (*42*) Further decades passed before chlorine dioxide was used as a disinfectant.

The first documented use of chlorine dioxide as a water disinfectant was in 1944 in Niagara. At that time, Niagara used water from the Niagara River for industry, food generation and drinking water. The water was contaminated with various pollutants by using water for every need. To purify the water, they use chlorine dioxide dosed at Niagara Falls in New York. (*40*) (*43*) Today, chlorine dioxide is in worldwide use and has many applications, such as water treatment plants (*44*), cooling water towers (*45*) and industrial waters (*46*) (*47*), to mention a few.

Chlorine dioxide is a stable inorganic radical. (*6*) The reactions occur through nucleophilic attack, with chlorine dioxide as the electron acceptor and organic and inorganic compounds functioning as electron donors. Therefore, chlorine dioxide selectively reacts over a nucleophilic attack with compounds with unpaired electrons or π-electrons (*6*). Chlorine dioxide has an oxidation potential of 0,95 V and is, therefore, also used as a potent oxidising agent. (*48*) An advantage over hypochlorite and chlorine is that fewer chlorine-containing degradation products are formed. The use of chlorine dioxide in drinking water treatment is prescribed in §20 of the Drinking Water Ordinance (German trinkwV 24.6.2023) and DIN EN 18087.

There are many ways to produce chlorine dioxide. The initial substances are usually ClO_3, ClO_2^-, ClO *or* Cl_2. Among the most relevant are the reactions R-1 to R-3 shown below.

$$\mathbf{2\,NaClO_2 + Na_2S_2O_8 \rightarrow 2\,ClO_2 + 2\,Na_2SO_4} \qquad \text{R- 1}$$

the hydrochloric acid method (R- 2)

$$\mathbf{5\,NaClO_2 + 4\,HCl \rightarrow 4\,ClO_2 + 5\,NaCl + 2\,H_2O} \qquad \text{R- 2}$$

and via the chlorine-chlorite process (R- 3).

$$\mathbf{2\,NaClO_2 + Cl_2 \rightarrow 2\,ClO_2 + 2\,NaCl} \qquad \text{R- 3}$$

A maximum concentration of 0,4 mg ClO_2/l is prescribed for drinking water, which is more than sufficient for microbial contamination of drinking water. (*49*) Chlorine dioxide can be produced by various processes, including the following persulphate process (R- **1**). All these processes are based on sodium chlorite. In addition, there are also other processes, for example,

based on chlorate, but they are not discussed here. A ready-made chlorine dioxide solution can produce pure chlorine dioxide obtained according to reactions R-1 to R-3 described above. By blowing air through the chlorine dioxide solution, the chlorine dioxide is transferred into the gas phase. The chlorine dioxide can be used directly as gas or dissolved into pure water. It is helpful to warm up the raw chlorine dioxide solution and cool the pure water to nearly the freezing point. Highly concentrated chlorine dioxide solution is orange, and in even higher concentrations, it precipitates and forms a red oily liquid. By cooling this pale liquid, it crystallises in the structure shown below as a red crystal (Figure 8). (*50*)

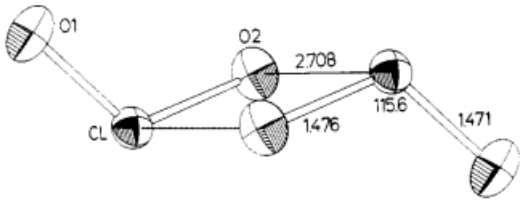

Figure 8: Structure of solid chlorine dioxide. (50)

It also forms gas hydrates in water, which are also called clathrates. (*51*) (*52*) (*53*) This is a cage structure of water in which chlorine dioxide is enclosed. Although this clathrate has hardly been investigated, it can be stored at low pressures and almost room temperature.

A sodium chloride solution is used as a reactant to prepare chlorine dioxide. The economic and environmental aspects depend highly on the byproducts. The byproducts at the point of electrolysis can be used again in the electrolysis, so the waste is minimal in this case. The other side is the energy consumption for heating and the electrolysis. (*54*) The Day–Kesting process to produce chlorine dioxide starts at brine and is the only one that starts at the beginning. In this process, electrolysis oxidises sodium chloride solution to chlorine at the anode and is directly hydrolysed. The hypochlorite, formed by hydrolysis, is then oxidised to chlorate at the anode. After that, the chlorate is reduced with hydrochloric acid to chlorine dioxide. The production must occur under controlled pH conditions and above 70°C. (*54*) (*55*) The chlorate formed is then reduced to chlorine dioxide and passed into a sodium hydroxide solution, leading to sodium chlorite formation. The sodium chlorite thus formed is then used as an educt to produce chlorine dioxide. (*56*) The chlorine dioxide solution is normally produced at the point of use because technical chlorine dioxide solutions are unstable. One exception is the method patented by a.p.f Aqua System AG for producing stable chlorine dioxide using an

improved persulphate process. (*57*) Several impurities, such as hydrogen peroxide, chlorate, and basic pH conditions, can cause the decomposition of other chlorine dioxide. (*58*)

Chlorine dioxide is an effective biocide. (*59*) (*60*) It works over various pHs, temperatures, and bacterial species. (*61*) (*62*) (*63*) Chlorine dioxide concentration is low compared to other advanced oxidation processes. (*64*) Chlorine dioxide is most effective against gram-positive and negative bacteria. Spores usually require slightly higher concentrations of chlorine dioxide, but these are also killed. (*65*) One important point is the target of chlorine dioxide. Because the bacteria are dying, the chlorine dioxide must destroy a critical point of the organism.

The inactivation of bacteria is an important part of chlorine dioxide research. Much research has been done in this field, but it is still not completely understood how the mechanism works in cells. This is caused by the huge complexity of the cells and species variation. From the literature, it is known that Chlorine dioxide does not attack the genetic information of microorganisms. (*66*) (*67*) (*68*) Yuang et al. study microorganisms that survive oxidation with chlorine dioxide. They collect the bacteria, incubate them in minimal medium, and then test for auxotrophic or asporogenous mutations. There is no evidence for mutations, but they found that the membrane permeability is damaged. (*66*) Further work from Shemesh focuses on the mechanism of the membrane. He shows chlorine dioxide lowers the membrane potential, causing surfactin production and histidine kinase activity. This membrane permeability of the cell is the probable trigger of apoptosis. Surfactin is also a quorum-sensing molecule that coordinates cell-to-cell interaction. This plays a critical role in many microbial activities like reproduction, growth, and biofilm production. (*14*) (*69*) Quorum-sensing molecules are oligopeptides that can be reactive against chlorine dioxide or its secondary oxidants, like chlorite and hypochlorite. Disturbed communication has potential effects on cell growth rates and normal behaviour, such as biofilm formation. It could be that the quorum-sensing molecules contribute to the detachment of the biofilms. If the necessary signals to maintain the biofilm are defective, this system may not be able to act properly. Unfortunately, there are no research results on this yet, but the oxidation of the quorum-sensing molecules should be investigated urgently. (*70*) TEM microscopy from Ofori et al. below shows that the membrane is uniform and smooth without chlorine dioxide but irregular with chlorine dioxide. (*62*) Various other groups have come to the same conclusion that the outer membrane is damaged first, and later, other oxidation can occur in the inner cell. (*68*) (*13*) (*71*) (*63*)

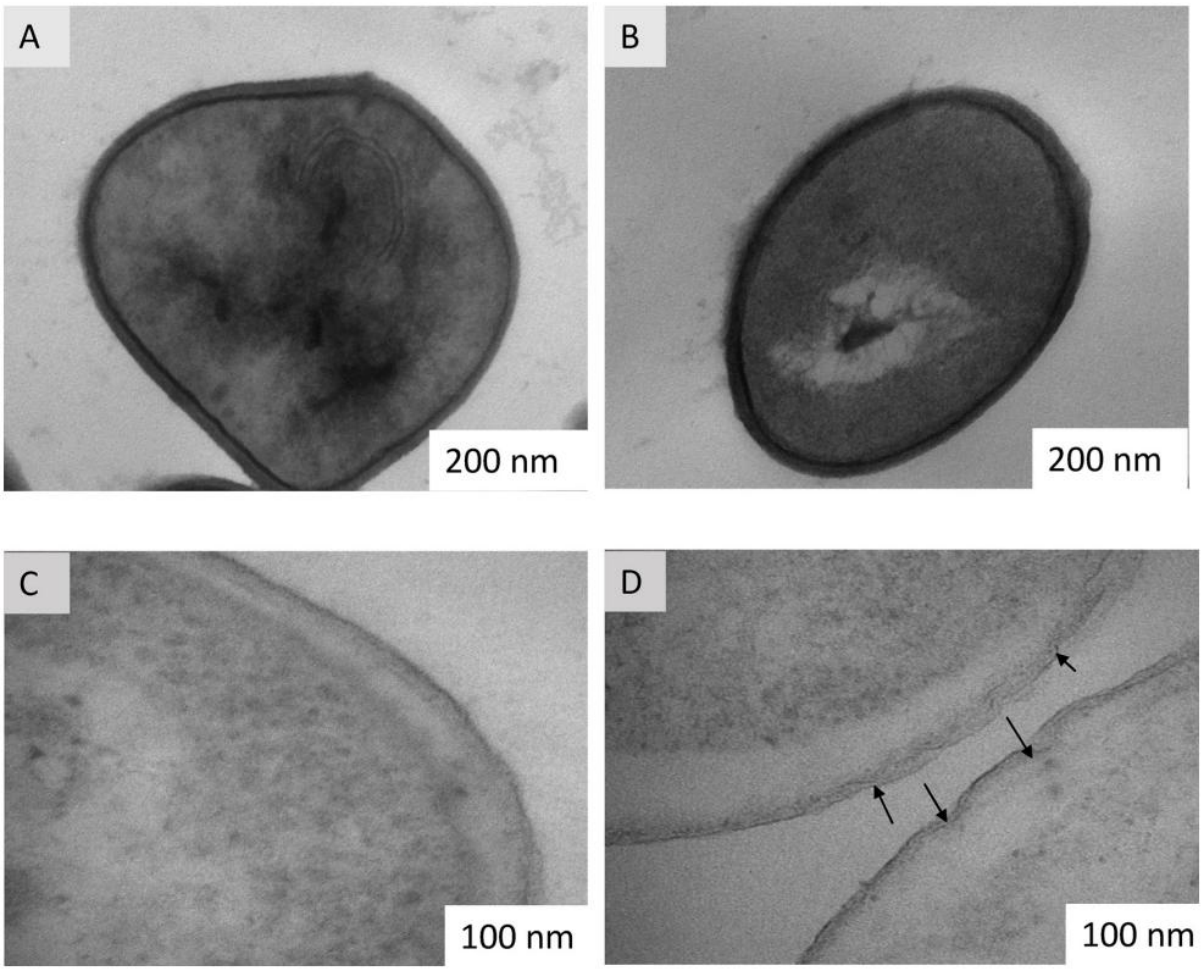

Figure 9: The chance of the outer membrane is slightly visible. The normally smooth membrane of (A) S. aureus and (C) P. aeruginosa before treatment and, in contrast, the drought-wall-treated cells (B) S. aureus and (D) P. aeruginosa show the effect of chlorine dioxide. Here, they use a chlorine dioxide concentration of 4 mg/l and get a 99,99% elimination. A more detailed concentration of bacteria is not available. (62)

There are many possible points of action. First, there is the outer cell membrane with its lipid layer. If the cell membrane is damaged, this breaks the whole wall, which, of course, leads to cell death. The cell wall does not look like it was broken. (*62*) The second option for killing the cell by destroying the wall is to ruin its permeability. This means denaturing membrane proteins. If the proteins are damaged, the cell cannot regulate its water balance, which leads to cell leakage. (*13*) Chlorine dioxide does not attack every amino acid. The main attack points are sulfur-containing cysteine and the aromatics tyrosine and tryptophan. A chlorine dioxide reaction is also observed with proline, hydroxyproline, and histidine if the pH value is over 6. In responses with a pH above 9, sulfur-containing methionine is also reactive. The other amino acids are also tested, but almost no activity exists. (*72*) (*73*) As previously described, the primary fluorescence comes from tryptophan. One possible way is to attack the indole system, which leads to a ring opening. (*6*) The attack on those leads to an unfolding of the protein.

The other possibility is to diffuse through the lipid membrane layer. After that, there are different antioxidative agents like NADPH, the whole energy system, different enzymes, and genetic material. Every one of those is essential for the bacteria; its destruction will lead to cell death.

3.6 Metalworking Fluids as an Example of Industrial Water

Water is utilized in various ways across different industries. In certain applications, high-quality water free from impurities is essential. However, more commonly, water is combined with additives. A notable example of this is cooling lubricants, which are highly complex mixtures. The key components of these lubricants are discussed here. Additionally, understanding their use requires some historical context.

Metalworking is a quite young field of research considering that metalworking is thousands of years old. The first cutting fluid might have been just water, which has good cooling properties but bad lubricating properties. After that, animal and vegetable oils were used to manufacture weapons and art. In the early 17th century, the first documented use of lubricants is present with oil for cart axles. Later, natural oils were replaced with crude oil because of the low price. However, scientific interest in metalworking started in the early 20th century. Currently, interest in replacing harmful substances for the environment and humans has grown. There is also the question of what we can expect from metalworking fluids (MWF) and whether they work. (*74*) (*75*)

Nowadays, MWF are complex aqueous mixtures containing oils, emulsifiers, corrosion inhibitors, anti-foaming agents, biocides, and extreme pressure and anti-wear additives. Lubricants are used in metalworking processes like grinding, milling, and forming. The task of the lubricating fluid is first to lubricate, second to cool, third to flush away chips, and fourth to protect the product, machines, and tools from corrosion. (*76*) With these properties, cooling lubricants contribute to the tools' lifespan and the working piece's surface quality and reduce the energy required, making it more cost-effective.

Cooling lubricants are visually sophisticated mixtures. Water-based lubricants can be divided into emulsions and real solutions. The picture below shows a non-soluble and soluble MWF

(Figure 10). The emulsions are not translucent; in most cases, they look white because of the scattering. The real solution normally has a colour but is translucent. A more detailed description of the components comes later.

Figure 10: left is a 10% MWF emulsion based on several oils. The right one is a 10% MWF solution based on polyglycol. Both contain almost 20 ingredients with several aromatic components that are fluorescence active and ingredients that are reactive with chlorine dioxide.

The industry requires this complexity due to the variation in materials and the ever-changing compositions produced by lubrication processes. The reaction conditions vary widely, from high temperatures to high pressures, depending on factors, e.g., cutting speed. Lubrication, a seemingly straightforward aspect, requires extensive research and is more complex than it appears. Nevertheless, it holds great potential for improving efficiency, reducing costs, and minimising environmental impact. (*74*) Researchers are focusing on various areas, including environmentally friendly lubricants (*77*) (*78*), additives that are not harmful (*79*) (*80*), and microbial growth, which is the focus of this work. (*81*) (*82*)

3.6.1 Synthetic and Natural Oils in MWF

The main compound is divided into water-soluble and not water-soluble. The main compound could be any slippery substance like oil or glycol that performs the lubrication; then, there is about 90% water for the cooling properties. The water-soluble compounds are, for example, glycerine, poly glycols, or ionic liquids (*83*), and every compound has its area of use (Figure 11).

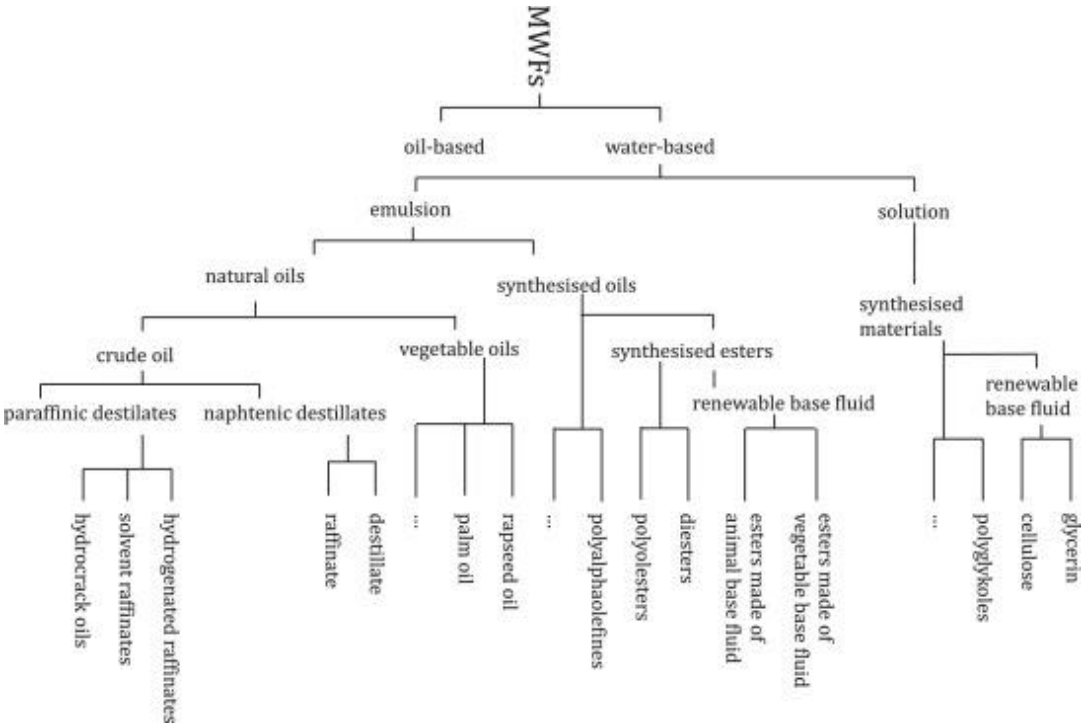

Figure 11: Metalworking fluids can be divided into several groups according to their ingredients (75)

The huge variety of base oils and additives makes it impossible to generalise MWFs, so compatibility with chlorine dioxide must be observed.

The non-water-soluble ones are divided into synthetic, semi-synthetic, and natural oils. The synthetic ones are modified hydrocarbons like polyalpha olefins (PAO), polyalkylenglycol, and various esters (Figure 12).

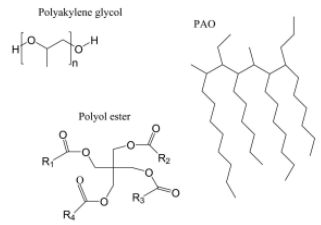

Figure 12: Synthetic main components of MWF.

They are designed to have good lubricant characteristics with a big structure, and it is easy to imagine that there is no direct contact if they are between the metals. As seen in the picture, there are no reactive groups, which explains why they are long-living and perform well in high-temperature and high-pressure applications but are also expensive. Due to their good stability, their biodegradability is not so good, which is why they have a poor biological effect. As MWF, they are used for aluminium working. R.S. Montgomery describes the effect of ester groups. He postulates that ester reacts with the aluminium, and the reaction product fills the gaps in the working tool and thus reduces wear. (*84*). Additionally, it can be shown that synthetic oils are better for aluminium than crude oil-based ones. Furthermore, the reactivity is described in more detail. The oxygen-containing group coordinate with the aluminium surface and reduces friction by forming a thin layer. The diols form aluminium alkoxide with the aluminium and the alkoxide hydrolysis and form aluminium hydroxide. (*85*) The synthetic oils are quite similar to the crude oil-based and can also be divided into paraffinic and naphthenic. (*86*)

Renewable natural oils can be categorized into two main types: animal oils and plant oils. Plant oils include rapeseed oil, castor oil, palm oil, and sunflower oil. Among these, palm oil, soybean oil, and rapeseed oil are the three largest producers globally. Various industries utilize these oils, particularly the metalworking industry, where they are used for lubrication. (*87*) (*88*) (*89*) From the chemical structure, the oils are triglycerides. They have glycerol backbone and long hydrocarbons, which can be saturated or not and in different chain lengths, as shown for several natural oils in the table below. (Table 1) There are also several other impurities like Vitamin E, sinapic acid, caffeic acid, etc. (*87*) While these impurities are difficult to remove completely, they exist in such small concentrations that they typically do not pose a problem.

Table 1: Natural oils are a good source for the chemical industry. They sustainably produce a large number of different components. These include various oils with chain lengths of 16-22, both saturated and unsaturated. This enables them to be used as a raw material for further modifications. However, other substances are also present in the oils. The percentage shares are shown in the diagram: A) ricinoleic acid 90%, B) resin acid, mainly abietic acid, dehydroabietic acid, pimaric acid (40-60%), and other fatty acids 20%

component	16:0	18:0	18:1	18:2	18:3	22:1	Other	source
Soybean oil	12	4	24	54	7			(*86*)
Sunflower oil	7	4	35	52	1			
Rapeseed oil	4	1	19	22	8	45		(*86*)
Palm oil	16	5	41	10				(*86*)
Olive oil	13	3	72	11	1			(*86*)
Castor oil			5	3			A	(*90*)
Tall oil	1	1	20	10	1		B	(*91*)

Animal fats are less reported than vegetable oils but can also be used for metalworking. (*86*) Tallow fat consists of triglycerides with a straight count of carbon in the carbon chain and fewer double bonds than vegetable oils. The main part is oleic acid; the rest are saturated, like palmitic acid and steric acid. (*92*)

Whether from animal or vegetable sources, triglycerides are a good source of environmentally friendly components. The main difference between various greases and oils lies in the chain length and the degree of saturation. The four common ways to make biolubricants more efficient for lubrication are in the picture below (Figure 13). The triglycerides can be used to make polyol esters over a transesterification. However, the double bonds of the fatty acids can also be used to get estolides. Epoxidation is also a common way to make more complex polyol esters. The chemical modification is also easy to make, but for the scale-up, it is important that there are just a few steps and mild conditions.

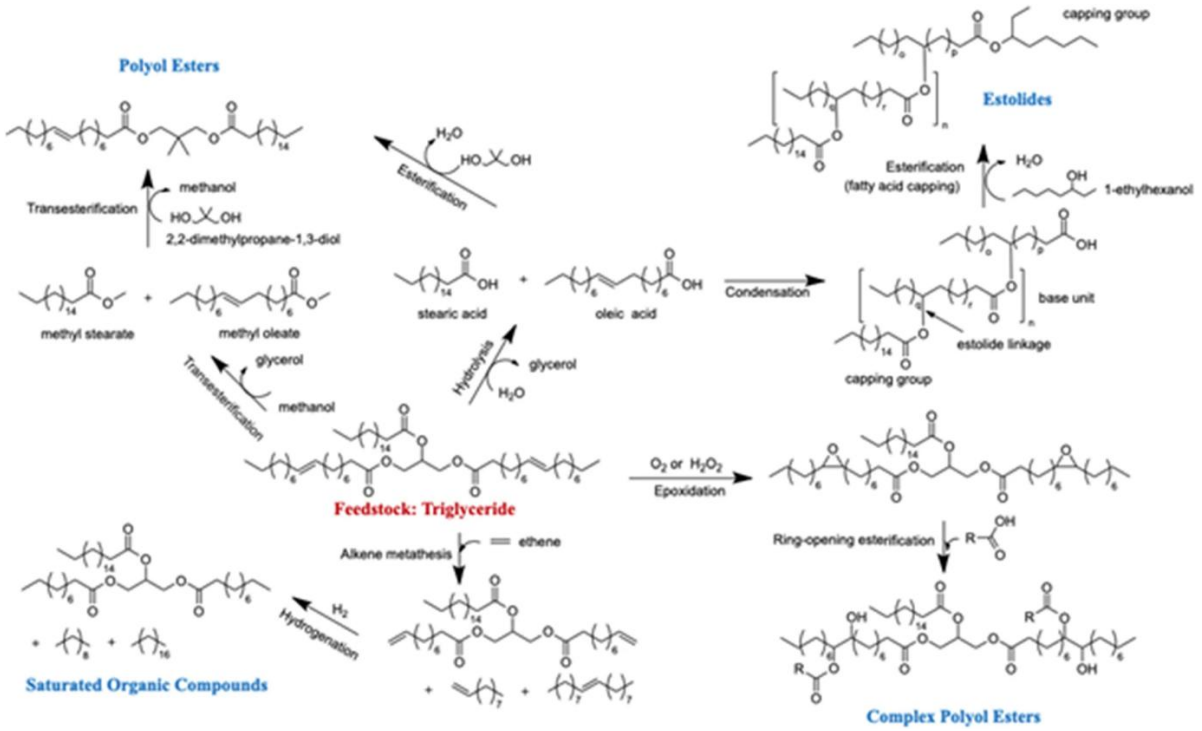

Figure 13: Modification of lubricants. (93)

Of course, the biological impact is the best, but they are not so stable against oxidation. Normally, those oils have double bounds in the structure, which makes it easier for microbiology to use them as a carbon source because of low activation energy. The oxygen from the air can attack the oil's double bonds, leading to oils with hydroperoxide groups. Those oils can react with the other oils and form wax. The second important point is the concurrence between industrial needs and food production. If farmers use their land to produce oil for metalworking, the capacity may be missing in another place.

Then there are the natural ones, which are crude oil based. They are divided into paraffinic and naphthenic oils. The paraffinic ones are, for example, the alpha olefins. They are cheap and have a long history. From the chemical side, they are quite inert. They are stable in oxidation and hydrolysis and are not so hard to attack by microorganisms. Furthermore, they have an ecological impact.

3.6.2 Extreme Pressure and Antiwear Additives

Extreme-pressure and antiwear additives are commonly used in MWFs to form a film between the working peace and the tool at high temperatures and pressure. Those additives contain organic chlorine, sulfur, or phosphorus components that react with the metal surface and form a thin layer. Each of the substance classes has a temperature range in which it lubricates well.

Order of extreme presser ability

phosphide > phosphate > sulfide > chloride

Order of antiwear ability

sulfide > phosphate > phosphide(*94*)

The diagram below shows that the lower the coefficient of friction, the better the substance lubricates. The lubricating properties of the substances are due to the reaction product being still hard at low temperatures and becoming soft as the temperature rises. The substances lubricate best in this state. If the temperature continues to rise, the compounds change to liquid form, and the lubricity is lost. (*95*) (*96*)

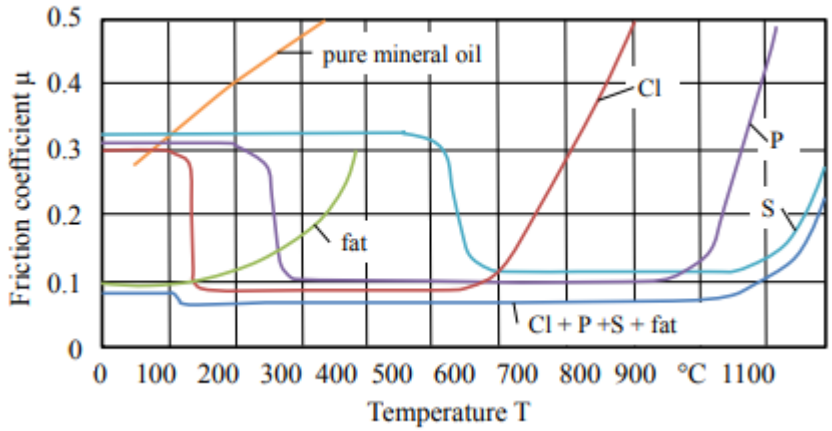

Figure 14: The selection of cooling lubricants is tailored to each process. Depending on their chemical composition, additives are chosen for low- or high-temperature applications. For processes generating significant heat, it is recommended to opt for additives with a low coefficient of friction in this temperature range. Using combinations that span a broad temperature range is often a practical approach. (95)

The chemistry behind these processes is not completely understood. The metals are covered by a protective oxide layer, and the additives require an oxide-free metal surface to react. Therefore, it is unclear how the protective surface comes between the tool and the workpiece. (*97*) Chlorine-containing components, for example, chlorinated paraffins, promote the

oxidation of the metal layer, resulting in a porous FeOOH layer. In the further reaction with Cl^-, this leads to the formation of iron chlorides. Subsequently, this leads to passivation of the surface, as shown in the reaction below (R- *4* - R- *8*). (*98*) (*99*)

$$R - CH_2\,CH_2Cl + Fe \rightarrow R - CH\,CH_2 + HCl(aq) + Fe(OH)^+ \quad \text{R- 4}$$

$$Fe(OH)^+ + OH^- \rightarrow Fe(OH)_2 \quad \text{R- 5}$$

$$4Fe(OH)_2 + O_2 + 2H_2O \rightarrow 4FeOOH \cdot H_2O \quad \text{R- 6}$$

$$2FeOOH \cdot H_2O \rightarrow Fe_2O_3 + 3H_2O \quad \text{R- 7}$$

$$Fe_2O_3 + 6HCl \rightarrow 2FeCl_3 + 3H_2O \quad \text{R- 8}$$

Chlorinated paraffins are not used anymore and are strictly regulated for health and waste disposal. (*100*) It could also be shown that chlorinated paraffin can be replaced when synthesis esters are used. For this purpose, pentaerythritol esters and chlorinated paraffins were compared, and the esters delivered similarly good results. (*101*)

Sulfur-containing additives are the second group widely used in MWFs, including sulfurised olefins, polysulfides, and sulfurised animal and vegetable oils. (*97*) Here, the sulfur content in the molecule is directly related to the EP and AW performance. (*94*) The important thing here is that the addition of energy enables the sulfur to bind to the iron, so the sulfur is located between the iron layers. With the sulfur-containing additives, the sulfur is deposited on the metal surface. As the temperature rises, the S-bonding breaks down, and the sulfur binds to the metal. As the temperature rises, the S-C bond breaks and the metal sulfide is formed (Figure 15). (*102*)

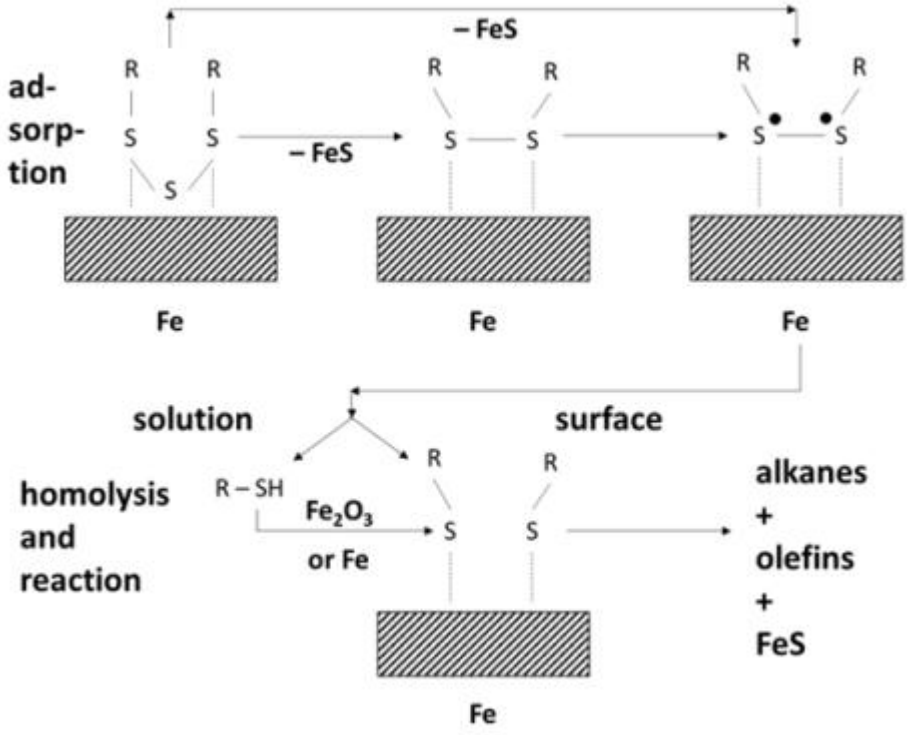

Figure 15: The process of sulfur-containing additive reaction on the metal surface. (102)

The wide range of additives also includes various petroleum-based products, but products from renewable sources are also used. Ricinus oil-based EP and AW additives increase the EP property of water by a factor of 8,7 and can be used well in cutting fluids. (*103*) Another important aspect here is the possible corrosion of copper. Sulfur-containing additives attack metals containing copper if these are present in high concentrations. Therefore, sulfur-free substances such as phosphoric esters could be used in such situations, but phosphorous cannot replace the sulfur additives because of a different reaction mechanism. (*94*)

The third group of EP and AW additives are the phosphorus-containing additives. They are used in middle- or high-pressure applications, but their AW ability is lower than that of sulfur. The reason they are not replaceable is shown in the picture below (Figure 16), where the film-forming reaction is shown. The following pathway is postulated as the reaction mechanism. First, the tricresyl phosphate is absorbed on the surface. Subsequently, an iron phosphate is formed, which reacts under high loading to form the phosphate. This results in the phosphatisation of the surface. The substitutes also have a major effect on the properties. With long chains, the AW properties are better, and with shorter chains, the EP properties are stronger.

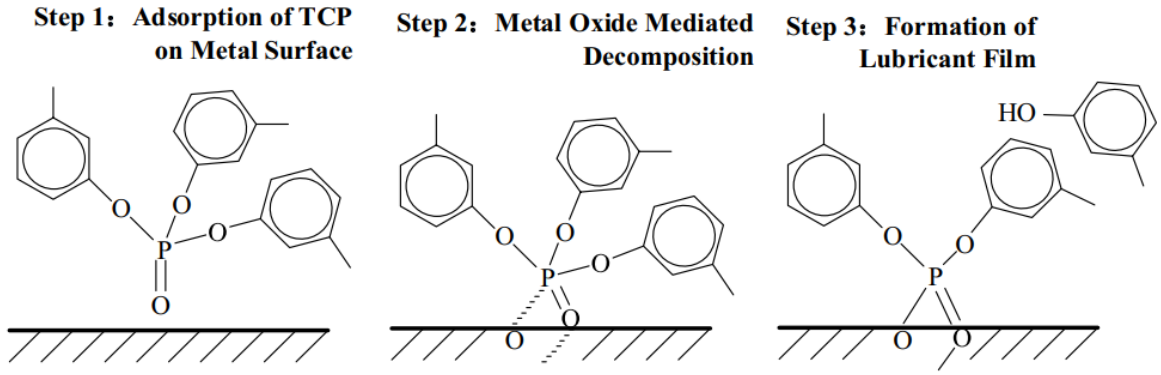

Figure 16: The process of phosphorous-containing lubrication. (97)

Then, there is the group of phosphite esters, which differ slightly from the mechanism of action. Therefore, these can interact with the metal surface via their free electron pair and are more strongly bound. When the temperature is increased, phosphatisation occurs. This means that phosphites have a better AW effect than phosphates. There are also various combinations of phosphates, sulphates, and amines, but this will not be discussed further here.

3.6.3 Antioxidants

Amines are widely used for MWFs. (*104*) It has long been known that amines are absorbed on metal surfaces and form a layer of molecules. This layer, in turn, prevents the metal from corroding. (*105*) It is also assumed that the amines can displace the water molecules from the metal surface. Here, amines with polar groups are better than the non-polar ones. In the case of polar amines, the free electron part of the nitrogen can interact with the metal surface and the polar remainder with the aqueous phase. (*106*) Their function as rust protection is not their only purpose; they also adjust the pH. Amines are strong Lewis bases, the strength of which depends on the functional groups at nitrogen.

3.6.4 Biocides and Alternatives

Biocides are widely used to prevent or inhibit the growth of microorganisms. Biocides are often used in low concentrations in the concentrate and are nevertheless very effective. Due to their biological activity, they are usually strictly regulated, and their use is also restricted. The permitted biocides listed in PT 13 (protective agents for processing and cutting fluids) contain 31 biocides. Among them are 2-phenoxyethanol and 1,2-benzothiazole-3 (2H)-one, which is investigated in this work. The biocides can be divided into formaldehyde formers, isothiazolinones, halogenated biocides, and phenols. (*94*) (*3*) An overview of the different functions of biocides and the point at which the biocide interacts can be found in the table below (Figure 17). (*3*)

Mechanisms of microorganism inactivation by different families of organic molecules with biocidal activity.

Types of Biocides	Mechanisms of action
Acids	Interaction with cell membranes
Active halogen compounds	Binding to -SH groups, inhibition and inactivation of proteins
Alcohols	Protein denaturation, dissolution of cell membranes
Aldehyde and compounds releasing formaldehyde	Binding to NH_2 groups, inhibition and inactivation of proteins and nucleic acids
Biguanides	Interaction with cell membranes, inhibition and inactivation of proteins and nucleic acids
Cationic surfactants	Modification of membrane potential, destabilization of cell membranes
Isothiazolinones	Inhibition of Enzymes
Oxidizing or chlorine releasing compounds	Oxidation of cellular components, interaction with cell membranes, inactivation of proteins and nucleic acids
Phenolic compounds	Protein denaturation, alteration of cell membranes

Figure 17: Different groups of antimicrobial substances with their mechanisms of action. (3)

In addition to conventional biocides, there are approaches to hygienizing cooling lubricants using physical methods or oxidising agents. Physical processes such as UV radiation, heat, or ultrasound can eliminate microorganisms in MWF. (*107*) However, these are very energy-intensive methods. (*108*) It has been shown that a reduction of 99% is possible with UV lamps (55W) in 3 minutes. However, the strong absorption of the MWF interferes here, so mixing is necessary to ensure hygienization. They also show that biocides can be dispensed with this

method. (*109*) In the case of oxidising agents, ozone was tested and showed a promising effect in terms of germ reduction. However, reactivity with some components has also been observed here. In addition, increased quantities of ozone are required in the range of several grams per hour, depending on how long the dosage is applied. This ranges from 1,5 g/h at 45 min to 15 g/h at 20 min, whereby no more germs could be detected in the dipslide test. (*110*)

3.7 Microbial Contamination of MWFs

MWFs provide an ideal environment for various fungi and bacteria, containing 5-10% organic compounds. Bacteria thrive on easily breakable carbon sources, nitrogen, phosphate, and other minerals, with favourable temperature conditions enhancing growth. Contamination sources include the water used, which often contains 10^4-10^5 CFU/ml (*111*), non-sterile equipment surfaces, airborne spores, and user contact with bare hands. This leads to strong and rapid microbial growth in MWF.

However, studies have shown that after only 12 hours, the bacterial load rises sharply to $6{,}9 * 10^6$ CFU/ml. (*112*) (*82*) In another study, a sampling of 44 locations showed that more than 10^9 CFU/ml are present in the cooling lubricants. Conventional methods often refer to cultivable germs, meaning many germs remain undetected. The qPCR technique has shown that up to 5 orders of magnitude, more microorganisms are present in the solutions. Precise methods such as flow cytometry, PCR, and plating would provide the most reliable results here, but this is often not feasible in practice for cost reasons. Alternatively, cheaper test methods are preferred, but they do not allow exact quantification and do not allow any statements to be made about the type of contamination. (*113*)

The picture below shows how much the dipslide test distorts the result. The dipslide test shows an average of only 1% of germs, which is a massive distortion of reality. In some cases, the test even shows that the emulsion is completely uncontaminated, although this is not the case (Figure 18). A simple and accurate measurement method is needed here. (*114*)

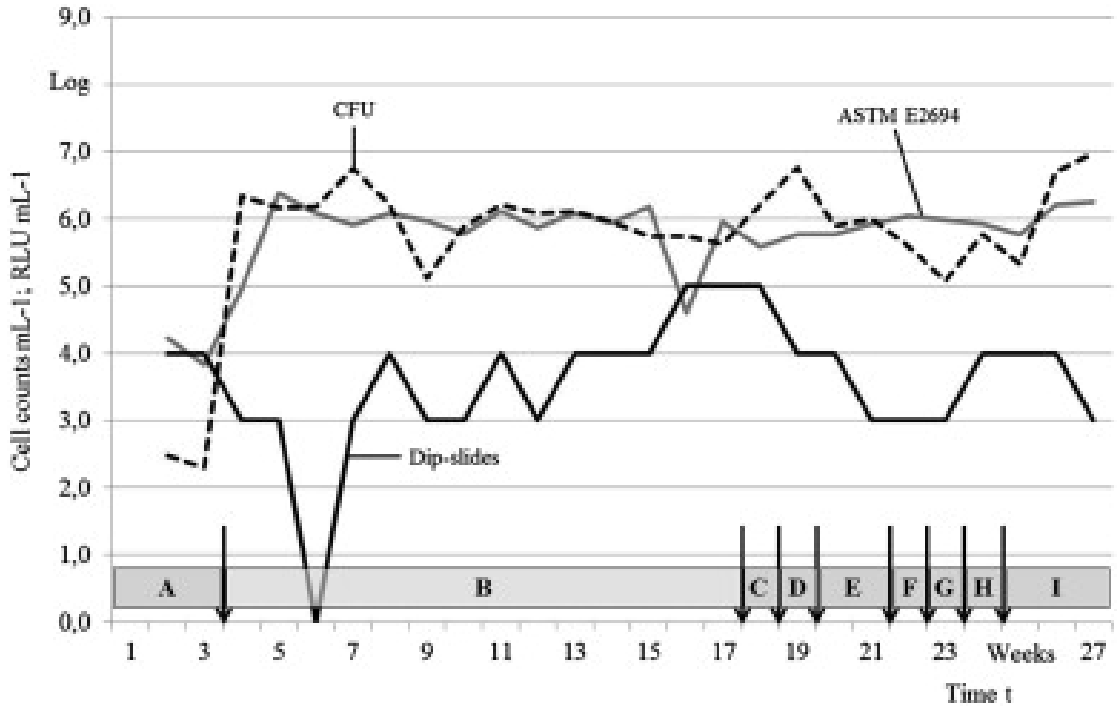

Figure 18: A 27-week monitoring of MWF by various microbial test methods shows the extent of the deviation. This emphasises the need to create cost-effective and functioning alternatives. (114)

As shown, MWF is a challenging fluid from both a microbial and analytical point of view. In addition, action is absolutely necessary from a sustainability and occupational health and safety perspective. MWF is also an extreme example. If a method works here, it can easily be transferred to other processes. This underlines the importance of this fluid for the further course of this work.

4. Results and Discussion

To achieve the objective of this project, an online-capable, real-time analytics system for microbiology is necessary. This system must accurately assess contamination levels, allowing for the adjustment of chlorine dioxide dosages according to the detected contamination. Spectroscopy is particularly well-suited for this purpose due to its speed and reliability. While absorption can be influenced by various substances, fluorescence presents a more precise option, as not all absorbing substances emit light.

NADPH serves as a prime target since it is a characteristic marker of living cells. A high concentration of NADPH indicates a substantial presence of living cells, enabling the determination of the total bacterial count. This, in turn, reflects water contamination levels, allowing for precise dosing of chlorine dioxide. The stable chlorine dioxide used in this work comes from a.p.f. Aqua System AG and is based on the patented persulphate process and DVGW W 224 (3.2023). (*57*)

4.1 Fluorescence Spectroscopy of NADPH

Fluorescence spectroscopy is a widely used analytical tool. There are numerous compounds in nature that fluoresce. Some of these substances are found in vital cellular processes. The quantification of such substances is a great challenge, but it can provide a lot of information about organisms. One promising substance is NADPH. It can be used here because only cells with intact energy balance can produce them.

First, the peak maximum of NADPH is determined. Subsequently, NADPH is determined in living cells, whereby the feasibility and the concentration in living cells can be determined. A concentration of NADPH was chosen that could be easily measured spectroscopically. The NADPH is measured under laboratory conditions in a concentration of 14 mg/l with a 3D fluorescence spectrometer. A pure sample of NADPH shows an intensive fluorescence signal at Ex. 270nm and 345nm and Em. at 460 nm, as seen in the picture below (Figure 19). The

position of the peak agrees well with the literature but the concentration is lower by a factor of 100. (*32*)

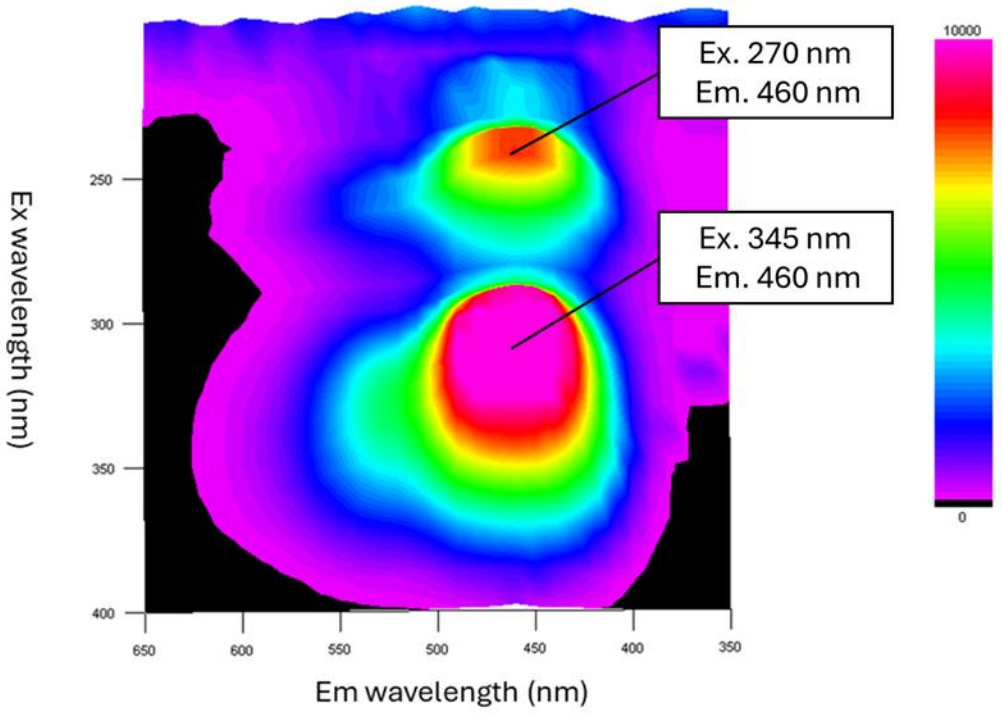

Figure 19: 3D spectra of NADPH in deionised water

Since NADPH is easy to measure, it is used directly as an indicator for living cells. For this reason, a fresh, live *E. coli* OP50 sample was prepared and analysed using 3D fluorescence spectroscopy. The bacteria are a modification of Escherichia Coli B from the bacteria strain OP50-1 ordered from the workbook. The bacteria were grown in LB Broth at 37°C for 24h. The bacteria were stored in a refrigerator until use. The harvesting is performed by centrifugation at 4000 rpm at five degrees for 20 minutes. The washing procedure was performed as follows: the pellet was resuspended in PBS (phosphate-buffered saline) and centrifugated; this was performed three times. The bacteria were diluted in PBS and were used immediately.

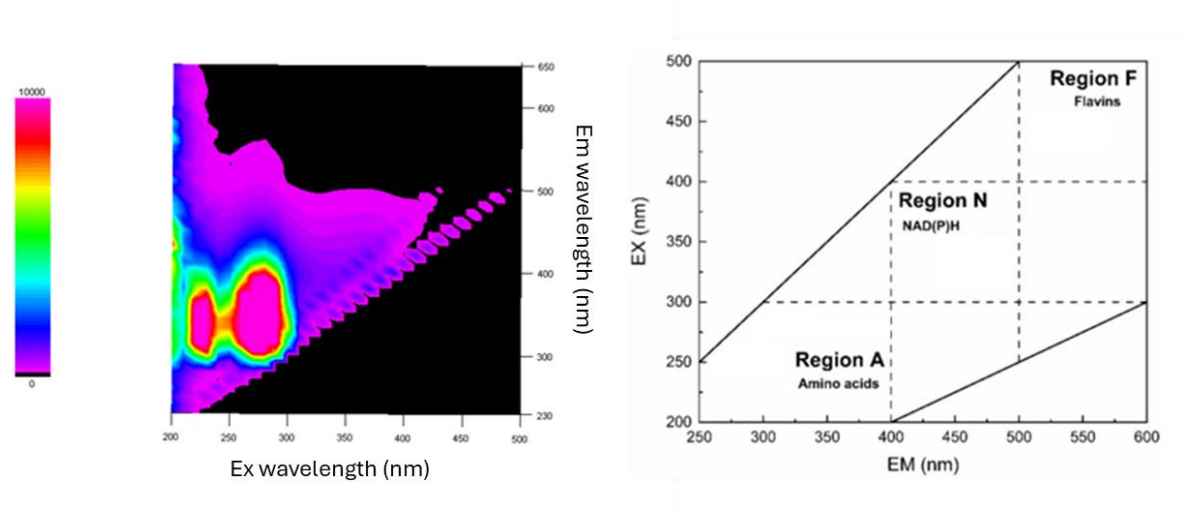

Figure 20: The left spectra show living E. coli in PBS, and the right one(115) shows an overview of important autofluorescence species in microorganisms. Only the fluorescence in Region A is visible.

The diluted sample did not exhibit fluorescence at the NADPH region as shown in the figure, and other fluorescence-active substances from the inner cell were not observed in the *E. coli* spectra (Figure 20). Below is a schematic representation of where bacterial fluorescence substances should emit fluorescence. The two figures show that the N-region in the *E. coli* spectrum has no peaks. However, two peaks are visible to the left below this peak. These match the position of region A.

However, the measurement of living *E. coli* shows no fluorescence in the range of NADPH. This could have several reasons. First, it could be a scattering effect. To test this, an emulsion is produced which is intended to represent the conditions in the bacterial suspension. For this purpose, octanol and water are mixed; this mixture should not fluoresce but scatter light. To make this emulsion more stable, it was emulsified with an ultra-turrax. This mixture did not show any fluorescence. After adding NADPH to the solution at a concentration of 14 mg/l, the fluorescence of NADPH was visible. Therefore, the reason for the scattering is unlikely.

Second, the light is not strong enough to go through the cell wall to the target and back through the cell wall to the detector. To eliminate the effect of the cell membrane, living organisms were crushed with the ultra-turrax and solid parts were removed by centrifugation. The liquid phase contained no cell membrane residues, but no NADPH was still visible. In addition, the solid components were suspended in PBS and showed no change in fluorescence. This means that the observation of fluorescence is independent of the cell membrane.

The third reason could be the detection limit. The NADPH concentration within cells may fall below the detection limit. To address this, we first determined the detection limit of NADPH using a fluorescence spectrometer. A solution with a concentration of 1,2 mg/l was prepared

and measured, yielding an intensity of 218. The noise from the zero measurement was 0,7, leading to a detection limit of 4,2 µg/l. Due to the absorption of other molecules in the bacterial cell, a signal swelling is expected when measuring; therefore, the detection limit is likely even higher.

According to the publication of Lilius et al, wild *E. coli* have a concentration of 1,8 µg NADPH per gram of *E. coli* dry mass. Therefore, a level of approximately 2,3 g *E. coli*/l is required to get above the detection limit. This highlights the significant quantity of *E. coli* required for detection. Given that an individual bacterium weighs approximately 0,15 pg and the measurement is performed in the range of 1,5 mg bacteria/l, it is evident that the current method lacks sufficient sensitivity. Without significant advancements in detection capabilities, reducing the detection limit by several orders of magnitude is unlikely, indicating the necessity for an alternative approach. (*116*)

The spectra show a strong peak at 330 nm, which is known as bacterial autofluorescence. (*115*) This fluorescence of bacteria has no evident area. It occurs from 300 to 350 nm, with the maxima at 325 nm and needs further examination. (*115*) (*21*) The characteristic fluorescence of peptides could cause it, but it requires a closer look.

4.2 Fluorescence Spectroscopy of Amino Acids and Peptides

The fluorescence discussed in the previous chapter is now analysed in more detail. It can be seen that the bacteria exhibit intense fluorescence (Figure 20). It is important to determine whether this fluorescence is also suitable for quantifying microbiology. If, through optimisation, a sensor can be built that can measure fluorescence at low levels, maybe even drinking water-relevant ranges can be achieved. Such a device could lead water disinfection into a new era. First, we examine the three amino acids that exhibit fluorescence in the range of A (Figure 20). These three are tryptophan, tyrosine, and phenylalanine. From these, the amino acid that most accurately represents bacterial fluorescence is selected as the model substance. Following this, the oxidation processes of these amino acids are investigated.

A 3D spectrum from the amino acids makes the actual maxima visible (Figure 21). For phenylalanine, the excitation is at 210 and 250 nm, and the emission is at 280 nm. There is still the highest concentration, and the impact is the smallest. Tyrosine also has two excitation maxima at 220 and 280 nm and emission at 300 nm. The emission is much smaller, but the concentration is the same as tryptophan's. The fluorescence of tryptophan has the same excitation as tyrosine, but the fluorescence is shifted to 350 nm (Figure 21). Tryptophan is the best option for modelling bacterial fluorescence and a good choice for understanding proteinogenic fluorescence (Figure 20).

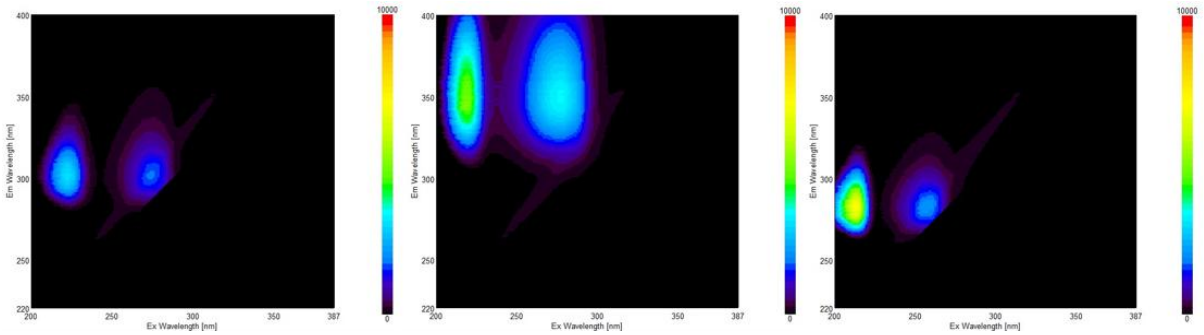

Figure 21: 3D fluorescence spectra of tyrosine (2,84µmol/l), tryptophan (2,86µmol/l), and phenylalanine (183 µmol/l) in deionised water. Left tyrosine, middle tryptophan, and right phenylalanine.

As shown the intrinsic fluorescence of bacteria is primarily caused by the indole group of tryptophan, one of the amino acids. While tryptophan contributes significantly to the fluorescence, it does not account for all of it. Tyrosine and phenylalanine also exhibit fluorescence, albeit to a lesser extent. These amino acids are present in the membrane proteins within the cell wall, and their proportions vary among different proteins. Consequently, the emission of individual proteins differs from that of tryptophan or tyrosine. (*38*) However, various microorganisms, such as Staphylococcus aureus, *E. coli*, Pseudomonas aeruginosa, and Legionella waltersii, have been tested for their fluorescence using 3D fluorescence spectroscopy, which has shown intense autofluorescence. (*117*) (*21*)

As described in the theory, chlorine dioxide is a very efficient and widely used oxidising agent that is well-suited for the elimination of bacteria. For further investigations, it is also important to know how fast the reaction of the amino acids with chlorine dioxide is. Otherwise, the reaction time could be too short or too long. The reactivity of chlorine dioxide with amino acids has only been reported in a few cases. The reaction kinetics of the amino acids have the order cysteine ($10^7 \frac{mol/l}{s}$) > Tyrosine ($10^5 \frac{mol/l}{s}$) > tryptophan ($10^4 \frac{mol/l}{s}$). (*118*) (*119*) (*120*) The

reaction constants clearly show that the reaction is very fast and will be completed in a few seconds. Long waiting times are therefore not necessary.

The oxidation of amino acids requires further investigation to understand the oxidation of living organisms. First, tryptophan is treated with defined amounts of chlorine dioxide. As tryptophan is usually bound, various peptides are also tested.

When chlorine dioxide was added to the solution, a noticeable reduction in the peak was observed. The oxidation of tryptophan with chlorine dioxide has been reported a few times, and the reaction products are known. The effect of chlorine dioxide is measured with fluorescence spectroscopy and shows an intense degradation with a low concentration of chlorine dioxide.

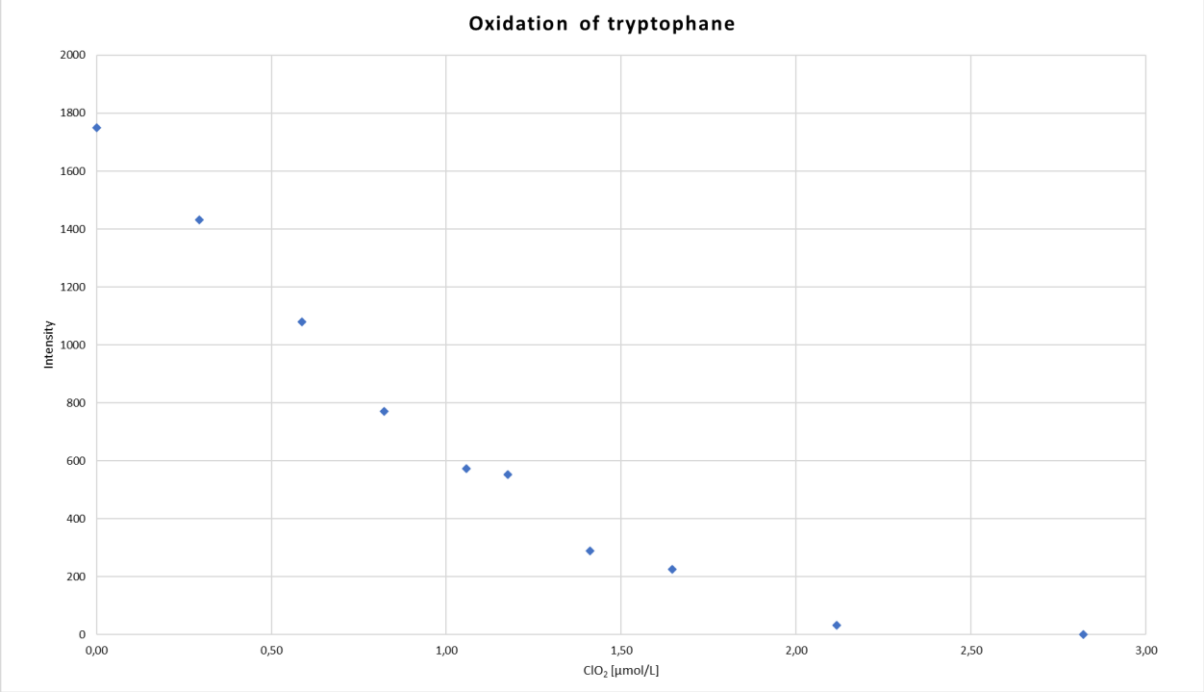

Figure 22: Oxidation of tryptophan with chlorine dioxide in different concentrations

The chart clearly shows how the fluorescence intensity decreases. At first glance, it appears to be a logarithmic decrease, but this represents the decrease very poorly. A better alternative is provided by two grades. One that represents the beginning of the oxidation and a second that represents the end.

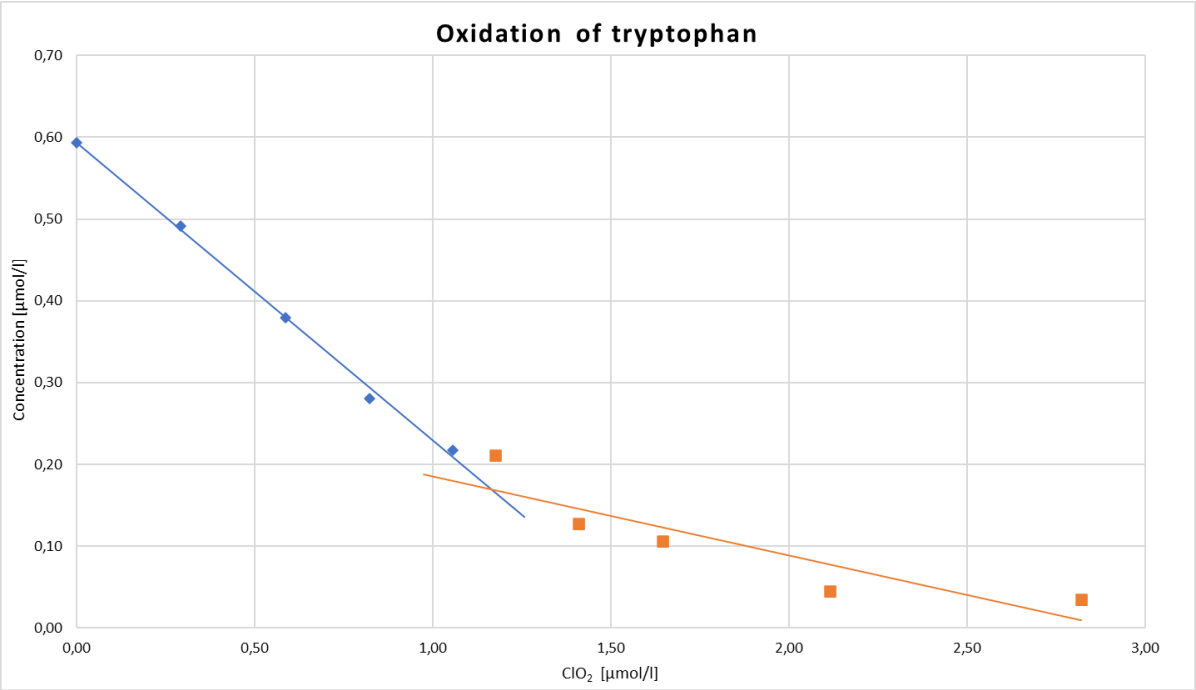

Figure 23: The degradation of tryptophan in different molar ratios and a two-linear correlation.

By using a calibration function it is possible to calculate the tryptophan concentration, with this data it is possible to get a molar ratio from the slope. Using this technique, the slope is for the first function 0,36, a molar ratio of 3 ClO_2 against one tryptophan, and then the other slope is 10 to 1 (Figure 23). This could indicate two groups of oxidation products. The first oxidation group has a more negligible fluorescence than tryptophan and easily forms with chlorine dioxide. This may be the oxidation of the indole structure. Then, there is a mixture of different components because of several oxidation products. (*120*) Several concentrations were measured to analyse the effect. This shows that the trend is independent of concentration and always works similarly (Figure 24).

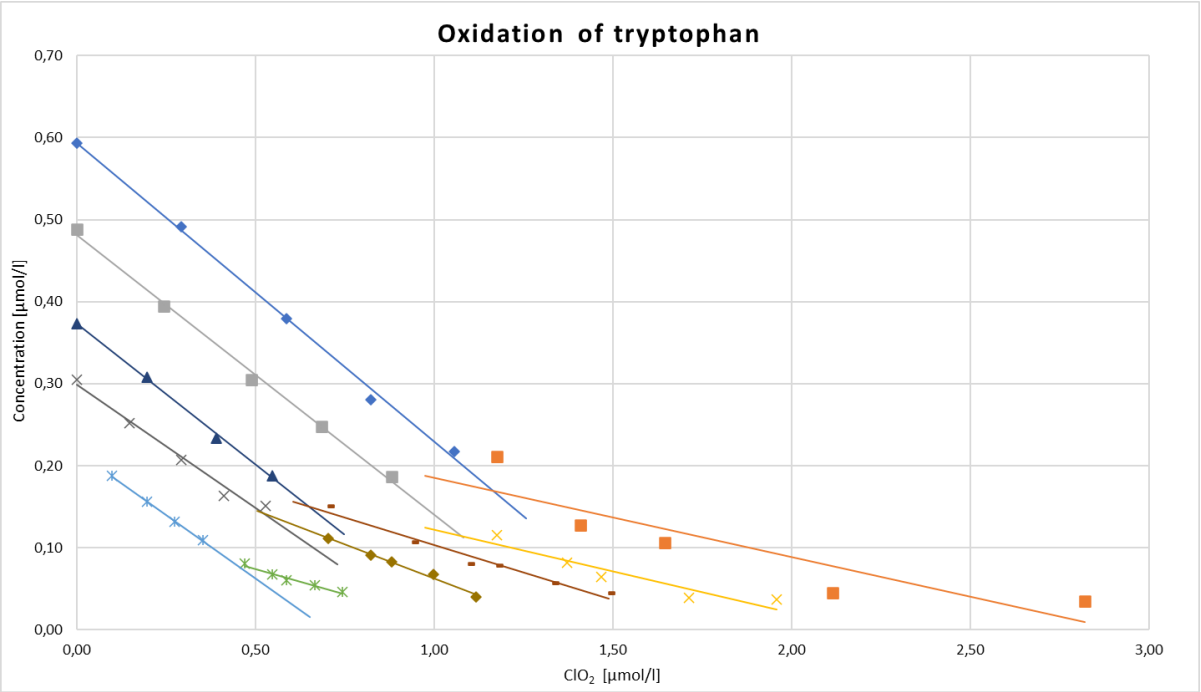

Figure 24: The degradation of tryptophan in different molar rations and two-linear correlations in various concentrations.

The slope of the straight line is the same over the entire concentration range and shows a good correlation with the linear regression. The values in the table show a slight drift. For the first degree, the slope increases with increasing concentration and for the second degree, it decreases. Nevertheless, the values show a clear trend of -0,33 for the first grade and -0,12 for the second (Table 2).

Table 2: The gradients of the tryptophan degradation.

Concentration (µmol/l)	the gradient of the straight one	the gradient of the straight two
0,588	-0,364	-0,097
0,490	-0,341	-0,101
0,392	-0,322	-0,111
0,294	-0,302	-0,167
0,196	-0,309	-0,122
	Middle: -0,327	Middle: -0,120

These results also fit with the known literature of D.J. Stewart, who measured chlorine dioxide and tryptophan. He used HPLC and ESI-MS to find the oxidation products shown below and postulate the reaction mechanism (Figure 25). (*120*)

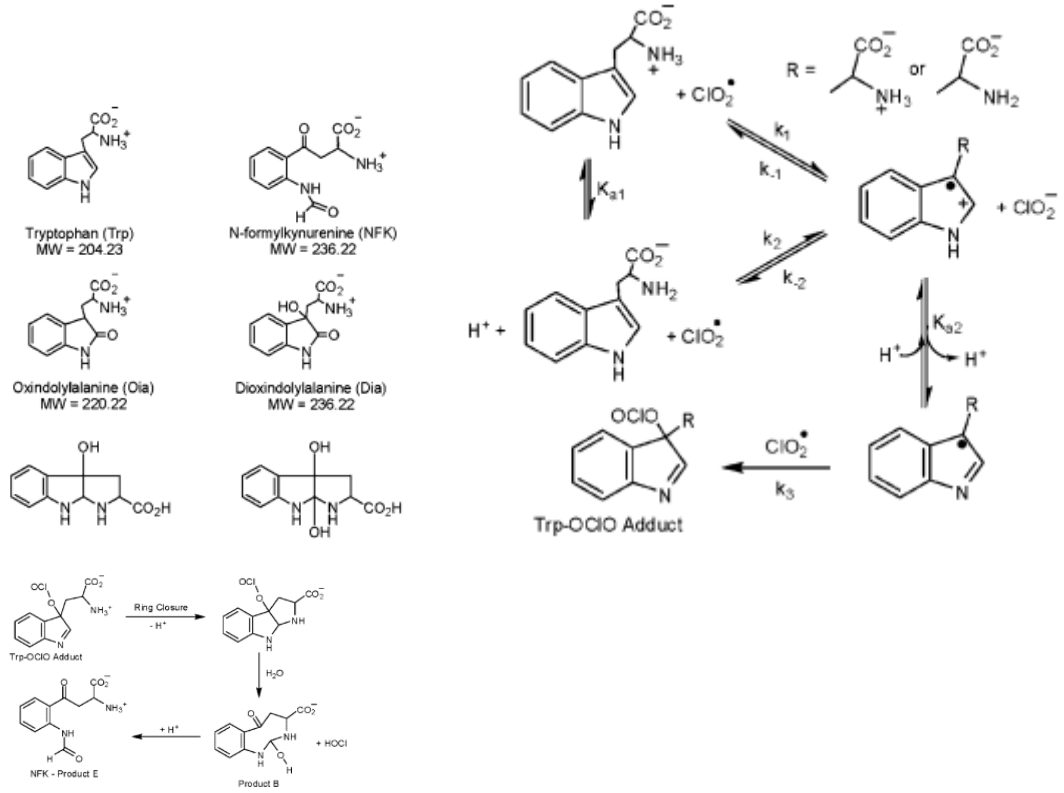

Figure 25: Postulated reaction mechanisms of tryptophan with chlorine dioxide and several products. (120)

The oxidation products are all generated with low concentrations of chlorine dioxide and form the oxidation species N-formylkynurenine (NFK) and oxidolylalanine. The formation of those species needs at least 2 chlorine dioxide. Then, considering that other species are also formed because the reactions are always competitive reactions, a ratio of 3:1 is possible. After the first oxidation, further oxidation will occur. Another publication also analyses the higher molar ratio of those oxidation products. (*121*) (Figure 26) They use derivatisation of the products and GC/MS with hard conditions. At this point, it should be noted that reactions by the analysis are possible, but the results are similar to those of D.J. Stewart. In any case, the reaction produces differ by a molar ratio higher than 1:2 critically. The indole-like compounds are reduced, and small acids indicate that the benzol ring is destroyed. The destruction of all aromatic structures will lead to a complete loss of fluorescence.

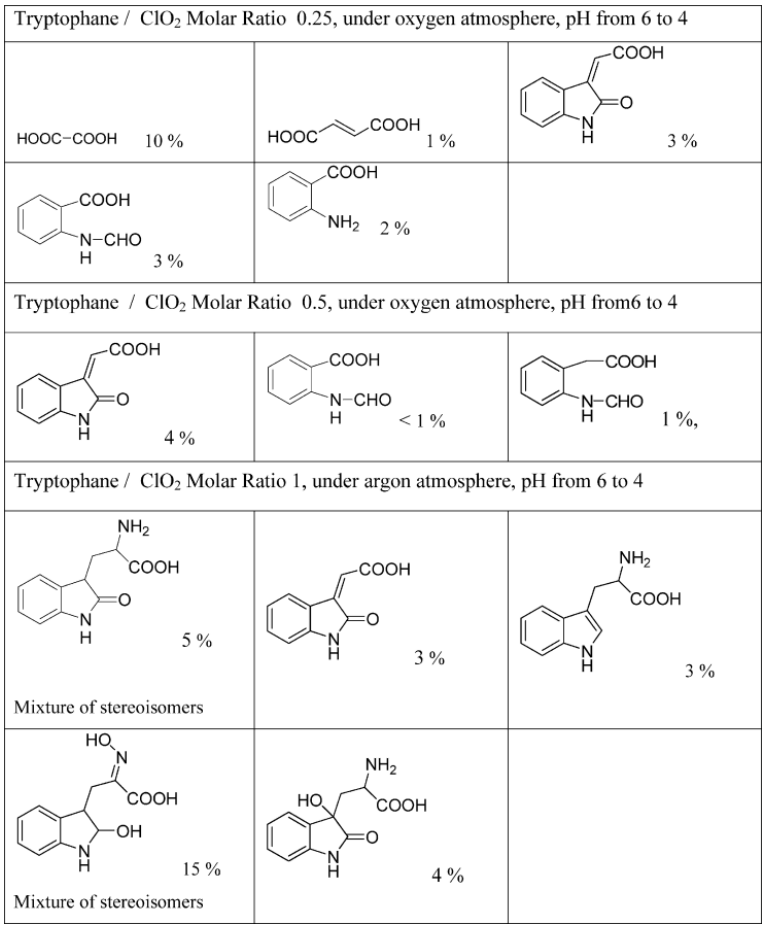

Figure 26: Reaction products that are found in the oxidation of tryptophan. (121)

The oxidation of free amino acids results in the degradation of tryptophan, leading to the formation of two oxidation groups: initially, oxidation group 1, followed by further oxidation to the second oxidation group 2 (Figure 23).

Since tryptophan is incorporated within the cell membrane, this can significantly influence its reactivity and fluorescence, warranting further investigation. Bound tryptophan cannot undergo the same reactions as free amino acids for two primary reasons: first, there is a difference in electron distribution, and second, the rotation of the molecule is restricted. The binding of peptides can alter the electron density under various conditions. Initially, peptides containing only tryptophan will be analysed. It is obvious that peptides containing only tryptophan will undergo similar degradation processes as tryptophan itself. However, because the chemical environment of tryptophans is different, differences in the reaction may occur.

The measurement shows that the amount of chlorine dioxide needed to eliminate fluorescence is independent of the amount of tryptophan. The amount of chlorine dioxide is just a bit higher

for the whole peptide than for tryptophan itself. The ratio for the first gradient is three chlorine dioxide molecules for one tryptophan molecule. For the second, 15 chlorine dioxides for 2 tryptophan molecules. The structure could explain this, as free tryptophan has other rotational possibilities and therefore other reaction products are also conceivable. In the case of free tryptophan, the rotation of the sidechain is easier. So, the oxidation way from tryptophan to NFK is preferred. In the case of the di- and tri peptides of tryptophan, the path to NFK is possible for just one of the tryptophans, and even this is not so easy. So, the way to other oxidation products might be preferred, like the oxidolylalanines. The fluorescence activity itself is also changed in contrast to tryptophan. The tryptophan has twice the intensity of the peptide, which will also be analysed later.

The tripeptide case shows that the reaction's molar ratio looks similar. The ratio for the first gradient is the same as above; for the second, it is one tryptophan to 7 chlorine dioxides. There might be similar reaction kinetics. A closer look at the results indicates that all peptides with only tryptophan react in the same ratio—the degradation analysis with two gradients instead of a logarithmic works well for peptides with only tryptophan. Since the two degrees offer a good correlation, it is assumed that it is a multi-stage oxidation process.

Since peptides in cells consist of different amino acids, the investigations are extended to peptides with different amino acids. The peptides where tryptophan is only on the side of the molecule Trp-Leu and Trp-Met-Asp-Phe are analysed. Like in the others, there is a clear trend, even if the results differ. Here, a small amount of chlorine dioxide is enough for oxidation. It is just half of the molar ratio needed for tryptophan itself. The reason for this can be the hindered side chain or electron density. The expectation would be that the longer side chain would block the attack of chlorine dioxide, but obviously, it does not. The effect of an even longer side chain is tested in the next. The longer chain makes it possible to achieve a more pronounced folded structure with which the tryptophan could be better protected.

In this case, the longer peptide does not affect the first oxidation, so other effects like electron density could play a role. In this case, the second oxidation differs significantly from the shorter Leu-Trp peptide. There were just four chlorine dioxides, which was enough to destroy the fluorescence, but here, it needs 56 moles for one. This is much more than expected, but from a closer look, it is seen that methionine and phenylalanine consume chlorine dioxide, which could be why they are so high. For the effect of tryptophan in the middle of the structure, H-Met-Pro-D-Phe-Arg-D-Try-Phe-Lys-Pro-Val-NH_2 is analysed. This one is quite different from all the others. It does not have two gradients, and all data points show an excellent linear

regression. Maybe the second gradient is there, but it is not visible, and measurements with higher concentrations of chlorine dioxide should be performed. The data show only a 90 % reduction in the fluorescence signal. A possible explanation could be the amino acids methionine and phenylalanine as they also react quickly with chlorine dioxide, which could be a reason for the higher molar ratio of 4 chlorine dioxide to 1 tryptophan.

Although the results are not completely identical and the quantity of peptides is limited, correlations can still be recognised here. Firstly, all peptide fluorescence can be degraded, and other peptides with reactive amino acids will be reactive. Second, the gradients that show the amount of chlorine dioxide are always in a similar range, and a slight molar excess is always necessary. Unfortunately, the second gradient is not so uniform here. Significant fluctuations can be recognised here, and the second gradient's complete disappearance is possible as is seen in the case of the oligopeptide. However, this leads to the conclusion that the first gradient allows a statement about the intactness of the fluorescent amino acid (Table 3).

Table 3: The results of the fluorescence measurements of the peptides were collected. This shows how much chlorine dioxide is needed to quench the fluorescence. The lower peptides are gastrin (Trp-Met-Asp-Phe) and oligopeptides (H-Met-Pro-D-Phe-Arg-D-Try-Phe-Lys-Pro-Val-NH_2).

concentration	the gradient of the straight one	the gradient of the straight two
Trp	3,0	8,3
Trp-Trp	2,5	7,4
Trp-Trp-Trp	2,9	6,8
Trp-Leu	1,6	4,0
Gastrin	1,5	55,6
oligopeptide	3,9	-

There is a clear trend in the measurements. Tryptophan is permanently attached to chlorine dioxide because the fluorescence goes down. The molar ratio that is needed for the destruction of almost all fluorescence is low. The rest of the fluorescence is much more stable, and the amount differs significantly. The effect of the position and size of tryptophan does not have a significant influence. In other words, no conclusions can be drawn about the molecule from the fluorescence because the differences are too small. On the other hand, it does not really matter what proteins are present because they always have very similar fluorescence intensity, which makes it possible to quantify the microorganisms. The relative intensity of fluorescence is also

an interesting part. A similar trend is found here, i.e., the bounded tryptophan has a much lower fluorescence than free tryptophan. The impact of two or three tryptophans is also tiny, and the oligopeptide is close to the intensity of only tryptophan-containing peptides. Then, the peptides with tryptophan at the side of the peptide have the smallest relative fluorescence. Therefore, the same pattern is visible here. The effect of the chemical environment is intense, affecting oxidation, and therefore it is an effect of the electron density. Trp-Leu and Trp-Met-Asp-Phe show a strong shift to tryptophan in an electron density map, while all the others have a more distributed electron density (Table 4).

Table 4: The relative intensity of tryptophan and peptides. The high molar weight peptides are gastrin (Trp-Met-Asp-Phe) and oligopeptides (H-Met-Pro-D-Phe-Arg-D-Try-Phe-Lys-Pro-Val-NH_2).

Molecule	Concentration (µmol/l)	Intensity	Intensity for 1 µmol/l	Intensity/Trp
Trp	0,59	1749,86	2978,12	2978,12
Trp-Trp	1,98	3559,12	1795,43	897,72
Trp-Trp-Trp	1,04	1921,23	1846,49	615,50
Trp-Leu	2,52	1657,39	657,53	657,53
Gastrin	2,61	1475,26	564,30	564,30
Oligopeptide	0,99	1777,24	1786,87	1786,87

The mechanism may be like the oxidation of peptides. For this reason, further analyses are performed with living organisms. Two critical aspects warrant further examination: first, whether the loss of fluorescence indicates that the bacteria are dead, and second, whether there is a correlation between the bacterial count and the fluorescence signal. Cumberland showed that *E. coli* can be measured using a simple fluorescence spectrometer. He found that *E. coli* can be measured with commercial devices in low range, but this was not true for other species. (*122*) Another study found that analysing several Ex./Em. pairs in combination with PLS analysis is a suitable detection method. Low detection limits are also achieved here with high accuracy. The dual wave lengths also make it possible to distinguish the individual species from concentrations of 10^4 CFU/ml. (*123*) The disadvantage of both, however, is that no statement could be made about the living/dead status, which greatly limits the benefits. The use of chlorine dioxide could possibly also clarify the status of the cell. However, further investigations are necessary to establish the connection between fluorescence and living germs.

4.3 Quantification of the Microbial Load

The appropriate wavelength pair was found, and now a method could be developed to detect microorganisms by fluorescence. First, the cell number must correlate with the fluorescence to find a measuring range. For this purpose, bacterial suspensions are cultivated on agar and counted. The fluorescence of the solution is measured in parallel. Second, it must be determined whether the disappearance of the fluorescence means that the bacteria are dead. For this purpose, the bacterial suspensions are treated with chlorine dioxide and measured as before. Third, the amount of chlorine dioxide required to eliminate the microorganisms must be determined from the collected data.

To correlate the number of living cells with fluorescence, it is essential to first determine the cell count. Since cell numbers can change rapidly, they must be reassessed frequently. Quantitative microbiological analysis presents greater challenges than chemical analysis due to the complexities associated with bacterial growth and death. As a result, multiple counts are often necessary to account for these variations. Bacterial load was evaluated using optical density at 600 nm (OD 600) through UV/Vis spectroscopy and Colony-Forming Unit (CFU) through plate counting. (*124*) OD 600 is the primary technique for estimating cell numbers in water-based samples. It offers a fast and straightforward approach. The OD600 value can only indicate the cell density, but it cannot make a statement about the number of living organisms, so cultivation experiments are necessary.

The bacteria were prepared as described in Chapter 4.1. To measure OD 600, quartz cuvettes with pathlengths ranging from 1 to 5 cm are utilised, and all suspension dilutions are prepared in PBS. Absorption is determined for a 5 cm cuvette, with an absorbance range typically between 0,1 and 0,5. The measurement has displayed strong linearity within the 10^6 to 10^8 CFU/ml (colony-forming unit per millilitre) range, leading to a reliance on optical density for further quantifications.

Cell count determination is performed with a dilution in saline and a sample volume of 1 ml. The sample was added to a petri dish, and 20 ml of agar was added with a 25 ml stripet. The plates grew at 37°C for 48h, and the CFU was counted according to DIN 8199(*125*)

Figure 27: The plate counting of E. coli (OP50-1) on an R2A agar. The plates are performed as triplicates; the white spots are the E. coli colonies.

After incubation, the plates show oval, slightly yellowish dots called colonies. These are located in the medium as the suspension is added in the medium itself. This can cause colonies to overlap or grow, so dilutions and good distribution are important (Figure 27).

Table 5: Results from the plate counting

	Dilution 1: 10^6	Dilution 1: 10^7	Dilution 1: 10^8
Measurement 1	276 Colonies	30 Colonies	4 Colonies
Measurement 2	256 Colonies	29 Colonies	4 Colonies
Measurement 3	248 Colonies	29 Colonies	6 Colonies

The table indicates that significant dilution is necessary to achieve the required measurement range (Table 5). The individual measurements show only minimal variations; from this data, it is possible to calculate the CFU/ml. For this, the volume of the original probe (3,33 µl), the total bacterial count for all plates for *E. coli* (882), and the reference volume of 1 ml are necessary. This information can be expressed as CFU/ml using the following formula according to DIN EN ISO 8199. (*125*)

$$\mathbf{C_s} = \frac{\boldsymbol{Z}}{\boldsymbol{V_{tot}}} * \boldsymbol{V_s} \qquad (5)$$

C_s = CFU/ml, Z = colonies on all plates, V_{tot} = volume of the original probe, V_s = reference volume. For the case represented in the table, the result is $2{,}65 * 10^8$ CFU/ml. The

measurements were carried out in a range from 10^6 to 10^8. The rest of the data is in the Appendix.

The data indicate a growing number of microorganisms exhibiting an increase in fluorescence, which suggests that quantification based on fluorescence is feasible (Figure 28). The quantification reveals an almost linear relationship. This proves that fluorescence is well suited to determine a bacterial count. This discovery proves the most important point: living cells fluoresce.

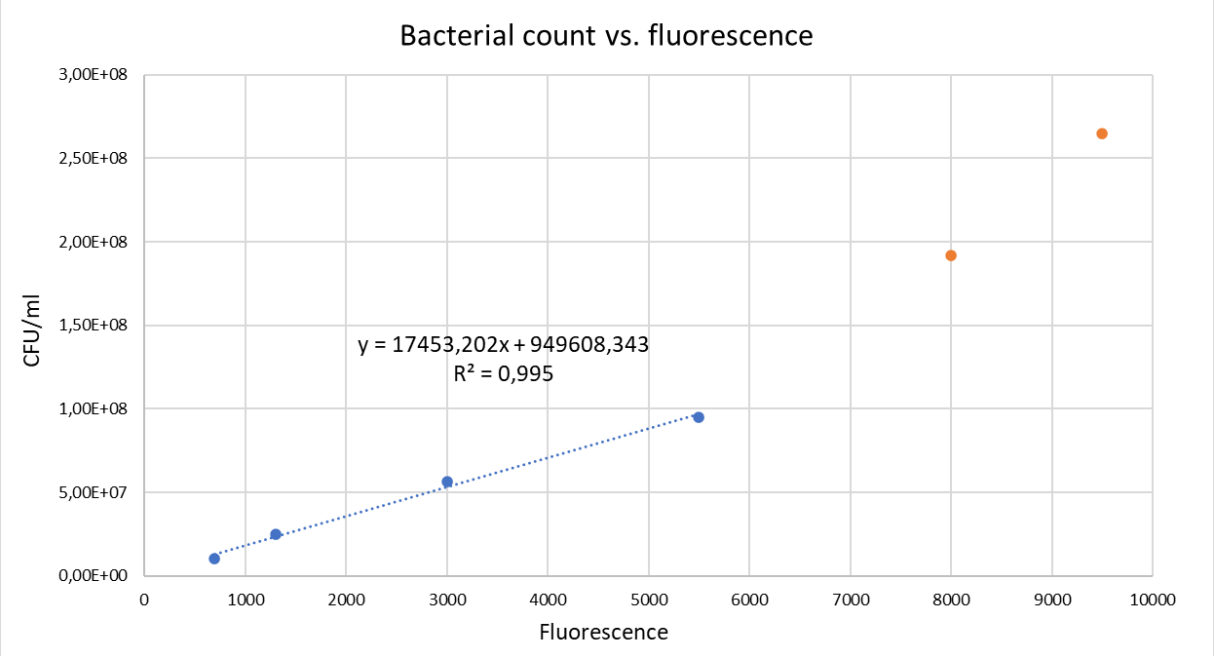

Figure 28: The plot of the bacterial count vs. fluorescence shows that the relationship is partly linear. The abbreviation of the grades can probably be attributed to the plating.

The linearity seems to be a problem here; to show that it is not a problem of fluorescence, a dilution series was measured that does not include a bacterial count determination but rather a stock solution with a known bacterial count. Samples were treated as in the previous experiments to confirm the linearity of the measurements by fluorescence. The stock solution was adjusted to an optical density similar to that of the plating. The samples were then measured by fluorescence spectroscopy. This showed a good correlation between the CFU/ml and the fluorescence. Attempts to make a dilution series here showed an even better correlation at close to 1 over the hole range. It can, therefore, be assumed that the most significant errors occur when measuring the living cells by plating. Nevertheless, the method above is quite

suitable with a correlation of 0,995. An untreated solution with a known optical density has a CFU/ml that can be calculated according to the function below.

$$\frac{\text{CFU}}{\text{ml}} = 17 * 10^3 * \text{Fluorescence} + 95 * 10^4 \quad (5)$$

To evaluate whether this method can effectively differentiate between dead and living bacteria, the bacteria are first treated with chlorine dioxide, which is well-documented for its strong antibacterial properties. At a bacterial count of $5{,}7*10^7$ CFU/ml and 1,5 mg/l of ClO_2, all bacteria are rendered inactive (1 CFU/ml). Fluorescence measurements indicate that this concentration is sufficient to extinguish fluorescence almost completely. The fluorescence decreases from 3000 to 80 fluorescence units. However, this observation merely confirms that bacteria killed by oxidising agents do not fluoresce.

It is known that heat can also kill bacteria. For instance, *E. coli* bacteria were subjected to a temperature of 70 degrees Celsius for four hours, effectively resulting in their demise. While a subtle shift in the peak was noted in the spectrum, indicating a modification in the tryptophan environment, the fluorescence signal remained detectable. This observation highlights that the presence of a fluorescence signal does not necessarily signify the presence of living cells; rather, it suggests that the tryptophan unit remains intact. Studies on tryptophan-containing proteins in milk have shown the effect of temperature. A slight reduction in the signal can be observed at temperatures above 90 degrees when held at these temperatures for more than 10 minutes. There is also a subtle shift of the maximum by approximately 20 nm. At higher temperatures, this happens within a few minutes. At a temperature of 80 degrees, no reduction can be observed. (*126*) Also, bacteria killed by heat have amino acid fluorescence. This aligns with the study, as temperatures of 90 degrees are usually not used for disinfection in water. The vegetative cells are already killed at 60 degrees. (*15*) To substantiate these considerations, the behaviour of tryptophan and tryptophan-containing peptides is investigated when they are oxidised with chlorine dioxide. The prominent fluorescence comes from tryptophan, tyrosine, and phenylalanine. In some cases, these proteins are pretty labile against oxidation (*119*), UV light (*127*), or heat, but not all. (*15*)

The fluorescence of bacteria has been proven, and as described above, fluorescence can be found in all bacteria. Fungi form a second large group of germs. Yeast also belongs to this group. In order to test whether these also show a similar behaviour to *E. coli*, baker's yeast is measured at a concentration of 10^6 and then treated with 1 mg/l chlorine dioxide. This led to

the same result as with the *E. coli*, with the exception that the fluorescence was higher by a factor of 10, which is due to the size of the yeast. After adding chlorine dioxide, this signal disappeared, which leads to the conclusion that it also works with fungi.

Living cells exhibit fluorescence, which correlates with cell count. This raises the question of how much chlorine dioxide is needed to kill bacteria. For this reason, different amounts of chlorine dioxide are added, and fluorescence measurements are taken before and after treatment. Plate counting is conducted using suspensions treated in the same manner as described above, with a known optical density. Each suspension is divided into several volumetric flasks, to which pure chlorine dioxide is added. The solutions are stored in the refrigerator for one hour before being plated. Several dilution steps are performed on each sample, with all measurements conducted in triplicate. After a cultivation period of 48 hours at 37°C, colonies are counted, and only plates with colony counts ranging from 0 to 300 are included in the analysis.

When chlorine dioxide solutions are applied, both fluorescence levels and bacterial counts decrease. This indicates that bacteria eradicated by chlorine dioxide exhibit reduced fluorescence. As previously demonstrated with the peptides, the relationship is not linear from start to finish. However, the results highlight that achieving zero fluorescence to eliminate all bacteria is not essential. Rather, what matters is the extent of change in the fluorescence signal. Therefore, it is crucial to consider the initial fluorescence value and its level following treatment. In the accompanying image, measurements of various bacteria-containing solutions reveal a similar degradation pattern for every concentration. This is a similar degradation as seen in the peptides (Figure 29). The bacterial count was determined for each data point. It could be shown that a linearity similar to the experiments with peptides exists. The fluorescence does not have to go to zero to kill all bacteria. The results are as expected from the previous results.

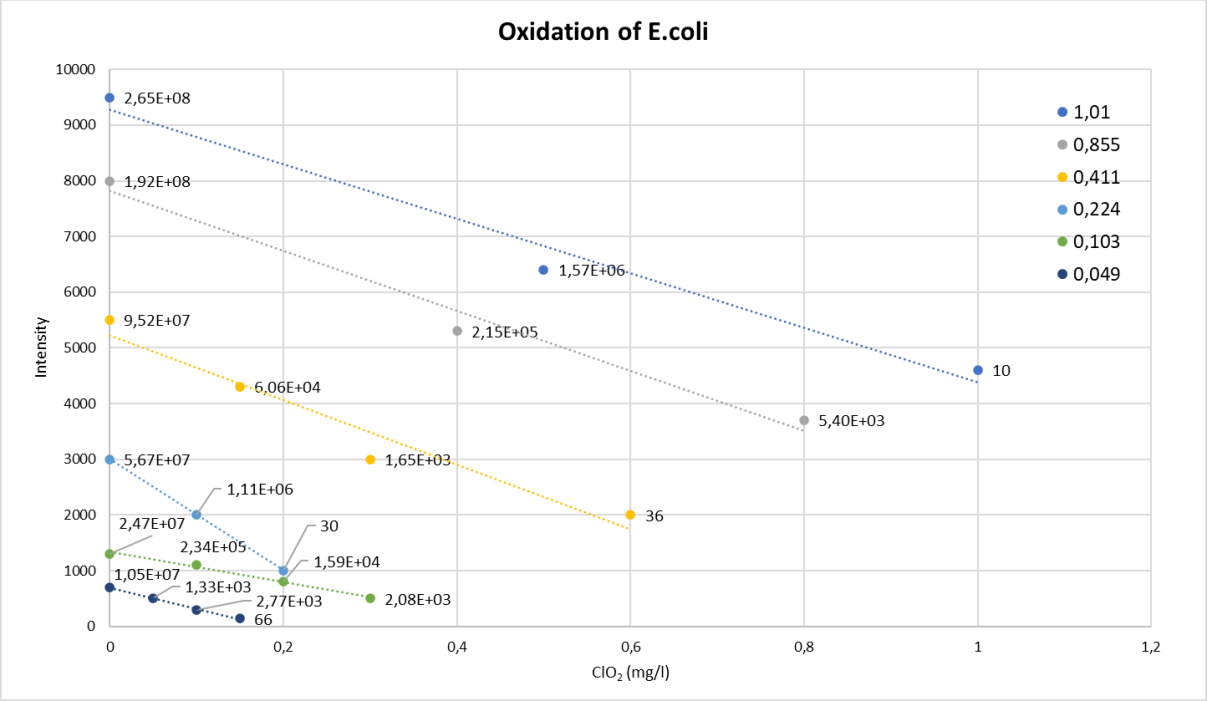

Figure 29: The measurement of the relation between chlorine dioxide hygienization and fluorescence.

It is essential to recognize the true challenges posed by the environment being studied. A few living cells among several million dead cells, all of which can potentially consume chlorine dioxide, represent a difficult situation for hygienization. These can severely impair sanitisation. Cell aggregation may prevent chlorine dioxide from reaching the inner bacteria. Additionally, bacterial regrowth after chlorine dioxide treatment is another contributing factor. Alternative methods like flow cytometry are necessary for a more precise measurement.

The analysis suggests that understanding the fluorescence levels before and after chlorine dioxide treatment makes it possible to estimate the presence of non-oxidised bacteria. It is important to note that fluorescence alone cannot determine the presence of living organisms. To confirm this, two *E. coli* samples were prepared. The first sample was stored in a cool environment, while the second sample was heated to 70 degrees Celsius for 4 hours. After this duration, fluorescence spectra were recorded from both samples. The results showed minimal differences between them, except that the heat-treated sample exhibited a peak shift of approximately 5 nm. For instance, bacteria killed through heat or similar methods can emit light. Conversely, dead bacteria with fluorescent amino acids in their membranes will react to chlorine dioxide, as will bacteria with damaged membranes. Therefore, simply observing the two points of action when chlorine dioxide is added is insufficient for determining bacterial

growth. To address this, a flow cell capable of continuous measurement over time must track and identify bacterial growth and oxidation.

To be able to assess the meaningfulness of the results, it is helpful to break them down. How much is a fluorescence unit and where is the limit of detection? Do the quantities of chlorine dioxide make any sense at all? According to the data available (Table 6), a fluorescence level of 1 corresponds to an approximate bacterial count of $5 * 10^5$ CFU/ml. This relatively high bacterial count suggests that a more sensitive detection method is needed to identify even lower contaminations. Consequently, the framework of the fluorescence measurement will be optimised in future efforts.

Table 6: Calculation of fluorescence for one bacterium

Fluorescence	CFU/ml	Fluo./KBE	Mittel w.
700	$1{,}05 * 10^7$	$6{,}70 * 10^5$	
1300	$2{,}47 * 10^7$	$5{,}25 * 10^5$	
3000	$5{,}67 * 10^7$	$5{,}29 * 10^5$	
4000	$9{,}52 * 10^7$	$4{,}20 * 10^5$	
8000	$1{,}92 * 10^8$	$4{,}18 * 10^5$	
9500	$2{,}65 * 10^8$	$3{,}59 * 10^5$	$4{,}9 * 10^5$

With the collected data and the literature, it is also possible to estimate the approximate amount of chlorine dioxide required per bacterium. It is evident that while the order of magnitude in the measurements remains consistent, the fluorescence per cell varies as the number of cells increases. This discrepancy can be attributed to the high concentration of microorganisms that lead to the absorption and scattering of light, ultimately decreasing the fluorescence yield in relation to the number of cells present.

The microbiological test shows that 0,2 mg/l is enough to set the CFU/l from $6 * 10^7$ to almost zero. The shape of bacteria is well known, as is the structure of the cell wall. From this point, it is possible to calculate that there are $9 * 10^{16}$ chlorine dioxide molecules for $3 * 10^9$ bacteria. This means there are $3 * 10^7$ molecules for one bacterium. One bacteria of the size r= 0,5 µm and l= 2 µm have an area of 9,4 μm^2, so there are 3 molecules per nm^2. Then, the membrane has a thickness of 200 nm, so there are $1{,}88 * 10^9\ nm^3$. So, this means there is not even one molecule for one cubic nanometre. One bacterial cell membrane contains about $7 * 10^5$

lipoproteins and $2 * 10^5$ Porins and OmpA. [10] So if all chlorine dioxide reacts with all the proteins on the wall, one protein reacts with 30 chlorine dioxide molecules. This is not much because one protein needs more than one chlorine dioxide. Therefore, the critical point is that chlorine dioxide will react with the proteins in the membrane, and the bacteria will die. It is not necessary to diffuse through the membrane to kill the bacteria.

Then, of course, the question is what happens if bacteria continue to grow and are then killed off again. This creates a cycle where new ones are created, they are killed off, and then new ones appear and so on. This was simulated by adding 1 ml of bacterial suspension to PBS and adding chlorine dioxide. The amount was adjusted so that a minimal residual fluorescence remained. This was repeated 10 times. A 3D fluorescence spectrum of this situation is shown below (Figure 30).

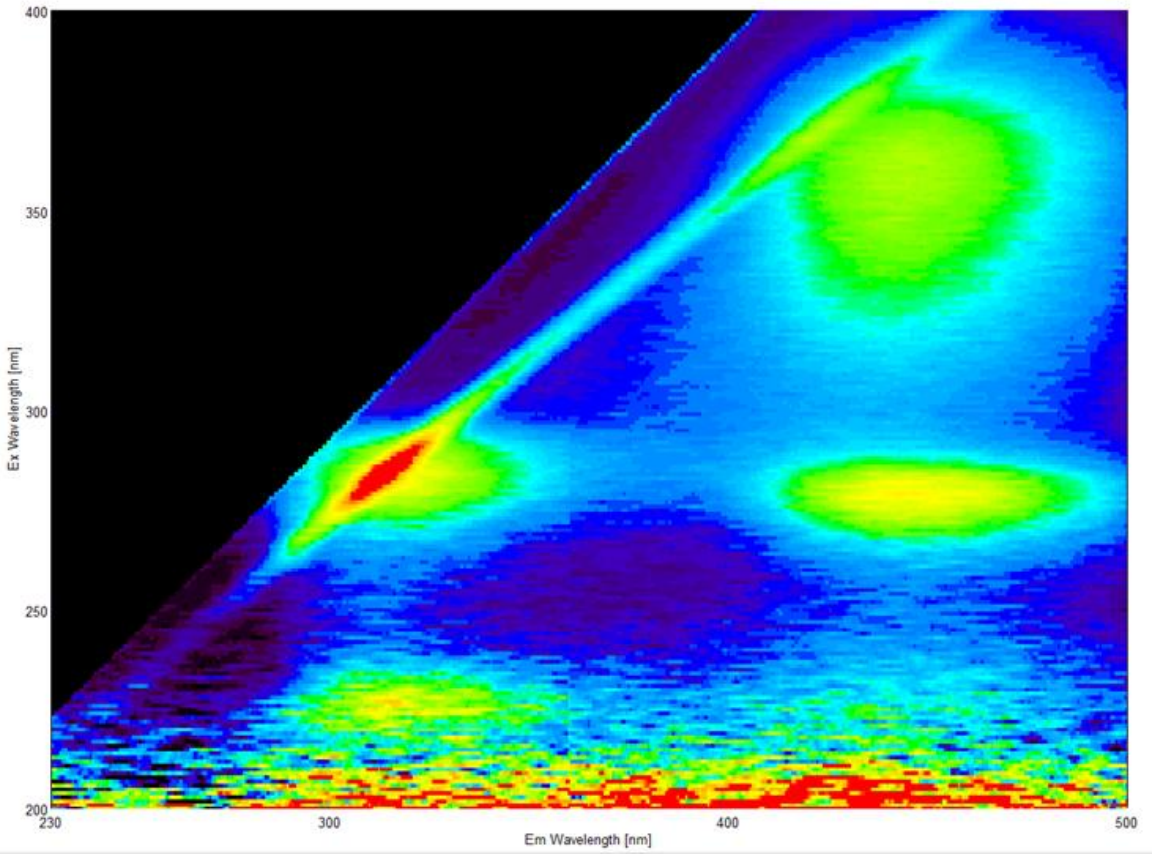

Figure 30: A probe of a longtime experiment showing that with time, other peaks become visible that are not identified.

The fluorescence spectra with a high bacteria load show how effectively chlorine dioxide destroys the proteinogenic fluorescence. Another effect can also be seen. After four hours, the spectra show another peak in the region of 550 nm. This peak could be a result of the oxidation

with chlorine dioxide. If chlorine dioxide destroys the membrane proteins, they cannot handle the osmotic pressure, leading to cytosol compounds leaking. However, it could also be that the cell count is so high that other substances that were previously below the detection limit become visible.

4.4 Fluorescence Detector and Characterisation

As shown above, the principle works. An existing flow fluorescence spectrometer is used for the first measurements. If this setup is functional over a longer period, the setup can be optimised. A control loop is crucial for addressing microbiology issues and the overuse of biocides, necessitating a reliable online sensor system for accurate microbial load and dosage data. This enables precise biocide administration to maintain low microbial levels safely. For fluorescence sensor development, an existing HPLC fluorescence detector was used to explore the measurement principle. This method allows for time-resolved measurements at a single wavelength (Figure 31).

Figure 31: First measurement setup with an HPLC fluorescence detector F-1080.

Since it is not necessary to observe a broad spectrum for the measurements, a simple fluorescence detector was constructed that measures only 10 nm area of the emission spectra

(Figure 46). First, a solution of tryptophan was measured. This already shows a strong fluorescence in the range of 0,5 mg/l. Bacteria could also be measured in this way. When measuring the bacteria, however, a high level of noise and outliers can be observed. This behaviour could be due to the scattering. For this purpose, $CaCO_3$ was dispersed and measured. This also shows strong disturbances. Subsequently, octanol was emulsified in water and measured. Both substances do not actually fluoresce but show signals in the measurements. This can be attributed to the dispersion. A bandpass filter was used to prevent the scattering of the incident light. The key point to emphasize here is the importance of minimising interference from scattering light. This phenomenon arises from a measurement error, as the detector is unable to differentiate between scattered light and fluorescence. To enhance our ability to distinguish between these two types of light, a bandpass filter (320 - 340 nm, OD 4) is installed. Further details on this will be discussed later in the prototype section.

Further measurements of *E. coli* indicate that readings can be obtained through the bandpass filter. To conduct these measurements, a flask was filled with phosphate-buffered saline (PBS) and 1 ml of bacterial suspension was added, resulting in a consistent increase in signal intensity. The introduction of chlorine dioxide resulted in a decrease in intensity, demonstrating that the setup can effectively measure bacteria and chlorine dioxide reduces the signal. Measurements with deionized water have also been carried out that show that the system shows only minimal fluctuations over several days. The next question is whether the system remains stable over the long term and is capable of measuring bacterial growth.

4.4.1Long-Time Experiment with F-1080

Long-term measurement is now of fundamental importance in recognising potential difficulties early and incorporating them into the development process. In this way, possible problems can be counteracted in later work. Using the HPLC detector discussed, measurements can now be conducted on actively growing microorganisms. These should exhibit an increase in fluorescence during growth and a decrease in intensity during dosing.

In this experiment, the focus is on observing the behaviour of bacteria over a 3-week period. An HPLC fluorescence detector, the Hitachi F-1080, was used along with an Arduino to read the analogue data. The bandpass filter mentioned earlier was also utilised along with a 70-litre tank equipped with a stirrer and a pump for circulating the liquid medium. The tank was filled

with 70 litres of deionised water and prepared with PBS, glucose, uracil, and ammonium chloride. *E. coli* OP50-1 was then added to the solution. Additionally, a flask of chlorine dioxide was connected to the tank via a pump. The chlorine dioxide is contained in a glass bottle wrapped in aluminium foil on the water tank (Figure 32).

Based on the fluorescence, the bacterial count should be in the range of 10^6 CFU/ml at a fluorescence of 50, which would require a concentration of 0,1 mg/l chlorine dioxide to kill all germs. Since mixing will take a certain amount of time, the concentration must be adjusted. This can be achieved by regulation. A fluorescence maximum is specified at which a dosage is carried out. After dosing, the concentration must fall below a defined count. This is followed by a rest phase or growth phase.

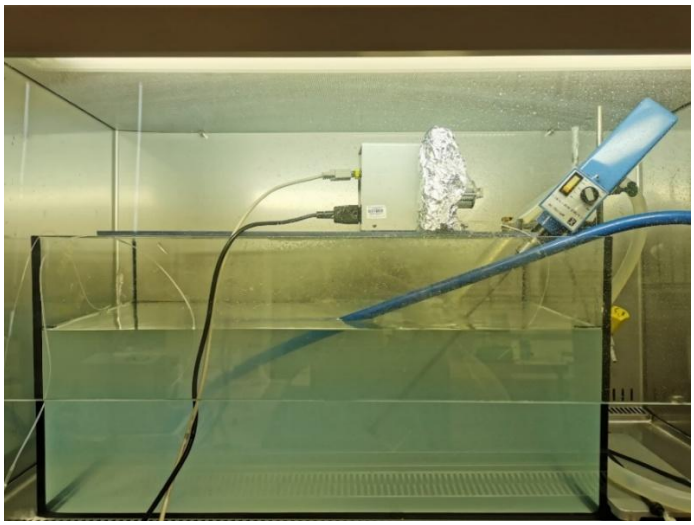

Figure 32: The 70 L aquarium with E. coli after three weeks. On top is chlorine dioxide wrapped in aluminium foil, a stirrer, and the pump.

Upon adding 0,1 mg/l chlorine dioxide, a rapid decline in the signal occurred, which is in line with previous findings (Figure 33). Under the specified conditions, the bacteria successfully adapted to the new environment.

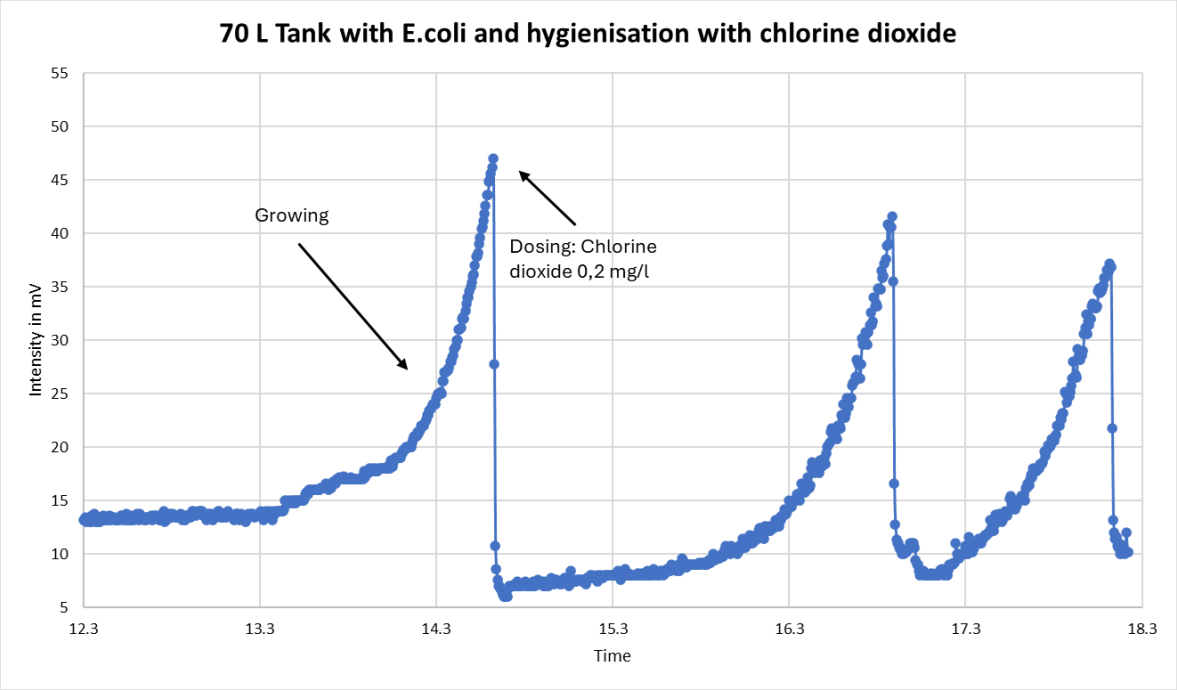

Figure 33: A small excerpt of a three-week period of growing and hygienization with chlorine dioxide.

Their growth was slow during this period, and they generated more cells emitting distinct fluorescent light, irrespective of their viability. The reaction of chlorine dioxide with the bacteria occurred rapidly, accounting for the sharp decline. Subsequently, exponential growth was observed during the initial week, which was halted by adding 0,2 mg/l chlorine dioxide. Following this, the bacteria rebounded and resumed exponential growth. The robust growth phase during the initial week was succeeded by a slower growth phase. The cause of this slow growth phase remains unclear. Several factors may be responsible: disinfection byproducts inhibiting growth, increasing chlorite and chlorate concentrations, hindered growth due to oxidised quorum sensing molecules, or the involvement of other species. Alternatively, it may be linked to a bacterial mechanism resulting in the formation of surfactin. Surfactin is a potent surfactant, which could account for the slight foaming observed after the experiment. Additionally, surfactin is recognised for its ability to inhibit bacterial growth, suggesting its potential as a biocide. Nonetheless, more detailed analyses are necessary to confirm the presence of surfactin. (*14*)(*128*) It may be due to food availability or other underlying mechanisms. To make a conclusive assessment, it is essential to analyse inorganic products like chlorite and chlorate to understand their impact. Additionally, it is important to analyse organic molecules, including quorum-sensing peptides. Comprehensive methods such as flow cytometry and MALDI TOF should be employed to identify living organisms. Notably, even at high chlorine dioxide concentrations (60 mg/l), fluorescence does not decrease to zero by

the end of the period. When minimum intensity is reached, there is a noticeable upsurge in intensity, possibly indicating cell regeneration, rapid growth, or a defensive response that involves storing more tryptophan in the cell wall or leakage of intracellular peptides.

In the experiment, the method works with tap water, which is the case in cooling towers, for example. For MWF, the fluid is an emulsion with high optical density and several compounds that might disturb the measurement. The data suggests a correlation between bacteria and fluorescence and a decrease in bacterial count with a specific amount of chlorine dioxide, which also correlates with fluorescence. Additionally, it is possible to construct a detector using readily available commercial materials. However, it is essential to evaluate how this system performs under real-world conditions where water might be stored for extended periods, leading to changes in various factors, including an increase in the number of dead cells over time.

4.5 Fluorescent Sensor Development

Previous investigations have demonstrated that a microbial sensor needs to irradiate at specific wavelengths (280 nm) and measure at a particular wavelength (350 nm). For this purpose, UV LEDs with a narrow emission bandwidth are suitable as the light source. Additionally, a quartz measuring cell must be used to avoid UV absorption. A bandpass filter is essential to block stray light, and a photodiode can be utilized as the detector. The collected knowledge is now used to develop a sensor. This should be small and robust, work without moving parts, and be reliable. First, the commercial fluorescence spectrometers have the option of varying the wavelength with a monochromator. This is not necessary for our application. An optical filter can be used well here. Secondly, a fixed wavelength radiation source is required. LEDs are well suited for this purpose.

This allows the sensor to be made more robust and simpler. The detector unit has an LED light source, a quartz tube, an optical filter, and a photodiode module. The schematic build-up of the measurement is shown below (Figure 46), and the working principle is shown in Figure 34. The housing drawings of the measurement set-up used are in the Appendix and milled from aluminium (9.6 Detailed Pictures of the Sensor). It is important to note that the housing has been manufactured to be completely light-tight. It has also been coloured completely black on

the inside to absorb stray light. Holders were used to minimise the distance between the LED and the cuvette as well as between the cuvette and the photodiode and to keep it at a 90-degree angle.

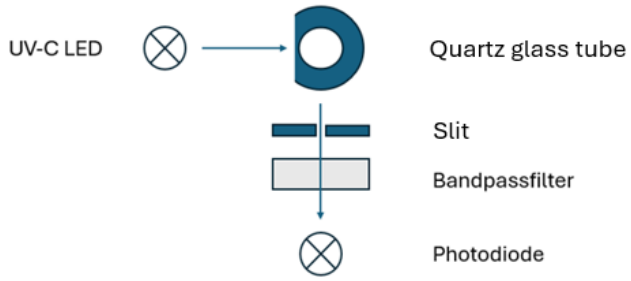

Figure 34: Top view of the fluorescence measurement setup.

The LED utilises a Nichia light source (NCSU434) that emits UV-C light. The source consists of a light-emitting crystal fixed in a ceramic field with a sapphire (Al_2O_3) cover and gold electrodes for the power supply (Figure 35).

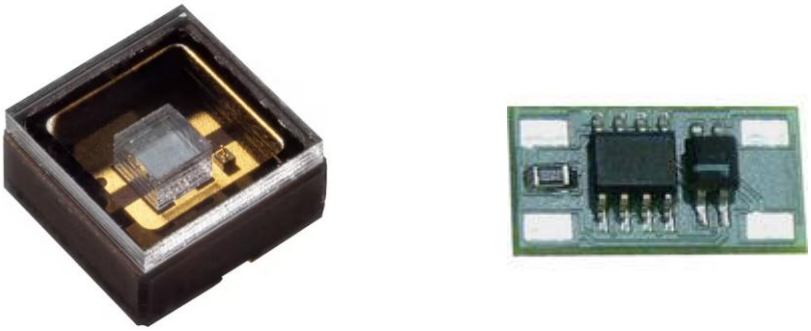

Figure 35: NSCU434 UV LED from Nichia with maximum intensity at 280 nm and a constant current supply MKSQ-50mA.

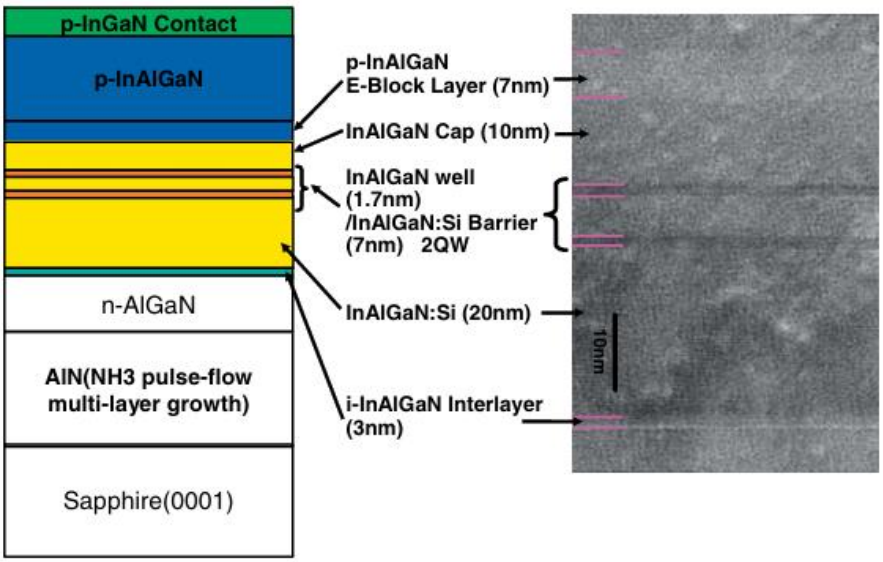

Figure 36: The schematic buildup of an InAlGaN crystal used in UVC LEDs and a TEM image from the crystal showing different layers of the structure. (129)

The LED power supply consists of a laboratory power supply unit with 13,5 V connected to a constant current (MKSQ-50mA). A 1K Ohm metal-chip resistor is used as the series resistor for the LED (Figure 37).

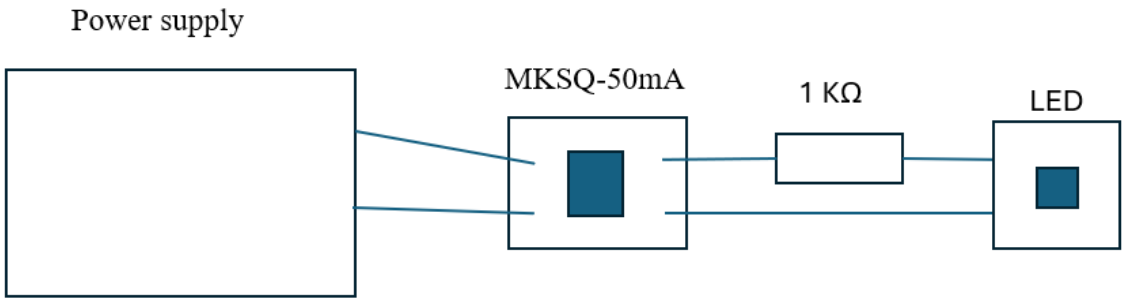

Figure 37: Schematic representation of the supply of the light source by a laboratory power supply unit, constant current source, series resistor, and LED.

There is also a protective device in the SMD LED device. The emission spectra are depicted below, with the emission peak at 280 nm. However, there is also emission extending from 260 nm to 310 nm. Due to the LED emitting light at a very high intensity and the photodiode measuring radiation in the 280 nm range, scattered light poses a significant challenge. The LED emits also slightly bluish light caused by emissions in the visible range. During this process, the LED emits light with a lower intensity at 560 nm and 840 nm (Figure 38). This leads to a

massive problem because the fluorescence is superposed. The detector cannot distinguish between the light from the light source and the fluorescence.

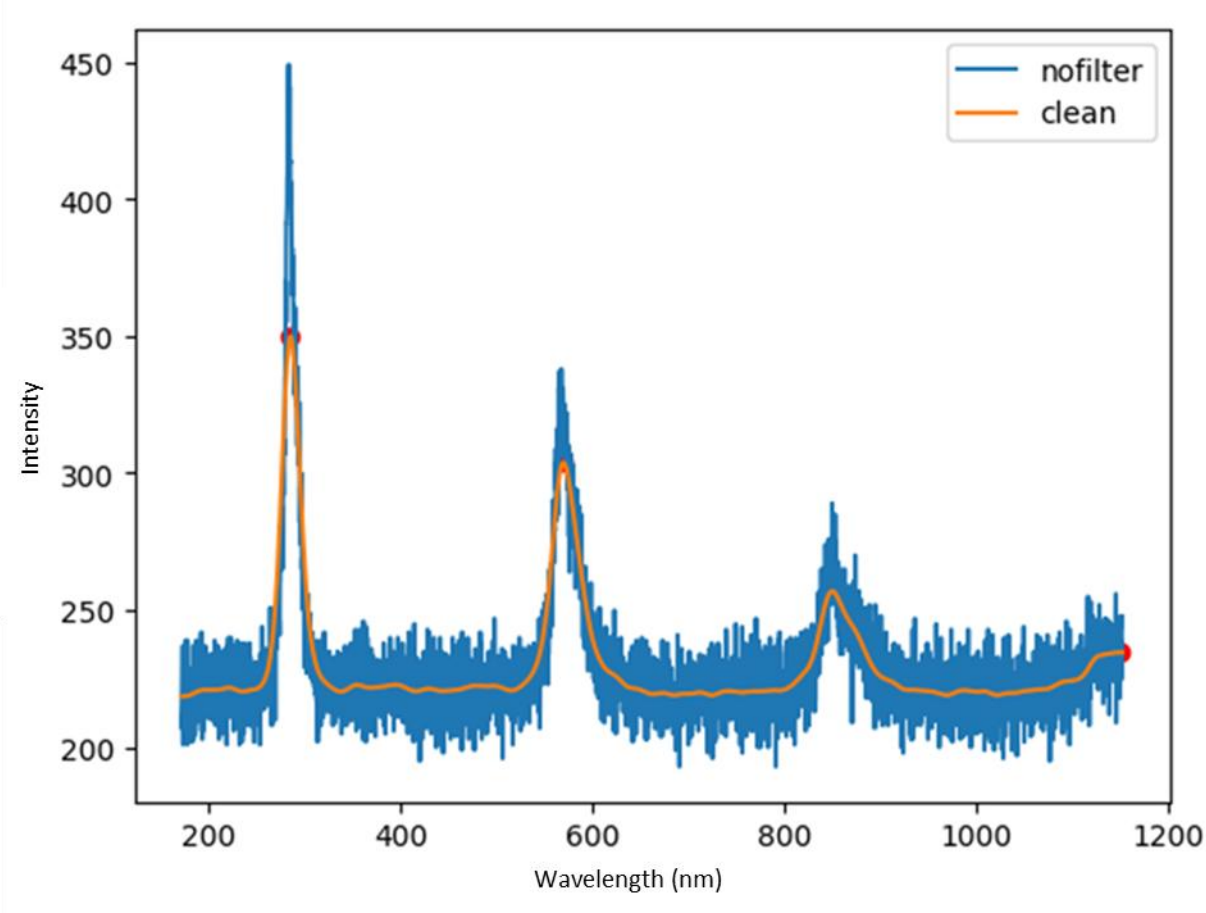

Figure 38: Full spectra of Nichia 280 nm (62 mW) LED showing light emission at 280, 560 and 940 nm.

As a result, the light leads to a high background load and the increasing absorption due to the rising microbial load leads to a reduction in intensity. To prevent this, a filter must absorb everything below 310 nm and above 520 nm. The fluorescence intensity depends mainly on the intensity of the light source, which is given here as light source intensity in mW. This relationship is dealt with in the theory in Chapter 3.2. In addition, three LEDs with an output of 10 mW, 62 mW and 110 mV were analysed. It was shown that the more intense the radiation source, the more intense the fluorescence signal. Not only is the intensity necessary, but the noise is also essential. A good measurement cannot be guaranteed if only the signal is high, but a high noise level disturbs the measurement. The detection limits achieved can be found in the table below (Table 7).

Table 7: The results for three different light sources at their optimum conditions with the detection limit of tryptophan.

Light source intensity	Limit of Detection
10 mW	20 µg/l Trp
62 mW	1,5 µg/l Trp
110 mW	1,2 µg/l Trp

Therefore, the detection limit for the respective LEDs is tested. This means that the most intense light source is chosen as it produces the best detection limit. The characterisation of the LEDs was carried out in the same way for all of them, although it should be mentioned that the 62 mW and 110 mW LEDs were identical and that the ten mW LED had a lens that reduced the beam angle from 120° to 30°. However, the effect of the smaller beam angle is minimal compared to the intensity. This is probably because the light source is directly at the measuring cell and most of the radiation enters the cell.

The characterisation is carried out using the most intense LED as an example. The system's long-term stability was assessed, providing practical insights into its future performance. Observations indicate that cold appliances undergo a gradual heating process following an initial phase of approximately ten hours. Initially (A), the system lacks a stable temperature, which is evident in the signal. Subsequently, the signal stabilizes, leaving behind only noise, steps, and drift. In phase B, the LED operates steadily with only minor fluctuations. These fluctuations arise from both the photodiode and the LED. After this phase, a slight drift is evident (C), indicating minor fluctuations in the devices (Figure 39).

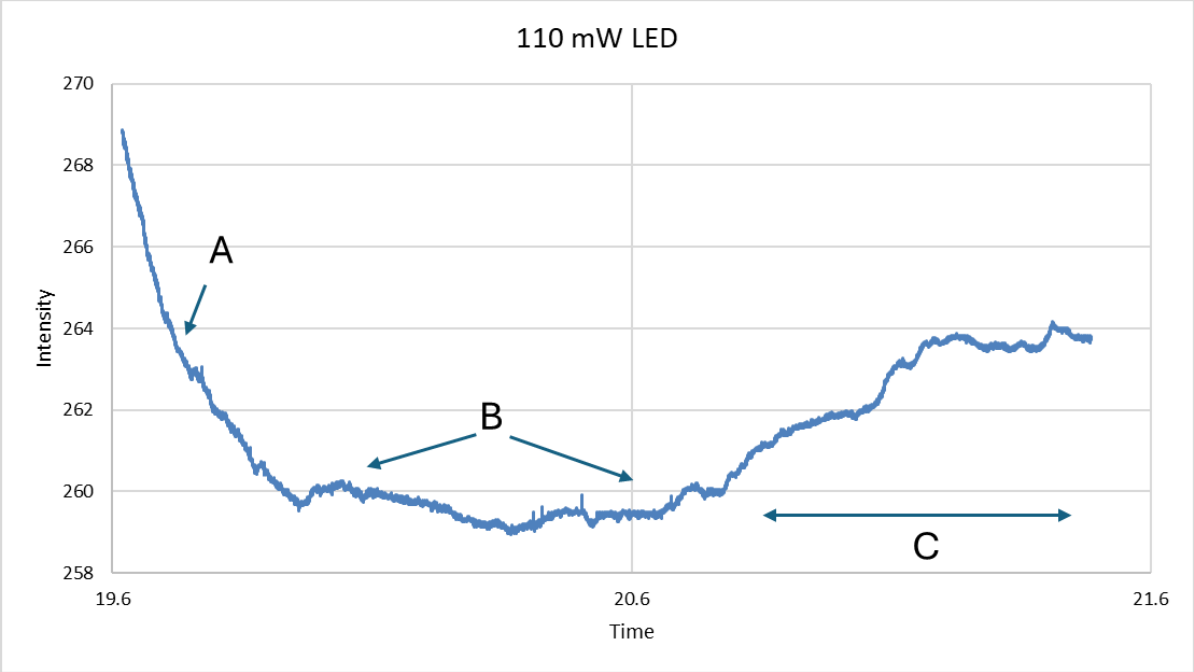

Figure 39: A long-time experiment with water to show the performance of the LED.

Changes in signal intensity that are not attributed to microbial growth can disrupt the accurate determination of the total microbial load. An increase in overall signal intensity might be mistakenly interpreted as microbial growth. Similarly, sudden fluctuations in intensity can also lead to errors in measurements. These issues can be addressed later—primarily through software designed to monitor microbial growth, as well as by adjusting the dosage. A dosage of chlorine dioxide, for instance, should typically result in a change in signal intensity. However, in this scenario, such a change might not occur, allowing the software to effectively identify the presence of technical issues. This capability helps resolve the issue of minor fluctuations in the signal. Furthermore, the solution may lack complete chemical stability; for example, light-absorbing substances may degrade over time, leading to a decrease in intensity. Additionally, impurities could enter the water and unexpectedly enhance the signal. As a result, the detector would continuously adapt to the changing background conditions, thereby minimizing measurement errors.

The noise significantly influences the limit of detection. The smaller the noise can be kept, the more accurate the measurement can be. However, the noise level is approximately 0,06 units due to small fluctuations in the current. Due to the design, the current is not completely constant and is subject to interference. However, these are tolerable at this point as all parameters are then optimised later using the values. Notably, rapid fluctuations in intensity are also noticed. For a more accurate measurement, those fluctuations need attention. The LED circuit regulates the current and the voltage accuracy has a direct influence on the signal. A constant current is

therefore necessary in the finished prototype. For this purpose, the current power supply is adjusted between 3 and 52 mA. The optimum resistance can be determined by changing the resistance.

Table 8: Measurement of signal intensity at different conditions with a 110 mW LED to find the optimal parameters.

Water (intensity)	Trp 1100 µg/l) (intensity)	Fluorescence (intensity)	Current (mA)	Resistance (Ω)	LD (µg/l)
50,44 ± 0,02	104,07 ± 0,02	53,63 ± 0,02	3,45	2000	1,25
87,36 ± 0,02	192,80 ± 0,06	105,45 ± 0,04	6,75	1000	1,19
187,83 ± 0,04	439,16 ± 0,25	251,33 ± 0,14	15,19	400	1,87
322,95 ± 0,23	767,22 ± 0,94	444,27 ± 0,59	28,11	207	4,36
541,96 ± 3,69	1294,56 ± 0,66	752,60 ± 2,17	49,08	103	9,54
604,13 ± 0,17	1445,94 ± 5,13	841,81± 2,65	52,46	40	10,38

An adjustable resistor is used to find the optimum current. A constant resistor is used for further experiments to avoid changing the current. It can be assumed that this lowers the noise and thus improves the detection limit. It can be seen that a detection limit of less than 2 µg/l tryptophan is achieved at a current of less than 15 mA. A strong change in the fluorescence intensity can be observed in the results, which behave linearly. When the current increases to approximately 30 mA, a change in linearity occurs. It can also be observed that the noise increases sharply from 30 mA, as the LED protecting device (z-diode) has to intervene more strongly. This leads to the conclusion that 15 mA is a suitable current for further experiments. This is characterised by a high-intensity yield and a low signal-to-noise ratio. Shortening connections between the components and better heat dissipation are applied to extract the full potential. In the further course, a constant resistor is attached to the housing with thermally conductive adhesive. This leads to a reduction in noise and thus to a better detection limit of 0,8 µg/l. These adjustments would have had no effect with the low current, as the noise was hardly present anyway. The fluctuation is so high at the high currents that no improvement could be achieved here.

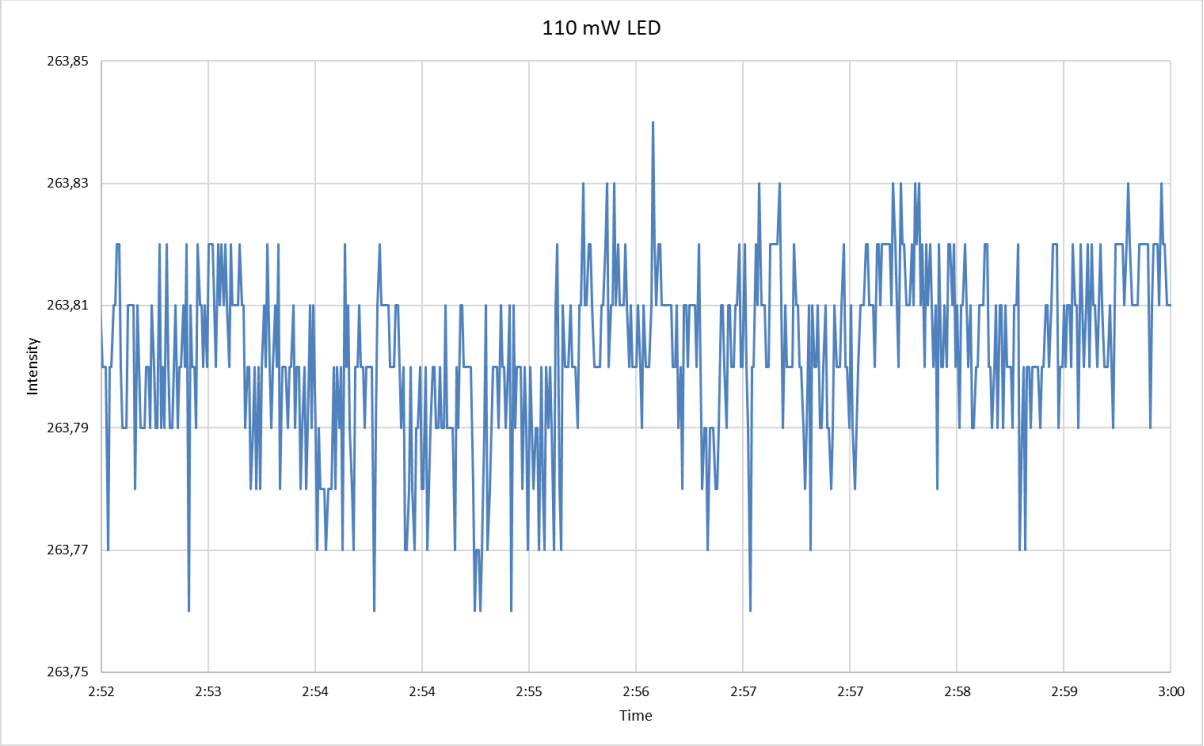

Figure 40: Noise level.

The next important element of the structure is the measuring cell. Absorption in the UV range must be avoided here, and scattering to the detector should also be kept to a minimum. Five different pipes were examined to optimise the flow cell. The pipes had inner diameters of 3, 4, 5, 6, and 7 mm and a wall thickness of 1 mm. Additionally, a 10 mm cuvette was tested. It is worth noting that the formula for fluorescence indicates that the layer thickness also influences it. Essentially, the thicker the layer, the more molecules are present that can potentially be excited.

It is crucial to note that scattering significantly impacts fluorescence yield. The LED emits at an angle of 120 degrees, which is further directed to the side by the rounding of the tube, contributing significantly to background noise. Understanding scattering's influence can help us better navigate its challenges in our work (Figure 41).

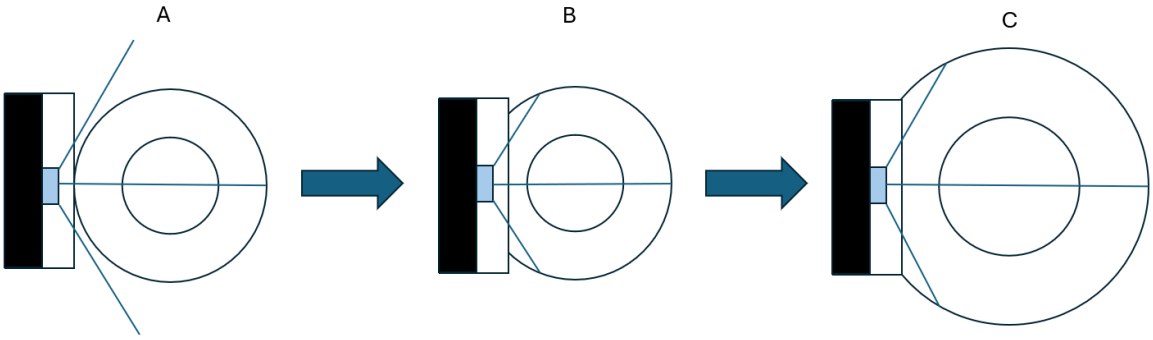

Figure 41: (A) The first setup with a round tube led to high background noise because of the high angle of the light source. (B) The optimization of the tube through grinding gave better results, but the light source was bigger than that of the grinding. On the side of the light source, a little light comes through. (C) Using a bigger tube made it possible to get the optimal fitting.

The flow cell is a quartz tube with a diameter of 4 mm and a wall of 1 mm that is cut to a length of 50 mm and ground straight on one side. Light passes through the tube and is absorbed by the liquid, causing fluorescent emission in every direction.

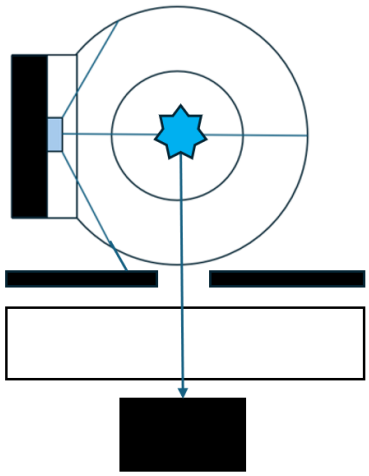

Figure 42: The flow cell improves the measurement enormously, but a lot of light gets into the detector that does not come from the fluorescence. The illustration shows how the light is blocked by the LED and the fluorescence is directed to the photodiode.

There is a slit that limits the emission of light to ensure it is low (Figure 42). After that, there is still light from the LED that goes to the photodiode. For this reason, a bandpass filter blocks the light of the LED. The spectra of that are shown below (Figure 43). That shows that the light from the source is almost completely blocked and cannot disturb the measurement. The

manufacturer's specifications indicate that it achieves an OD10 block at 280 nm, with lower blocking at higher wavelengths. At 560 nm, the blocking is only OD 6; at 840 nm, it is only OD 4, allowing a small amount of light to pass through the filter. While this amount is relatively small, it will certainly contribute to the background signal (Figure 44).

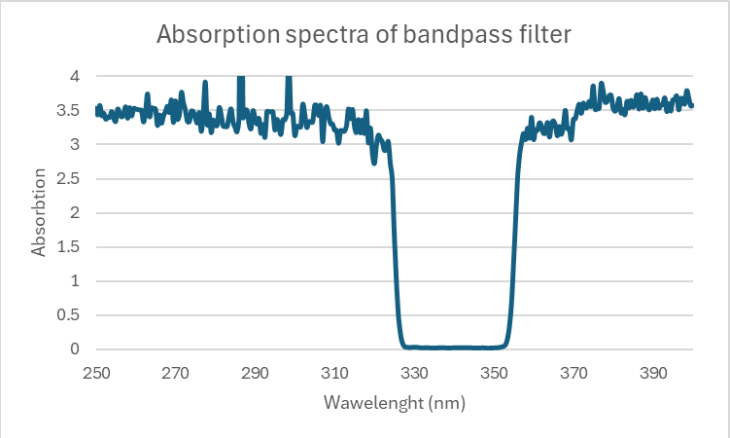

Figure 43: The measurement of the bandpass filter shows that there is a sharp cut at 328 and 352nm. The correct absorbance is at 6, but the measurement range goes only to 4. This leads to the wrong image, which shows that the blocking is only OD 3,5 instead of 6.

Figure 44: Bandpass filter spectra adapted from Edmund optics.

To minimise the impact of this light, we select the measuring direction at a 90-degree angle. This allows us to detect only the light scattered to the side. Additionally, we utilise a slit that is aligned directly with the liquid, requiring the light to pass through the medium, further weakening it. The actual blocking of the photodiode module is a photodiode module from Hamamatsu with a SiC photodiode (Figure 45). The diode's response to radiation in a specific area indicates that it also receives a signal. At 840 nm, the detector's sensitivity is approximately three times higher than at 340 nm, underscoring the significance of the filter.

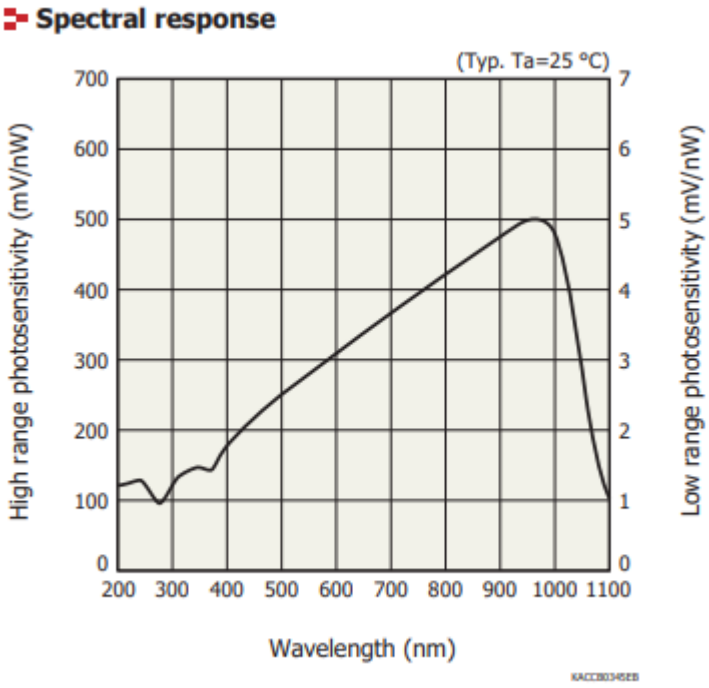

Figure 45: Sensitivity of the fluorescence detector unit.

To illustrate the minimal impact of the light source, we can conduct a straightforward thought experiment. By analysing the emissions at 280, 560, and 840 nm and applying intensities of 1, 0,5 and 0,25 while using blocking factors of 10, 6, and 4, we arrive at resultant transmission intensities of 1^{-10}, $0{,}5 * 10^{-6}$, and $0{,}25 * 10^{-4}$. This indicates that the radiation at 840 nm is the dominant factor. Moreover, when we consider the fluorescence produced by the radiation at 280 nm, which is 1 with a quantum yield of 0,13, there exists a 1000-fold contrast between the incident light and the fluorescence. Admittedly, this is a simplified representation and is still significantly affected by the angle and other factors, but it underscores the importance of the setup.

The test shows that the tube splits the light so that a part of the LED light gets to the photodiode. Even if almost all light is filtered, the diode sees it. This leads to a high background signal. To get the maximum fluorescence and the minimum of scattering light, there should be a slit that saves the photodiode from the source light. All these results are then combined in a detector to test the interaction (Figure 46).

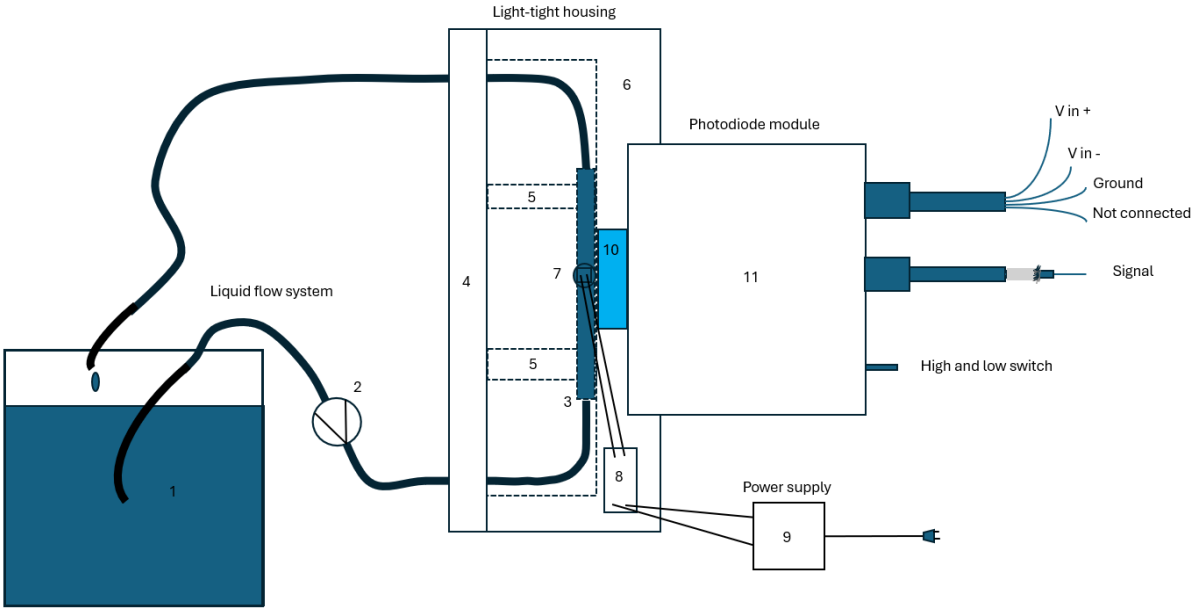

Figure 46: The set-up of the measurement showing the whole sensor: (1) water that contains bacteria; (2) a peristaltic pump; (3) a quartz glass flow cell; (4) an aluminium lid; (5) holders for the flow cell; (6) the body of the housing; (7) an LED light source 280 nm; (8) a constant current source; (9) a power supply of the LED; (10) an optical bandpass filter with 340 nm gab; (11) a Photodiode module.

The aluminium housing is completely light-tight (4 and 6). This is ensured by seals that are used at the connection points. The complete housing is then operated in a large metal box shielding electromagnetic and light radiation. The photodiode module (11) is a weak point here as it is not entirely light-tight. The individual electronic components will be discussed later. The flow cell (3) is supplied by a peristaltic pump (2), which pumps the liquid (1) in the circuit. The signal is sent via a coaxial shielded cable to a 16-bit converter and then processed by an Arduino. The Arduino and the bit converter are located in a separate metal housing, which protects against electromagnetic radiation.

Tests with an 0,5 mm slit that moves along the photodiode window of 9 mm show that the scattered light has to be maxima at 2 mm and 5 mm position. Almost no light is visible outside

this area, and between this is the minimum of scattered light. Tests with tryptophan also show that the fluorescence maximum is between these areas. This is shown in the picture below (Figure 47).

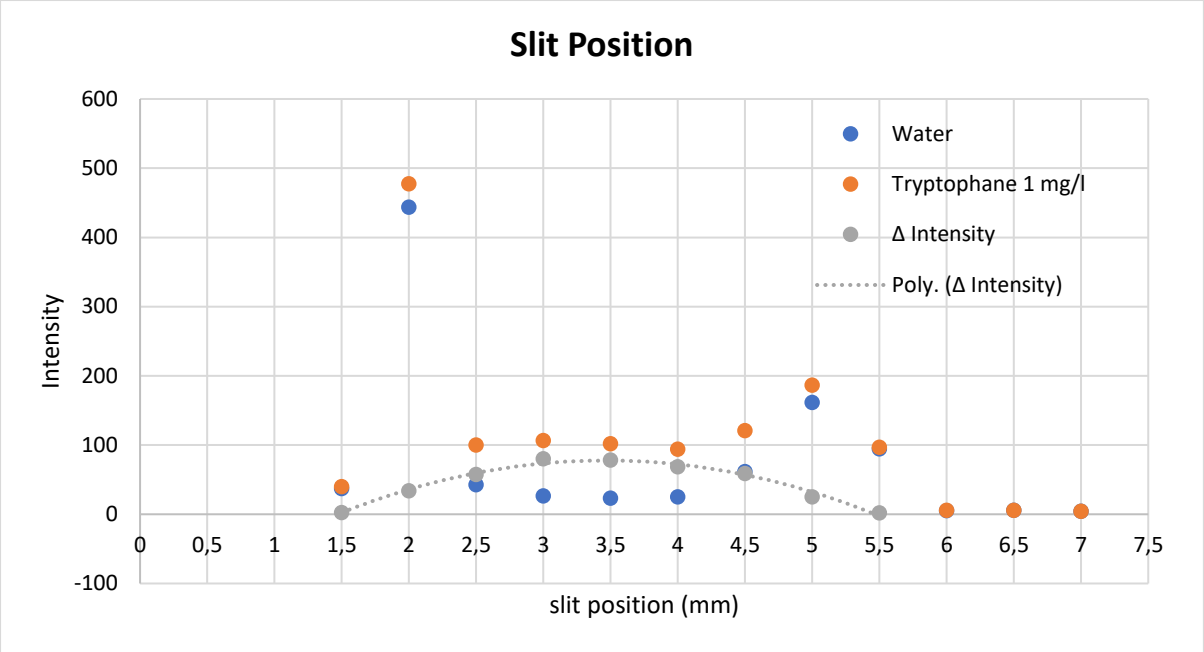

Figure 47: Results from the slit position measurement.

The second factor is the slit width, and according to the slit position test, the maximum point is at 3,5 mm, and this is always the middle. The useful area is about 4 mm, but with a width of 3 mm, almost all possible fluorescence is caught. In our experiment, the slit is 1,5 mm, which leads to low scattering and high fluorescence yield. In the pictures below can also be seen that the linear range of the slit is not the complied area (Figure 48). The linear growth ends at approximately 1 mm, but the linearity is not important for this experiment; it is only related to the background and the signal.

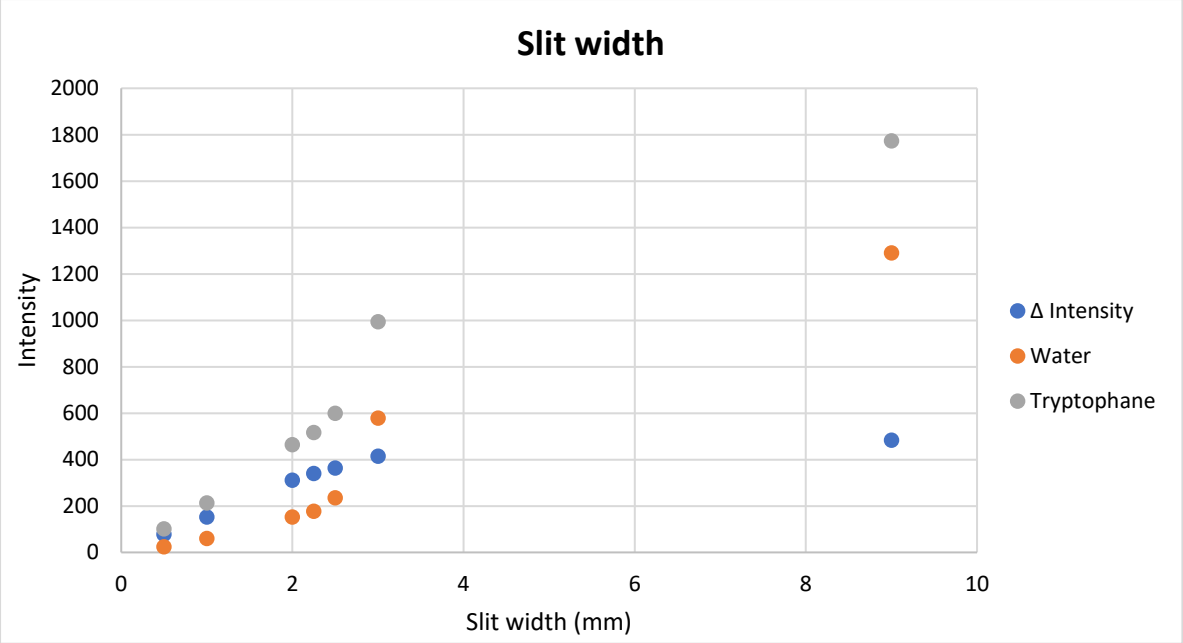

Figure 48: The slit width measurement shows that with 3 mm almost all light is collected, and the background is minimised.

By measuring pure water for several hours, a slight drift is visible. Those 40 000 measurement points are shown in the data below. It is possible to calculate a standard deviation of 0,05 and a middle intensity of 98,55 with the consequence that the detection limit is 98,70. This low noise level and sensitivity makes it possible to detect tryptophan in a low concentration of 1,35 µg/l. The data points run over two days (data is not shown here) with similar noise. Several data points now have outliers, but interestingly, all outliers are positive and not negative. The conclusion is that the points are caused by small air bubbles that influence the scattering. Some drift is also visible here, mainly from the light source, which is not completely stable (Figure 49).

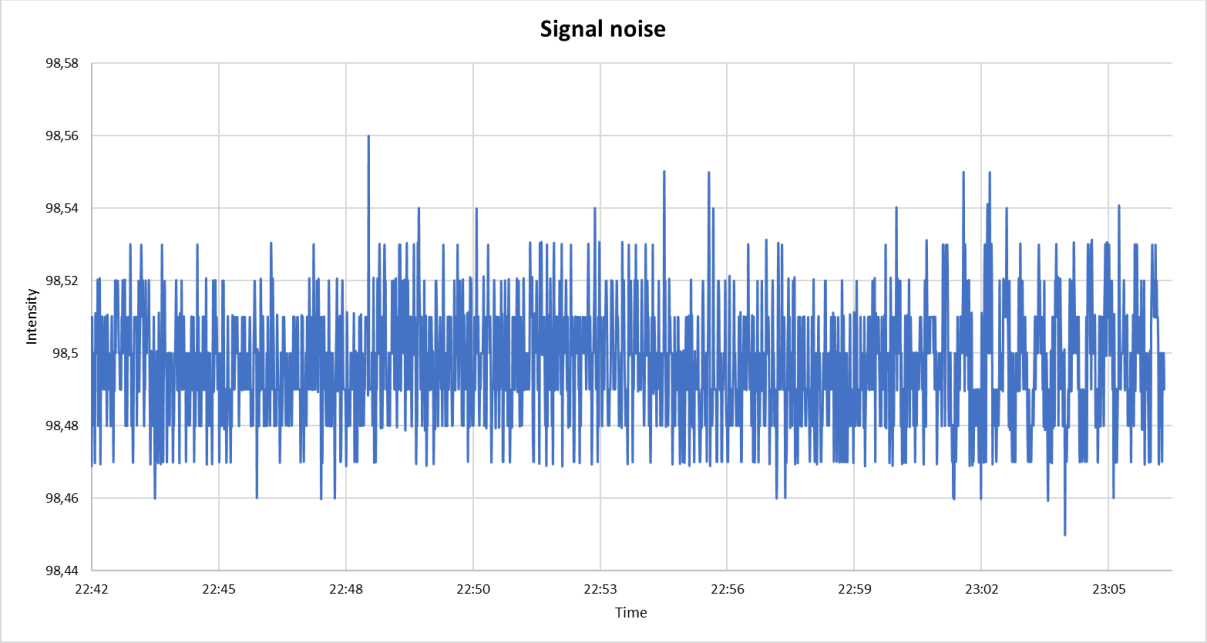

Figure 49: detector noise over several days.

Not only is the detection limit important but also the measurement range. Tryptophan is measured from 20 µg/l to 10 mg/l, but a theoretical minimum is 1,5 µg/l. Over the whole range, the intensity is linear, and no saturation occurs (Figure 50).

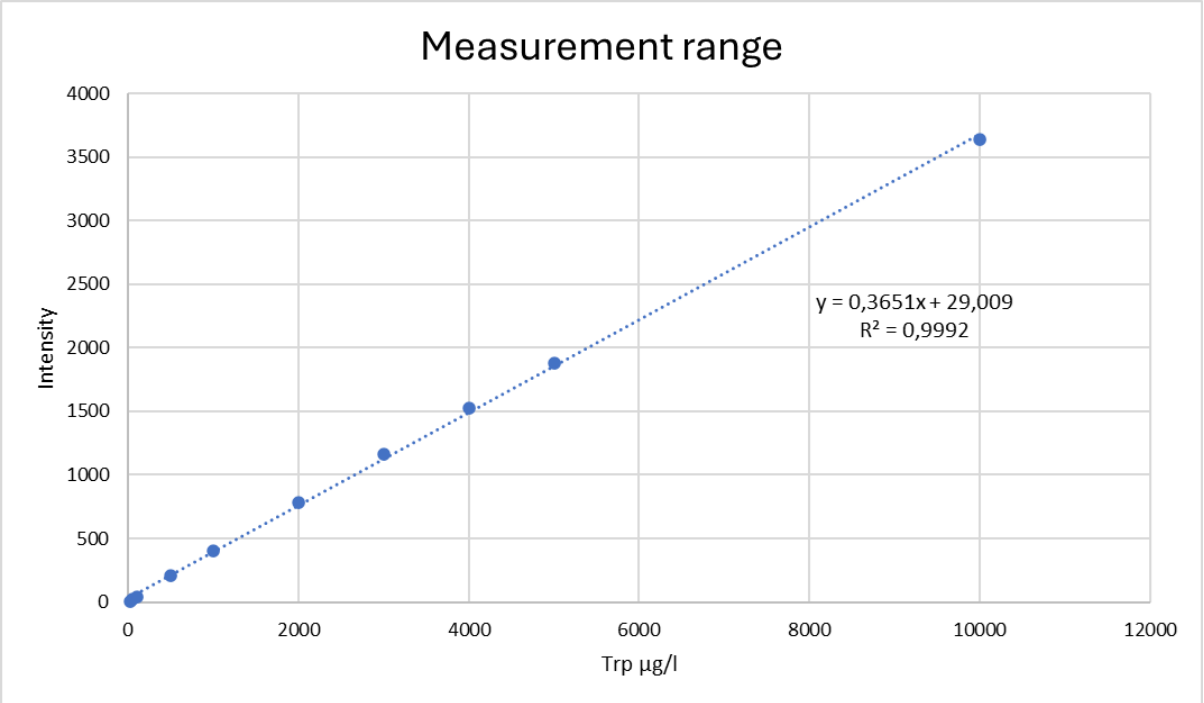

Figure 50: Tryptophan solutions were measured in a concentration range from 20 µg/l to 10 mg/l. The measured values are shown in the graph, and the grade shows a strong linear behaviour. This shows that measurements are possible over a large measuring range.

As described earlier, the measurement can be adapted for living organisms. In this case, the reproduction of bacteria should be visible as an increasing signal. When the oxidation agent chlorine dioxide is added, the signal should drop.

Regarding the photodiodes, two candidates with different current supply types will be explored and optimised in the subsequent stages of the project (Figure 51).

Figure 51: Left Hamamatsu photodiode S1227-33BQ and right Hamamatsu photodiode S16586. The form factor of the active area of the two diodes is entirely different. The active area of the one on the right is smaller, but it is more sensitive. These two models will be compared for further tests to determine a favourite for a photodiode module.

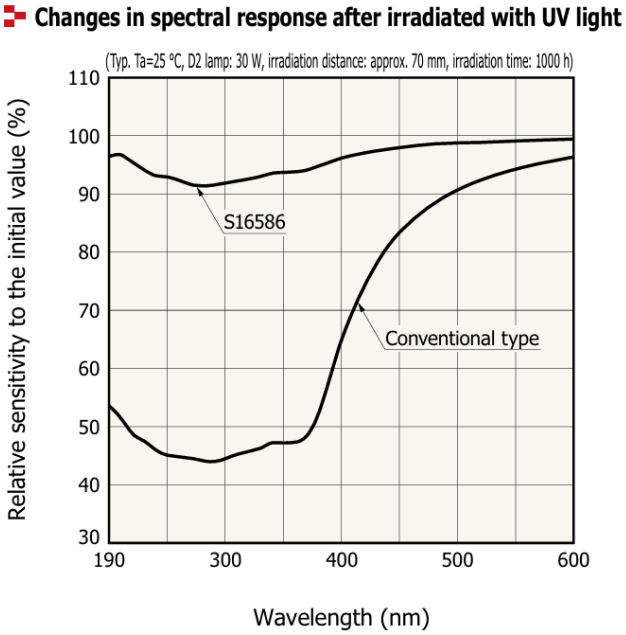

Figure 52: The relative sensitivity of S16586 to a conventional type shows that it is a good alternative to the older model S1227-33BQ.

The newer one (S16586) is significantly smaller than the older model (S1227-33BQ) but could still be better due to its better noise behaviour. Four boards are produced to test the diodes and the supply voltage. Two with a reference voltage and two with a plus/minus voltage. The boards are fitted once with the new photodiode and once with the old photodiode. Both diodes are

potentially well-suited and can both be considered. The S16586 has a smaller surface area of 0,5 mm^2 but is more sensitive, whereas the S1227-33BQ has a significantly larger surface area of 5,7 mm^2. The question is how much of the surface area can be actively used and whether the sensitivity or the surface area will be the decisive factor (Figure 52). However, only a limited percentage of the area will see the light, so it is impossible to choose the best without tests. For this purpose, two circuit boards that differ in the photodiode were designed. The measurements show that signals can be measured more intensively by a factor of 10 with the S1227-33BQ, which can be easily argued as being based on the area of the diode. The noise of the two diodes is also essential. If the noise level is low enough, the results could be better with the small diode. For this reason, the variance of the data is a good indicator. In the case of S1227-33BQ, the variance is twice as much as in the case of S16586. But this is not enough compared to the effect of the area. The best case here would be the new diode type with large areas, but this is not available, so further work is performed with S1227-33BQ.

The circuit of the photodiode is a critical point in the work. The photodiode operating in a range of pA is converted into a voltage signal via a trans-impedance amplifier and amplified by a factor of 1000. Two options were tested for the voltage supply. The plus/minus circuit and the direct current circuit. The voltage is equalised with the plus/minus supply, and a measurement against the ground then provides the final measurement signal. This setup can often be precisely adjusted and can give excellent results. With DC voltage, measurements can be made against a voltage signal (reference voltage).

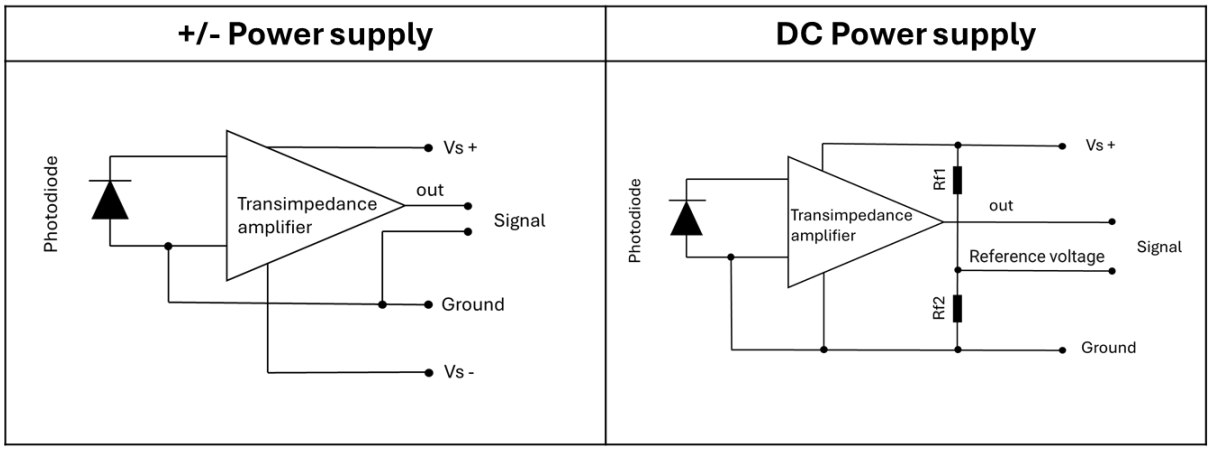

Figure 53: On the left is a circuit featuring a photodiode connected to a +/- voltage supply and a current-to-voltage converter that includes amplification. The signal is measured relative to the ground in this configuration. On the right side is a DC voltage supply paired with a current-to-voltage converter. In this setup, however, the signal is measured not against the ground but against a reference voltage.

As the two signals fluctuate equally, good results can also be achieved. The measurements with the different supply voltages show no significant difference in behaviour. They are very similar. The noise is in the range of a few µV in both cases. The F-test is used to make a valid statement here. This static method compares two groups with each other—in this case, the measuring points of the two voltage supplies. The data can then be used to determine whether these two groups differ from each other and which has a lower noise level. The requirements for the F-test are met in all cases.

Table 9: The F-test result for zero measurement without LED and water.

	ref	*Plus/minus*
Mean value	34035,0	-1592,7
Variance	63,0	49,7
Observations	2000	2000
Degrees of freedom (df)	1999	1999
Test variable (F)	1,3	
P(F<=f) one-sided	$7{,}0 * 10^{-8}$	
Critical F value for a one-sided test	1,1	

The F-test showed that the variance at the reference voltage is 27% higher. In addition, the critical value was exceeded, which means that the values are not equal with a probability of 95%, and the null hypothesis is therefore rejected. The very small P-value also shows a statistically relevant difference here. A lower detection limit can be achieved with the plus/minus voltage for the subsequent measurements.

The results for the photodiode in the cycles are shown above. Light behaviour could be different, so the LED variable is also considered. Measurements are made with deionised water and a ten mg/l Trp solution. The table below shows the results with pure water (Table 10).

Table 10: The F-test result for zero measurement with LED in Deionised water

	ref	plus/minus
Mean value	2898199	2837193
Variance	61014	46871
Observations	2000	2000
Degrees of freedom (df)	1999	1999
Test variable (F)	1,3	
P(F<=f) one-sided	$2 * 10^{-9}$	
Critical F value for a one-sided test	1,1	

In this case, the variance in the reference measurement is 30% higher. The results for water remain consistent, with the plus/minus voltage once again delivering the best outcomes. However, the variance has notably increased in both scenarios, likely owing to fluctuations in the light source as well. The next table shows the measurement of tryptophan (Table 11).

Table 11: The F-test result for measurement with LED and ten mg/l tryptophan.

	ref	plus/minus
Mean value	3091021	3038929
Variance	22911	10664
Observations	2000	2000
Degrees of freedom (df)	1999	1998
Test variable (F)	2,2	
P(F<=f) one-sided	$2{,}7 * 10^{-64}$	
Critical F value for a one-sided test	1,1	

A similar trend occurs when the ten mg/l Trp solution is passed through. The variance of the +/- voltage supply is approximately 50 % less than that of the reference voltage. The +/- voltage supply is, therefore, the favourite. This clarifies that the plus/minus voltage must deliver the best results. The measurement data show a detection limit for tryptophan of 15 µg/l for the plus/minus voltage and a detection limit of 24 µg/l for the reference voltage. One reason could be that the reference signal is subject to fluctuations that are not symmetrical with the voltage from the operational amplifier circuit. This can cause a disturbance that manifests itself as increased noise.

The manufactured circuit board (Figure 54) features a photodiode that converts light into a current signal. Because this signal is minimal and unsuitable for direct processing, a trans-impedance amplifier transforms the current into a voltage and amplifies it. However, this amplification can also boost interference signals, necessitating proper shielding measures. The resulting analogue signal is then converted to a digital format by an analogue-to-digital (AD) converter and subsequently processed by a microcontroller, which is also shielded to reduce interference. The digital signal can be translated through software into tryptophan concentration, which can then be utilised to estimate bacterial counts.

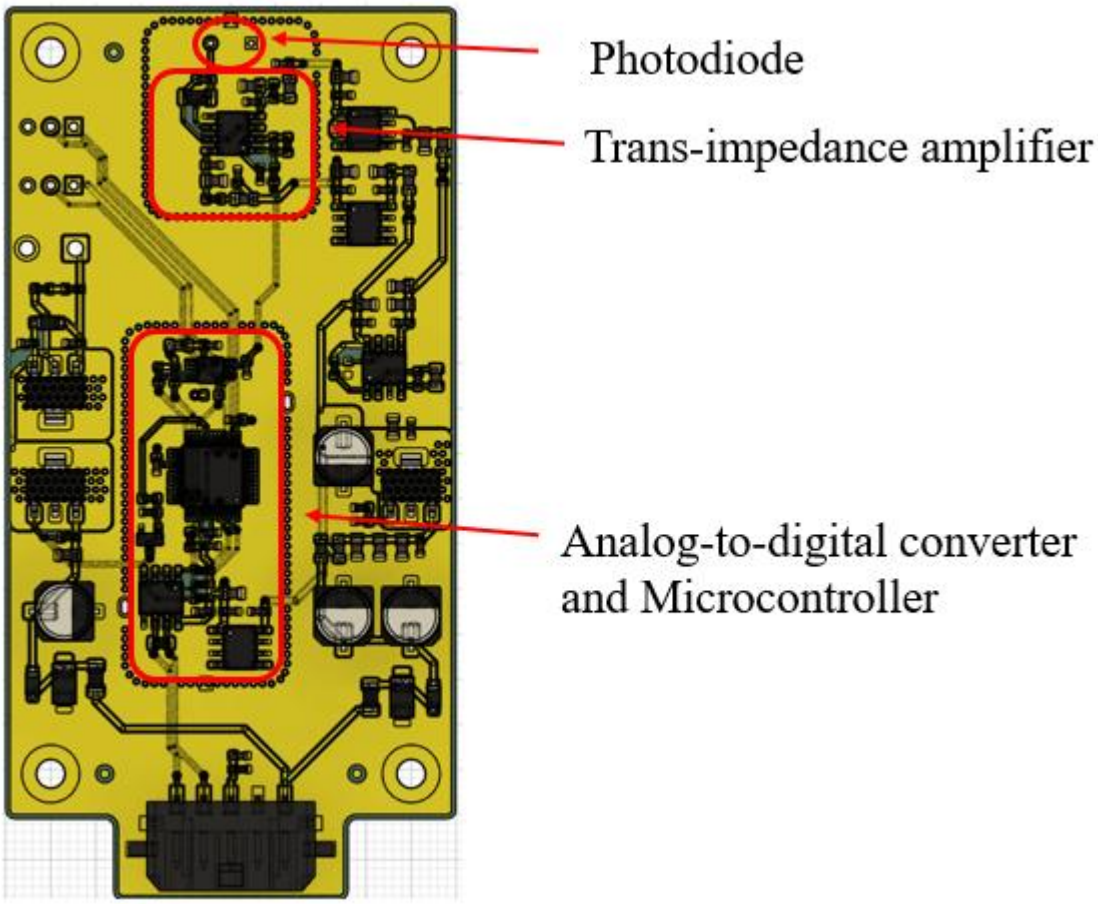

Figure 54: Photodiode board with a built-in trans-impedance amplifier, AD converter, and microcontroller.

By optimising the circuit board for the photodiode, power supply, and shielding of critical components, a signal noise level of 35 µV can be achieved. This optimisation is crucial for attaining a low signal-to-noise ratio. The measurement range extends from a detection limit of 105 µV to a maximum of 3,6 V. It is important to note that this range does not represent the linear measurement range but rather the minimum and maximum limits within which measurements can be obtained. Additionally, tryptophan measurements ranged from 5 µg/l to 83 mg/l. The measuring range is not entirely linear, as illustrated below. The gradient begins to change at 35 mg/l, after which it continues linearly but with a different slope. The presence of triple noise results in a detection limit of 1,9 µg/l, with the lowest measurable point set at five µg/l. Due to the increasing inaccuracy at these levels, measurements at the detection limit have been excluded. Despite the inability to utilise the entire range, achieving measurements with exceptional precision and a substantial dynamic range across multiple orders of magnitude remains possible. It should therefore be noted that measurements over a range of 2 µg/l up to a maximum of approximately 30 mg/l are possible. The figure below shows the end of the linear measuring range (Figure 55).

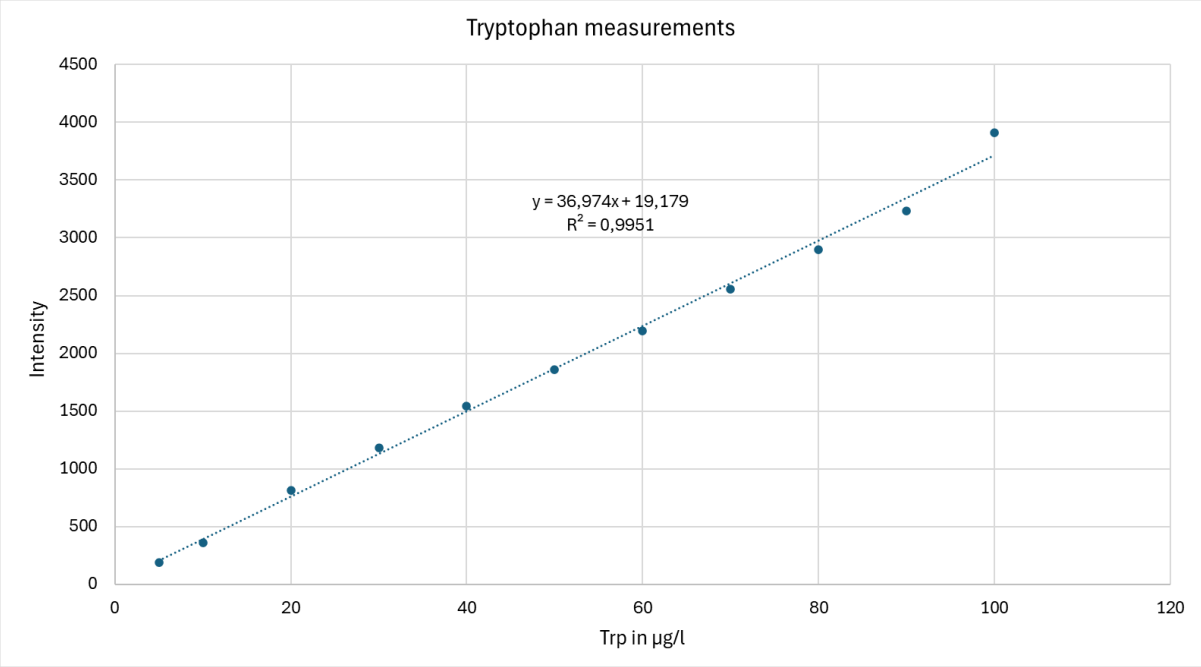

Figure 55: Measurement of tryptophan from 5 µg/l to 100 µg/l in water.

Due to the linearity and the low detection limit, measurements of bacteria in low concentrations are also possible. Further measurements are necessary to show how the optimized sensor behaves under laboratory conditions.

4.6 Creation of a Prototype

For further optimisation and to produce a prototype that can be mass-produced, all components are replaced as much as possible with commercially available components. In this section, the prototype is tested in real industry. The previously used prototype is useless for the industry because series production of these prototypes is not feasible due to factors such as price, repeatability, and automation. In order to enable series production, it is necessary to transfer the prototype to industry standards. In concrete terms, this means that expensive custom-made products must be avoided. These aspects were also considered in the course of the work. Therefore, all components are available in a modified form. The components used for the finished detector are shown in the figure and listed in the table below (Figure 56 & Table 12).

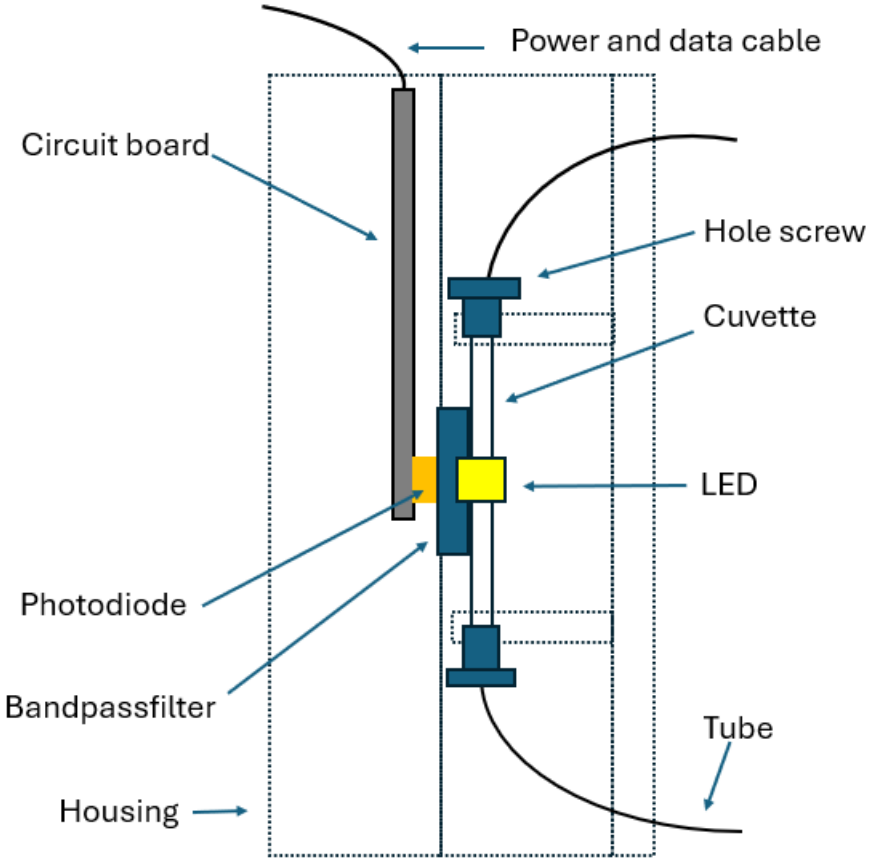

Figure 56: The improved design of the fluorescence sensor is shown in the figure.

Table 12: List of components for the industrial fluorescence detector.

component	product description
housing	3D printed
Photodiode	S1227-33BQ (Hamamatsu)
LED	NCSU434B (Nichia)
Flow cell	MQC401 (Machined Quartz)
tube	PTFE-Chemieschlauch – standard 92548
Hole screw	RCBAS5-8 (Misumi)
Bandpass filter	340 nm (edmundoptics)

The components of the detector are quite straightforward, as outlined in the list. The key elements include the LED, the optical filter, the cuvette, and the detector itself. Most of these components, including the optical filter, the UV LED, and the cuvette, have already been tested in the preceding chapter. It is important to note that the selection of commercial cuvettes is quite limited; consequently, the findings from the initial prototypes identified only one suitable candidate.

4.7 Fluorescence Sensor Test

A prototype sensor was developed as a result of the investigations conducted that were specifically designed for the detection of microorganisms. Previous studies have demonstrated that long-term measurements can be achieved using a commercial flow-through fluorescence spectrometer. This report now confirms that measurements with the prototype are also viable. To test this, a 70 L tank was filled in the pilot plant, as outlined in Chapter 4.4.1, and *E. coli* was introduced. The tank operated for several weeks, during which microbial contamination became evident, both visually and through fluorescence readings. When the fluorescence reached a predetermined intensity, chlorine dioxide was administered. This produced results comparable to those in Chapter 4.4.1, thus confirming the functionality of the sensor.

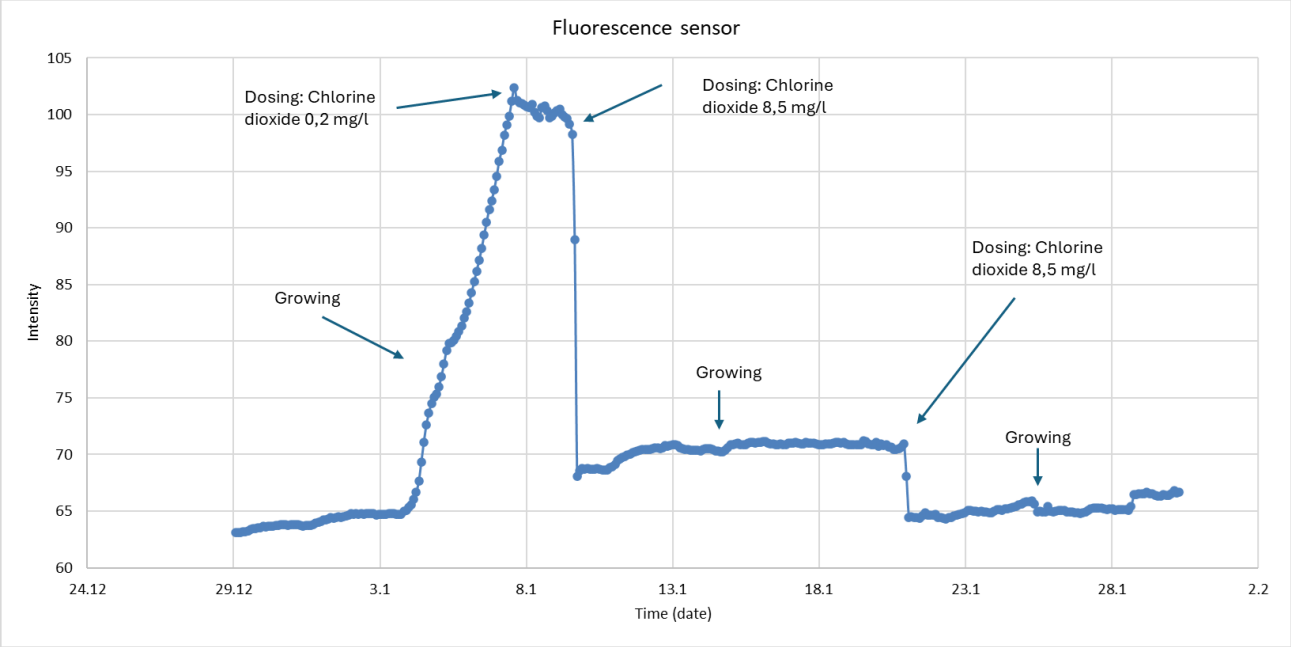

Figure 57: A 70L tank filled with water and inoculated with E. coli in PBS. The long-term measurements show the growth of microorganisms and the effect of the addition of chlorine dioxide.

The initial phase of measurement reveals a significant growth of microorganisms, accompanied by the formation of biofilms and turbidity in the tank. At this stage, a low dosage of 0.2 mg ClO_2/l is administered, which leads to a stabilization in growth. The assumption is that the bacteria have reached a steady-state status, where new bacterial growth is offset by the death of some existing bacteria. Consequently, while growth can be curtailed, a substantial number of microorganisms remain viable. An increased dosage of 8 mg/l results in a marked reduction in microbial count. However, it takes several days for growth to resume, likely due to the very low count of surviving bacteria, which need time to recover. The subsequent dosage also results in a notable decrease in fluorescence.

The results indicate that the prototype performs comparably to a commercial device. As previously discussed, the detector is intended for use in industrial water applications, where the water is often contaminated. A particularly extreme example of this is found in cooling lubricants. The next step is to explore whether such solutions can also be effectively monitored by the sensor.

5. MWFs as an Example of Industrial Water

Thus far, the research has demonstrated that tryptophan fluorescence is highly effective for detecting microbial contamination. Additionally, chlorine dioxide has proven to be an excellent choice for sanitization. However, it is important to note that these studies were conducted under laboratory conditions, which typically involve very clean environments.

In contrast, this sensor will ultimately be employed in industrial settings, where water quality is often compromised. MWFs serve as an extreme example of industrial water. As discussed in the theoretical framework, these fluids contain various components, each serving a specific function. It is crucial that the efficacy of these components is not significantly diminished by chlorine dioxide and the sensor is able to measure under these conditions. Therefore, first, the individual components are evaluated for their reaction with chlorine dioxide. This evaluation allows us to determine if a reaction occurs. Second, it is essential for chlorine dioxide to be evenly distributed throughout the emulsion rather than localized in a single phase to effectively target all microorganisms. This distribution can be assessed using the octanol-water partition coefficient. Third, there must be no interference with the fluorescence by the components involved in the fluorescence measurement. To ensure this, spectra of the various components will be recorded and compared to that of tryptophan. Fourth, once all these factors have been addressed, the method will be tested under real conditions.

As shown in the literature, many species are present in MWFs. Fungal species have a high natural occurrence and for this reason, have a significant impact. Characterisation of MWFs shows several types of fungi, such as Cladosporium, Aspergillus, Alternaria, and Candida albicans. (*130*) Candida albicans is a well-studied fungi. The analysis of the chitinase gene of Candida albicans, which is at the outer layer of the fungi, contains several tryptophan molecules. (*131*) Also, the most prevalent fungi, Cladosporium herbarium, contains tryptophan. (*132*) Nevertheless, there are many challenges that require intensive research, as will be shown below.

5.1 Oxidation of MWF Compounds

The reactivity of chlorine dioxide with organic compounds is apparent at equimolar concentrations, but a greater understanding of the low concentration range of chlorine dioxide is required. This low concentration range is crucial for the industrial application of chlorine dioxide to eliminate bacterial contamination in industrial water. In this scenario, slight oxidation of the product is not critical because there is a massive excess of it. The concentration of chlorine dioxide used is 10 mg/l, which simulates an extreme situation with a high bacterial presence. In typical cases, a concentration of a few hundred µg/l is sufficient to control an MWF, but it is too low for accurate photometric measurements. Several techniques are being tested for detecting chlorine dioxide in a high organic-load solution. The first is iodometric titration, a standard method for detecting oxidising agents, but organic components affect the measurement. Due to these disturbances in the matrix, it was not possible to determine the exact end point. This led to the exclusion of this method, as chlorine dioxide had to be determined in small concentrations. The addition of unsaturated oils leads to the formation of a brown colour, making it impossible to observe the iodine colour. The second method to measure chlorine dioxide is through photometry. Chlorine dioxide has a characteristic absorption spectrum with a maximum of 359 nm, which is easily visible even in solutions with high organic concentrations, enabling quantification. The absorption spectra for each component of the MWF were measured. To ensure that the components were not interfering with the measurements, a comparative spectrum was recorded to assess whether the components were excessively impacting chlorine dioxide absorption. However, none of the measurements indicated such an impact. The chlorine dioxide spectrum remained detectable despite the matrix lifting the entire signal. The lubricants and additives are technical grades. The lubricants are used in concentrations of 5% and 10% in deionised water in round bottom vessels with low gas phases, and they were filled with 100 ml of the solution or emulsion. The emulsions were centrifugated for 10 minutes before measurement. The aqueous phase was removed from below the organic phase using a syringe, and then the solution was measured the same way as the other solutions. Ten mg/l distilled chlorine dioxide is added to the solution, and all vessels are closed vapour safe. The samples were stored at room temperature in the dark under constant swirling. The first probe is measured after five minutes, and the spectra are checked for chlorine dioxide. All solutions were bubbled for one hour after the first

measurement and measured for a blank. Each sample was purged to eliminate the matrix's influence until the chlorine dioxide spectrum vanished. Subsequently, the concentration of chlorine dioxide could be determined using the Lambert-Beer law (2) in the following table (Table 13).

Table 13: The zero measurement of PEG 600 for a 5% solution without PEG 600 to see the maximum concentration of the measurement.

Cuvette (cm)	Absorbance 1	Absorbance 0	Δ Absorbance	mol/l	mg/l
5	0,8599	0,0020	0,8579	$1{,}454 * 10^{-4}$	9,8077
5	0,9417	0,0026	0,9391	$1{,}592 * 10^{-4}$	10,7360
5	0,8713	0,0029	0,8684	$1{,}472 * 10^{-4}$	9,9277
5	0,8653	0,0023	0,8630	$1{,}463 * 10^{-4}$	9,8660

An error analysis requires a minimum of 12 measuring points, which we currently lack for a single point. Nevertheless, we can still conduct a relative error analysis. We performed seven measuring points, each repeated four times, resulting in 28 measurements.

Table 14: The data of PEG 600 measurement.

Time (h)	Concentration (mg/l)
0	10,08
0,5	9,61
2	9,60
5	9,60
24	9,25
48	8,78
165	7,09

The precise measured values and their errors are heavily influenced by concentration and are unsuitable for determining the total error. However, the relative error remains consistent across all measurements, as it is not significantly dependent on the absolute concentration. A total standard deviation can be derived by summing the squares of the standard deviations, reflecting

the standard deviation across the entire measurement. It is important to note that this relative error may vary depending on the substance being measured. In the case of PEG 600, the error is 2%. The remaining data are listed in the Appendix.

Table 15: Data analysis of PEG 600.

Time (h)	Standard deviation	Mean value	Relative standard deviation	Square of relative standard deviation
0	0,4372	10,0843	0,0434	$1{,}9 * 10^{-3}$
0,5	0,0666	9,6108	0,0069	$4{,}8 * 10^{-5}$
2	0,1583	9,6050	0,0165	$2{,}7 * 10^{-4}$
5	0,0534	9,6042	0,0056	$3{,}1 * 10^{-5}$
24	0,1828	9,2547	0,0198	$3{,}9 * 10^{-4}$
48	0,0410	8,7831	0,0047	$2{,}2 * 10^{-5}$
165	0,0851	7,0891	0,0120	$1{,}4 * 10^{-4}$

This data can also be used to calculate the reaction constant of chlorine dioxide for the respective substances. For PEG 600, this is $7{,}5\ \mathrm{x}10^{-11}\ \frac{mol/l}{s}$ and is therefore very small compared to the reaction constants of tryptophan is in a range of $10^{5}\ \frac{mol/l}{s}$ (Table 14).

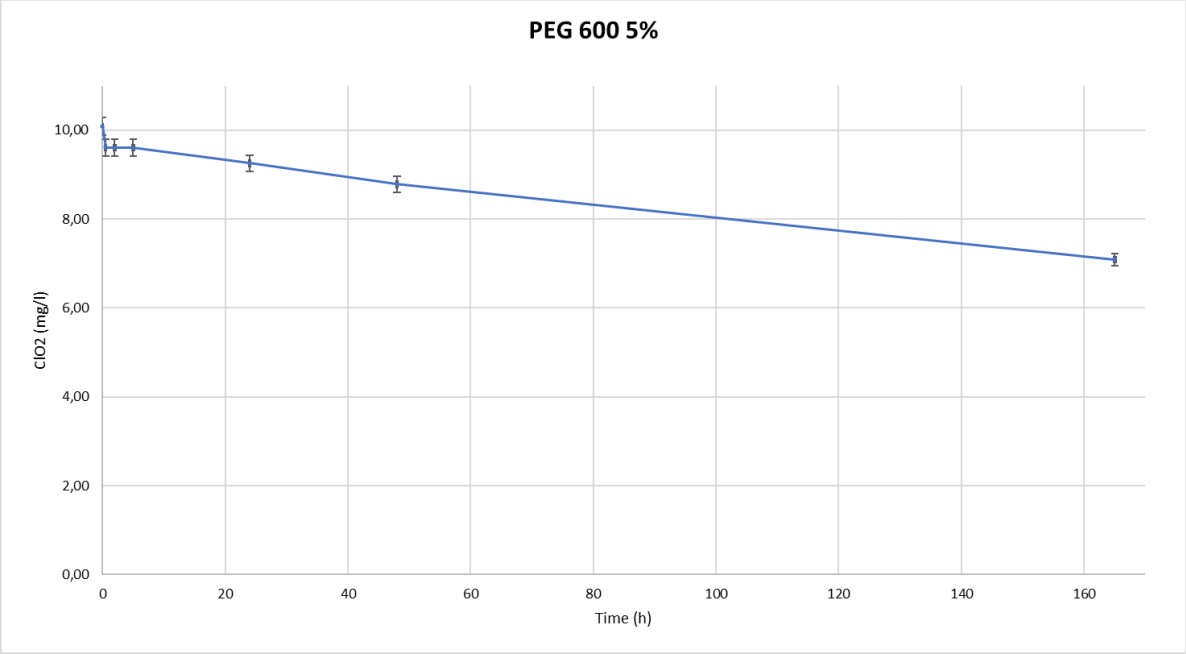

Figure 58: Degradation of chlorine dioxide in a PEG 600 solution over several days.

The results indicate weak reactivity of chlorine dioxide with PEG, PPG, glycerin, and mineral oil. Those compounds have no electron-rich moieties, so there is no point in attacking chlorine dioxide. The slight decrease in chlorine dioxide can be explained by a reaction with slow reaction kinetics. Those are, in most cases, impurities or the end OH-groups. The polyethene glycol and polypropylene glycol are shown below (Table 16). In all cases, the decrease in chlorine dioxide is not problematic when using chlorine dioxide. This measurement shows that oxidation occurs faster for components with higher middle molar weights than for components with lower molar weights. So, the high molar components are easier to break, which is not that logical. The reason for that could be impurities, but the substances were pure; therefore, this should not be the reason. High molar components do not form translucent solutions, so they are not completely soluble. Chlorine dioxide might diffuse into the solid part, where the reactivity is faster. However, this is not the focus of this research, and there is a need for more experiments to prove that because it could be that only some show this behaviour. Polypropylene is more reactive than polyethene glycol. This could be because the longer propylene side chain affects the electron density.

The non-soluble ones were rapeseed oil, castor oil, tall oil, olein acid methyl ester, and naphthenic mineral oil. Rapeseed oil methyl ester was also tested, but the reactivity with chlorine dioxide was too fast to be observed with this method. The sample is centrifugated to measure the chlorine dioxide loss, then the water layer is analysed. In the case of methyl oleate,

the reactivity is much faster than that of the other components. Compared to the other oils in the diagram, they have a high purity, and the background in the UV/Vis measurements is more defined. This makes the measurements here easier. This may be one reason the measurements seem to be better here. The measurements show that the castor and rapeseed oil are well-suited and show an approximately linear decrease, whereas the tall oil and olein acid methyl ester are logarithmic. The rapid oxidation of bacteria will not prevent sanitisation but will increase the amount of necessary chlorine dioxide.

It is good to know that chlorine dioxide's reactivity with unsaturated components is slow and that overdosing can lead to chlorinated products. (*133*) (*134*) The reaction products are also analysed with GC/GC-MS and show hydroxylation of the double bond. Chlorinated products cannot be found. The decrease in chlorine dioxide concentration is slow, depending on the reactivity of chlorine dioxide with bacteria. The reactivity with bacteria is a few seconds; therefore, the reactivity with the oily compounds is negligible.

The reaction constant offers valuable insight into the individual components' relative reactivities. All components show a slower reaction rate with chlorine dioxide compared to tryptophan. Even when the concentration of an element is doubled, resulting in a corresponding doubling of the constant, there remains an approximate 15-order-of-magnitude difference between the reactants, as shown in the table below.

Table 16: Reaction constants with MWF main compounds in two concentrations; doubling the concentration leads to a doubling of the constant.

compound	Reaction rate in 5 % solution ($\frac{Mol/l}{s}$)	Reaction rate in 10 % Solution ($\frac{Mol/l}{s}$)
PEG 600 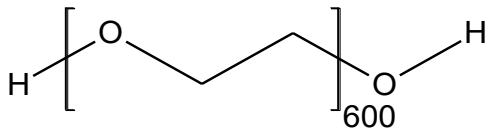	$7{,}5 * 10^{-11}$	$1{,}7 * 10^{-10}$
PEG 6000 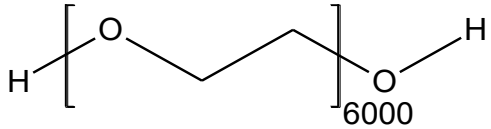	$8{,}9 * 10^{-11}$	$1{,}4 * 10^{-10}$

PPG 400 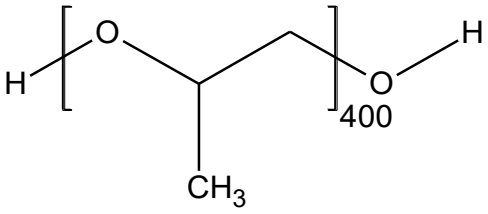	$2{,}1 * 10^{-11}$	$2{,}3 * 10^{-10}$
Glycerol 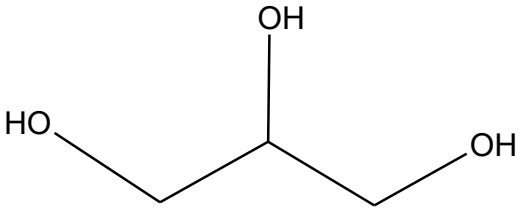	$1{,}1 * 10^{-10}$	$2{,}8 * 10^{-10}$
Olein acid methyl ester 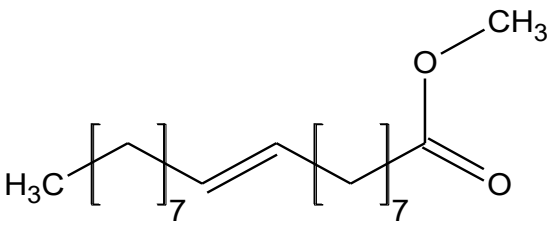	$1{,}9 * 10^{-8}$	-
Tall oil (Table 1)	$2{,}1 * 10^{-7}$	-
Castor oil (Table 1)	$8{,}9 * 10^{-9}$	-
Rapeseed oil (Table 1)	$9{,}2 * 10^{-9}$	-
Mineral oil	$2{,}2 * 10^{-10}$	-
Hygold T9	$2{,}6 * 10^{-10}$	-

The second important group are the emulsifiers. These are also measured as described above. The measurements were focused on the lower concentration range of emulsifiers, as they are typically used in low concentrations. Emulsifiers are usually only soluble or emulsifiable in low concentrations in water-based systems without additional substances. It is likely that the substances used are slightly below the usual level, which could result in slightly higher consumption than indicated by the results. However, the findings suggest that high emulsifier consumption is not expected.

MTP 090 is an ethoxylated and propoxylated oleyl alcohol with no defined structure. Walloxen is a polyester with alcohol groups and a small proportion of unsaturated compounds. SNS is a petroleum-based sodium sulfonate. Akypo is a polyester with a double bond and an acid group. The structure generally consists of an olefin (hydrophobic part) and an anionic group (hydrophilic part). Since no precise structure is available, explaining reactivities or postulated reactions is complicated. The knowledge that fewer electron-rich moieties are present explains the reactivity, but overall, the slow reaction kinetics do not hinder the use of chlorine dioxide. The reaction rate constants for the components MTP, SNS, and Walloxen are in the range of $10^{-10}\ \frac{Mol/l}{s}$, while Akypo's are in the range of $10^{-9}\ \frac{Mol/l}{s}$. The slow reaction is also evident in the table below (Table 17).

Table 17: Surfactants in metalworking fluids.

Compound	Reaction rate ($\frac{Mol/l}{s}$)
MTP 090	$3{,}8 * 10^{-10}$
Walloxen SP20	$4{,}3 * 10^{-10}$
SNS 467	$1{,}9 * 10^{-10}$
Akypo RG 90 VG 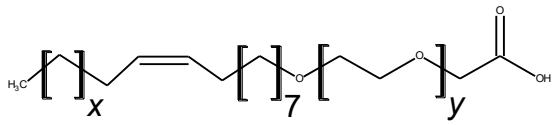	$5{,}7 * 10^{-9}$

Surfactants are unproblematic if they lack electron-rich groups. In addition, many groups exhibit slight reactivity but do not pose a problem for chlorine dioxide because they may have a steric hindrance. Consequently, chlorine dioxide could be applied in settings requiring disinfection and involving high surfactant concentrations, such as industrial laundries and large kitchen dishwashers, where hygiene is paramount.

The third important group to be tested are the performance additives. The tested additives are presented here. Lakeland is a phosphoric ester with an aromatic system. Additin is an olefin linked via sulfur bridges. CS is a versatile additive that functions as both an anticorrosive and

a high-performance additive comprising a phosphorus ester. Ilcolubes are polymer esters, and similar to the other components, they lack a defined structure.

Depending on the additive, the additives are tested in a concentration of 0,1% solution or emulsion. Several types of additives show good compatibility with chlorine dioxide. The tests are performed for a period of 24 hours, but the results are only recorded for the first 3 hours. Importantly, no problematic degradation was observed—a favourable outcome reinforcing the additives' compatibility with chlorine dioxide. After all measurements, chlorine dioxide is still available, at least in a concentration of 5 mg/l, indicating that even if a large amount of chlorine dioxide is in contact with the additives over an extended period, there should be no problems. The error bars are highest for Lakeland at 8% and Additin at 4%. The rest are about 1%, showing only a small variance between all measurements.

The presence of sulfur and phosphorus in the additives is not a significant problem. It is surprising that the unsaturated components have such a low reaction rate. This means that the electrons are not available to the chlorine dioxide, leading to the conclusion that they are bound in a form for which no reaction is possible (Table 18).

Table 18: High-performance additives.

Compound	Reaction rate ($\frac{Mol/l}{s}$)
Lakeland PPE 1614	$8{,}1 * 10^{-10}$
Additin RS2540	$8{,}7 * 10^{-10}$
Ilcolube 5000	$8{,}9 * 10^{-10}$
Ilcolube 7030	$4{,}4 * 10^{-10}$
Fosfodet CS-0606	$1{,}9 * 10^{-10}$

Next, the anti-corrosion additives and biocides are shown. The anti-corrosion additives are tested in a concentration of 0,1 %, which is 100 times lower than in common MWFs, and the biocide is in a concentration of 0,1 %, which is common in MWFs. Many additives contain small amounts of biocides added to the fluid later because of resistant microorganisms. Those compounds are problematic in combination with chlorine dioxide. The typical components are not the best option here; other biocides and rust protection agents should be tested. Compounds that are suitable for use as corrosion protection and are not so reactive towards chlorine dioxide

could be polymerised amines. Nutiu et al. also describe that sulfonates, organic boron compounds, amine phosphates, zinc dialkyl dithiophosphate, and fatty acids can be used as protection. (*135*) Several possible alternatives could be found under those compounds. In addition, phosphorous esters and carboxylic acids could also provide suitable corrosion protection. The biocide 3-Iodoprop-2-yn-1-yl butyl carbamate may be an alternative for the benzothiazole derivates. This would not be a problem for use in the plant, as chlorine dioxide would take over the task of the biocides. However, a small amount is necessary to store the products in the bins. This amount would decompose over time in the plant due to the addition of chlorine dioxide. As a result, the biocides would be tolerable, even though they interfere with the measurement.

Nevertheless, the experiment shows an intense chlorine dioxide degradation, also known from the literature. The reaction of the components is in a range of seconds, and they are problematic in combination with chlorine dioxide (Table 19). However, it is also obvious that this is not the right way to show reactivity with those fast components. It is quite clear that later in the MWF, the MWF components are in the solution and the bacteria. Therefore, there should be some competitive reaction. This reactivity is intensively discussed later.

Table 19: Reactivity of rust protection amines and benzothiazole derivate as a biocide.

Compound	Reaction rate ($\frac{Mol/l}{s}$)
TEA 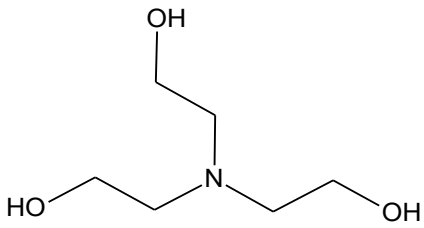	$\gg 10^{-6}$
MDEA 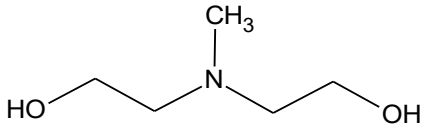	$\gg 10^{-6}$

DCHA 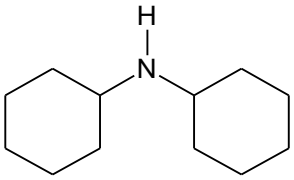	$\gg 10^{-6}$
AMP 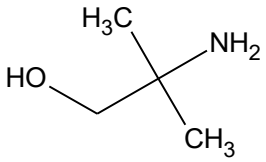	$\gg 10^{-6}$
Acticide B20 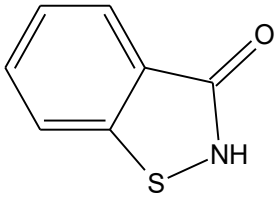	$\gg 10^{-6}$

5.2 Distribution of Chlorine Dioxide Between Organic and Aqueous Phases

After assessing the oxidation stability of the components, we must consider how chlorine dioxide is distributed within a two-phase system. This distribution first impacts the measurements of non-water-miscible components, and second, it provides insights into the behaviour of chlorine dioxide in cooling lubricants under real-world conditions. To ascertain whether chlorine dioxide is present in the polar or non-polar phase, we calculate distribution coefficients for different substances.

Chlorine dioxide is an angled molecule with a central chlorine atom and two oxygen atoms, and the electronegativity difference is 0,7. This means the electronegativity is not as high as in water, and no symmetry neutralises the polarity. Chlorine dioxide is likely also soluble in less polar substances. Chlorine dioxide may not have been degraded in the experiments but remains in the organic phase. Since chlorine dioxide is only determined in the organic phase, this can lead to errors.

The octanol-water coefficient (P) dictates whether a substance resides in the lipophilic or hydrophilic phase. In this instance, we measure the change in the concentration of chlorine dioxide in the aqueous phase. To prevent octanol from consuming chlorine dioxide, we conducted long-term experiments. These experiments revealed that the concentration remains stable over an extended period after reaching equilibrium. The coefficient can be determined using the formula below (6). If the value is less than one, the substance is more soluble in water, and if the value is greater than one, it is in the non-polar phase.

$$P = \frac{c_o}{c_w} = \frac{(m_{ClO_2\ theoretic} - m_{ClO_2\ water})/V_o}{m_{ClO_2\ water}/V_w} \quad (6)$$

Where P is the coefficient, c_w is the chlorine dioxide concentration in the water and c_o is the chlorine dioxide concentration in the organic phase. $m_{ClO_2\ theoretic}$ results from the amount of chlorine dioxide added, and $m_{ClO_2\ water}$ from the measured amount in the aqueous phase. The volume of the organic phase is V_o and V_w for the volume of water. Since chlorine dioxide has different absorption properties in the organic phase, the measurement in the organic phase is not used here. The concentration of the organic phase is therefore an approximation. The idea that everything that is not in the aqueous phase must be in the organic phase only works if nothing is in the gas phase and nothing is reacting. This study was conducted for various substances, and the results are presented in the table below. The data indicate a trend: Highly non-polar substances, such as isooctane, have values below one. Alcohols with slightly more polarity due to hydroxyl groups fall in the range of 2-3, suggesting chlorine dioxide will be slightly more soluble in the organic phase. The more polar dichloromethane and the methyl ester exhibit the best solubility. These results indicate that chlorine dioxide is more concentrated in the organic phase than in the aqueous phase, depending on the substances used. However, the concentration difference is not significant enough to render the measurement of solutions infeasible. Most importantly, the initial measurements can be influenced by

distribution, underscoring the importance of long-term experiments. While equilibrium is reached within a few hours, if concentration changes after days, it can be assumed that the chlorine dioxide is reacting.

Table 20: The chlorine dioxide distribution coefficient for several organic components with chlorine dioxide in water.

	P(O/W)
Isooctane	0,9
2-Octanol	2,0
1-Octen-3-ol	2,8
Dodecane	2,5
1-Decanol	3,0
Dichloromethane	8,6
Myristinsäuremethylester	7,4
TMP (isostearic acid)	1,0
Paraffin oil	0,7
Mineral oil	0,5

The distribution between the organic and aqueous phases is essential, but the gas phase also plays a role. According to the literature, a solution in equilibrium with the gas phase is more concentrated than the gas phase. At 25 degrees in a closed flask, chlorine dioxide is 23 times more concentrated in the aqueous phase than in the gas phase. (*56*) This suggests that the gas phase is less influential when significantly smaller than the aqueous phase. The distribution's influence is minor in the experiments because the water phase is the biggest. The distribution is only slightly higher in the organic phase, and the gas phase is on the side of the water.

5.3 Fluorescence of MWFs

Fluorescence is a widespread phenomenon. Strongly fluorescent substances can interfere with the measurement. Since it cannot be completely ruled out that cooling lubricants fluoresce, and as there is no thorough description of the substances used, these must be analysed. To measure if the solutions are problematic for the measurement setup of this research, solutions and emulsions with a concentration of 1% of metalworking components are added to deionised water. The sample is measured with a 3D fluorescence spectrometer. After the measurement, tryptophan is added to the solutions, and the concentration is approximately 1 mg/l. The solutions are measured again. These solutions should show the characteristic tryptophan peak compared to the initial solution. Chlorine dioxide was added to the solutions in a 10-fold molar excess concerning tryptophan. The fluorescence should decrease in these solutions (Figure 59).

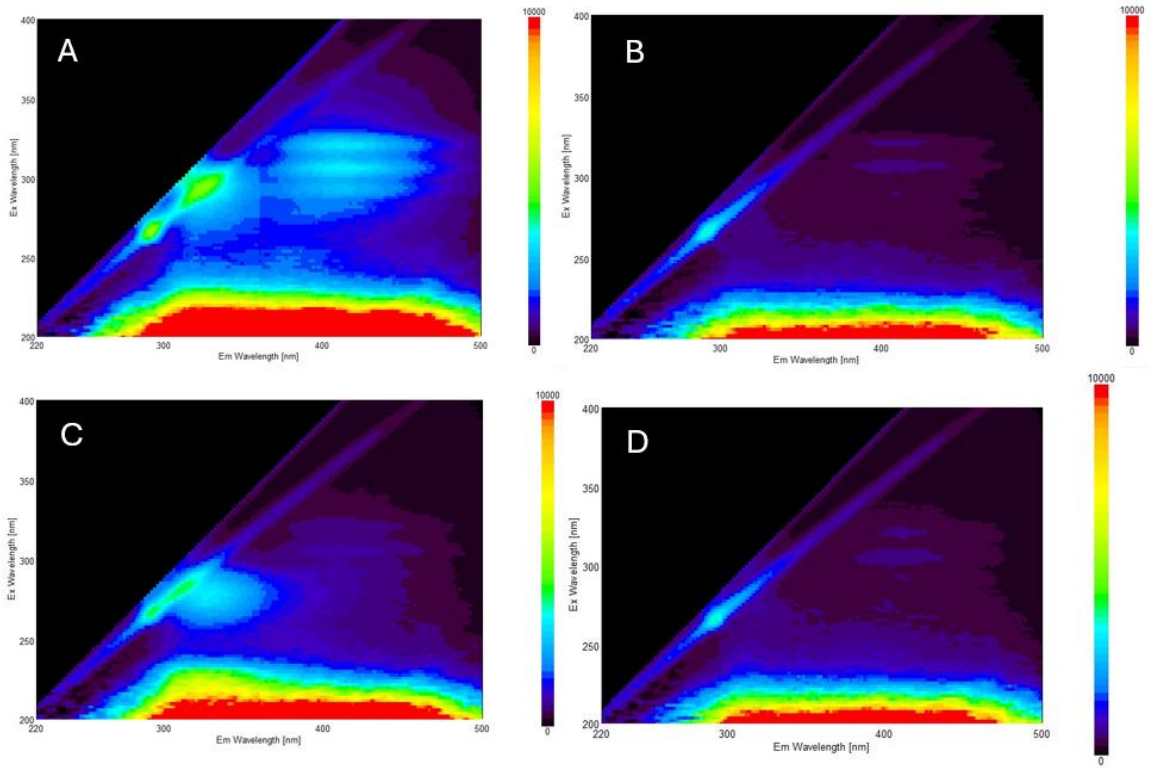

Figure 59: The natural fluorescence can be eliminated with chlorine dioxide. The addition of bacteria is also visible and possibly degraded, meaning that several components can be used in MWF.

The components of the MWF often have impurities from the process. In the case of rapeseed oil, the oil should not be fluorescence active, but the product can be seen in the figure. Picture A shows the fluorescence spectra of 5 g/l rapeseed oil in water with several fluorescence spots.

The reason for that is the presence of several natural aromatic components that could not be removed during purification. The fluorescence in the area of Ex. 300 nm and Em. 400 nm is weak and not resistant to chlorine dioxide (B). A small amount of chlorine dioxide destroys the fluorescence there. Then, the intense fluorescence in the Ex. 200 nm and Em. 300-500 nm region is not problematic. It is not strongly affected even if chlorine dioxide is added and does not reach the important measurement area. The area where the detector measures is also fluorescence, which could be proteinogenic. Adding *E. coli* to the emulsion shows a significant peak in the expected area (C). This leads to the fact that even if the oil fluorescence is small, it is possible to detect bacteria in low concentrations. After that, an average amount of one mg/l is added to the emulsion, leading to the complete degradation of the *E. coli* peak (D).

For this reason, all components are scanned with a 3-D fluorescence spectrometer in a concentration range of 5 g/l. The measurement was performed by excitation from 200nm to 500 nm and emission from 220 nm to 700 nm. Most of the fluorescence spectra show fluorescence activity. The *E. coli* (OP50) was purified as in the previous chapters. All substances were tested with 10^6 KBE/ml of OP50 for the cross-sensitivity of the measuring method. The expectation is that the signal rises. After that, chlorine dioxide is added to the solution, which should cause a significant reduction of the fluorescence signal. In the table below, the fluorescence intensities at Ex. 280 and Em. 350 nm are shown. The example of rapeseed oil shows a basic fluorescence of 3105. After the addition of bacteria, the fluorescence goes up to 7831 and after the addition of chlorine dioxide, it goes down to 4736. It can be seen here that the addition of bacteria has no effect and the addition of ClO2 has no effect either. The summary of the components is below (Table 21).

Table 21: Schematic demonstration of the fluorescence change caused by bacteria and chlorine dioxide.

	Intensity Pure	intensity with OP50	intensity with ClO2
T9 (Hygold 60)	10000	10000	10000
Rüböl Raff	3105	7831	4736
Rizinusöl	2178	6448	2599
Tallöl Dest 25/30	9993	10000	10000
SNS 467	10000	10000	10000
MTP 090	6505	9498	6149
Walloxen SP20	1666	5396	4811
Fosfodet CS-0606	9566	10000	10000
Ilcolube 5000	1932	4545	4074
Ilcolube 7030	173	5867	2193
Akypo RO90	10000	10000	10000
Lakeland PPE 1614	10000	10000	10000
Additin RC 2540	10000	10000	10000
DCHA	9194	10000	10000
TEA99	142	10000	10000
AMP 95	398	6003	5017
MDEA	694	6010	5935
Acticid B20	2	4	-2

The main components consist of mineral oils and natural oils. First, the mineral oil T9 contains highly polymerized unsaturated hydrocarbons. While these hydrocarbons are stable against oxidation, they exhibit fluorescence, which complicates their use.

Next, we have natural oils: rapeseed oil, castor oil, and tall oil. Tall oil is a byproduct of the wood pulp industry. All these oils are fluorescent, although not all fluorescence is problematic. Both rapeseed and castor oils display slight fluorescence in the range of tryptophan fluorescence, but measurements can still be performed. In contrast, tall oil is more fluorescent than the others.

Emulsifiers can also pose challenges, primarily due to impurities. For example, some emulsifiers, like SNS, are mineral oil based. There are emulsifiers with low fluorescence, such as MTP 090, which exhibit no cross-sensitivity. However, it is difficult to generalize, as different technical products may contain varying impurities.

Performance additives share similar issues with emulsifiers, with purity being a crucial factor. Some components can appear similar yet differ significantly; for instance, IL 5000 and IL 7030 have identical structures, but IL 5000 contains biocides that contribute to its fluorescence.

While amines themselves are not fluorescent, they can affect tryptophan fluorescence and interfere with the reaction of chlorine dioxide with amino acids. Acticide B20 is highly

fluorescent and can completely mask the detection of other fluorescent substances. Other biocides may provide viable alternatives.

Given these complexities, a thorough examination of the components is essential, and careful observation is still required. Directly using the instrument with all MWFs can be problematic. Using high-purity products that are free from fluorescent substances can work effectively, but this places significant limitations on the types of MWFs available.

An alternative approach would be to measure the products directly to determine the fluorescence of the composition. However, omitting certain substances from the mixture is usually not feasible, as this can lead to the emulsion breaking.

5.4 Reaction of Reactive MWF Additives

Some components, especially amines, react rapidly with chlorine dioxide, complicating the monitoring of its concentration. Various amines were examined: triethylamine (99% purity), methyldiethanolamine (99% purity), diethanolamine (98% purity), and 2-amino-2-methyl-1-propanol (95% purity), along with tryptophan at 99% purity diluted in deionized water with phosphate buffer. Tryptophan provides a stable solution, unlike bacterial cultures, which can fluctuate.

The free electron pair is a perfect target for chlorine dioxide. The kinetics of amines and chlorine dioxide do not get much attention in the literature, but the reactivity is shown in several compounds. (*136*) Also, the reactivity of triethylamine is studied, and the reaction kinetics are rapid. (*137*) It is also well known that the tertiary amines are the fastest, as observed in these studies. In the group of secondary and primary amines, there are significant differences in the kinetic, which depend on the functional groups. Those groups with an I+ effect push the electron density to the nitrogen, which increases the reactivity. Also, high pH increases the reactivity because deprotonated amines are strong electron donors. (*6*)

The properties of amines come from the lone electron pair at nitrogen. Depending on the order of the amines and the substituent, the lone electron pair is more or less associated with nitrogen. The weaker the attraction of the nitrogen to the free electron, the faster chlorine dioxide attacks

it. The literature shows many reactions from chlorine dioxide and nitrogen-containing molecules. (*6*)

Tertiary amines have the fastest reaction rate constants with chlorine dioxide from the amines, in the 10^1 - 10^2 $\frac{mol/l}{s}$ range. This is just a little slower than that of tryptophan, which means that chlorine dioxide destroys both in equal concentrations. However, tryptophan is in traces, so chlorine dioxide is almost completely consumed by tertiary amines. The disinfection in this kind of solution would not work.

Second and primary amines are, in many cases, hundreds or thousands of times slower than tryptophan. The reaction of the amines takes so long that the kinetic is on the side of tryptophan, even if there are a lot of amins.

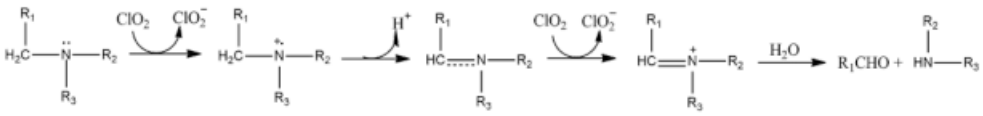

Figure 60: Reaction of amines with chlorine dioxide. (6)

As shown, the reaction of tertiary amines with chlorine dioxide leads to secondary amines and the corresponding aldehyde. In the case of enough chlorine dioxide, the oxidation goes further to ammonia.

Rapeseed oil is notably reactive due to its double bond and the presence of impurities. This study illustrates that the oxidation of tryptophan occurs at such a rapid pace that the oxidation of the oils can be regarded as negligible. As discussed below, the reaction kinetics of tertiary amines with tryptophan is comparably swift.

In this experiment, varying concentrations of amines were utilized while a constant amount of tryptophan was added. Following this, chlorine dioxide was introduced, and the fluorescence was measured. The decrease in fluorescence provides insight into the concentration at which the reactions between tryptophan and the selected amine occur at similar rates. The results reveal a logarithmic decrease in fluorescence.

For triethylamine (TEA), it was noted that the oxidation rate of TEA aligns with that of tryptophan at a 3-molar excess. In contrast, for diethylamine (DEA), half of the fluorescence is eliminated at a 70-molar excess, whereas for amine propylamine (AMP), this occurs at a 1000-molar excess. We expect that both reactions exhibit a similar likelihood of occurring.

Another commonly used tertiary amine in MWFs is methyl diethanolamine. This compound demonstrates a kinetic reaction that is nearly equivalent to those of TEA but shows a stronger correlation with the data and the logarithmic fit.

While secondary amines are no longer used in MWFs, they align well with existing literature, falling between the behaviours of tertiary and primary amines. Tertiary amines indicate that even minimal concentrations can significantly impede tryptophan oxidation. In contrast, primary amines still facilitate oxidation even within a typical MWF concentration range. Consequently, the use of primary amines in MWFs, in conjunction with chlorine dioxide, is a viable option (Figure 61).

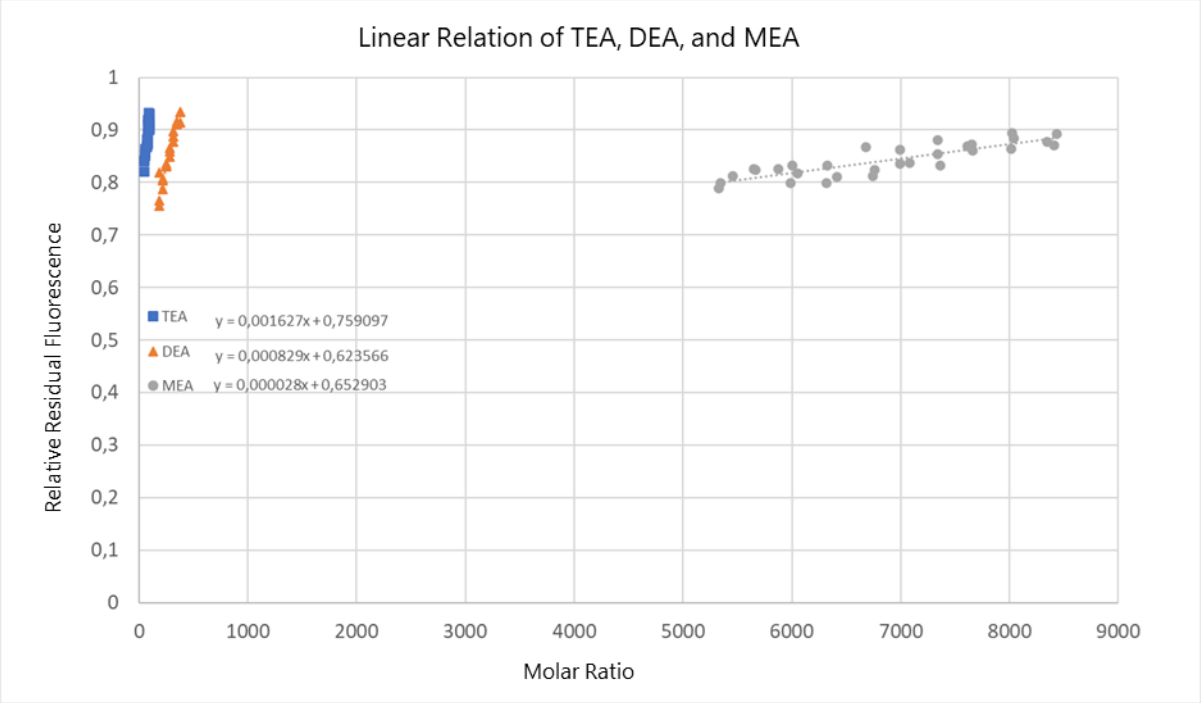

Figure 61: Summary of the competition reactions with primary, secondary, and tertiary amines with tryptophan.

Primary amines are seldom used, but monoethanolamine (MEA) and aminomethyl propane (AMP) are still used. They are the slowest, according to the literature.

The linear application of the degrees in the diagram shows that the difference between tertiary and secondary amines is not big, but for the primary ones, it is. This relation shows that using primary amines in MWF should be possible.

5.5 Measurements in a Model MWF

As previously discussed, MWFs are optically very dense emulsions that make measurements very difficult. Before measurements are carried out with living organisms, it must first be checked whether the solutions do not absorb too much. For this purpose, both the excitation wavelength 280 nm and the emission wavelength 330 nm of the prototype are examined. The solutions were measured in concentrations of 10%, 5%, and 1%. The penetration depth of the light is determined using a UV/Vis spectrometer. The measurements with a UV/Vis spectrometer show that even emulsions as low as 1% absorb almost all the light in the UV range, making the measurements difficult.

Table 22: Calculated results for the absorbance for different MWF concentrations. The results show that the light-source radiation is completely absorbed, and the fluorescence is almost completely absorbed.

Concentration of MWF	280 nm	330 nm
1%	2,31	0,55
5%	11,56	2,77
10%	23,13	5,54

As the absorption depends on the visible thickness and concentration, optimisation can easily be carried out at these points. The solutions that are passed through the measuring cell can be diluted just before they enter the measuring cell. In addition, a measuring cell with a short path length can be selected. The dilution enables excitation at 280 nm, and the fluorescence at 330 nm is only slightly weakened. Dilution by a factor of 10 logically increases the detection limit by a factor of 10, which is sufficient for MWFs. Measurements in the 100-1000 CFU/ml range would, therefore, shift to 10^4 or 10^5 CFU/ml. As work in these areas is often still carried out in the 10^8 CFU/ml range, the device would nevertheless significantly improve work. However, the detection limit must not be too high; otherwise, the measurements will not provide any benefit. The combination of 1% emulsion and 3 mm flow cell offers the best interference effect, providing a clear direction for our future work in this area. Measurements with yeast show that in the detector 10^6 yeast cells per ml cause a fluorescence that corresponds to that of 1100 µg/l tryptophan. With a detection limit of 2 µg/l tryptophan, this would correspond to a detection limit of 3600 CFU/ml. The measuring range extends up to 83 mg/l,

which would correspond to a maximum range of 10^8 CFU/ml. By measuring this, the signal can estimate the bacterial count and adjust the optimum dosage of chlorine dioxide accordingly. This allows the bacterial count to be reduced to a defined level or even to be eliminated completely. The device also has fantastic long-term stability. Over several days, only a slight drift of approximately 1 fluorescence unit can be observed.

To prove that measurements in emulsions are possible, we prepared a concentrate with rapeseed oil, MTP 090, Ilcolube 7030, and MEA. The structure of the setup is similar to the previous one in Chapter 4.4.1. The setup is shown below (Figure 62).

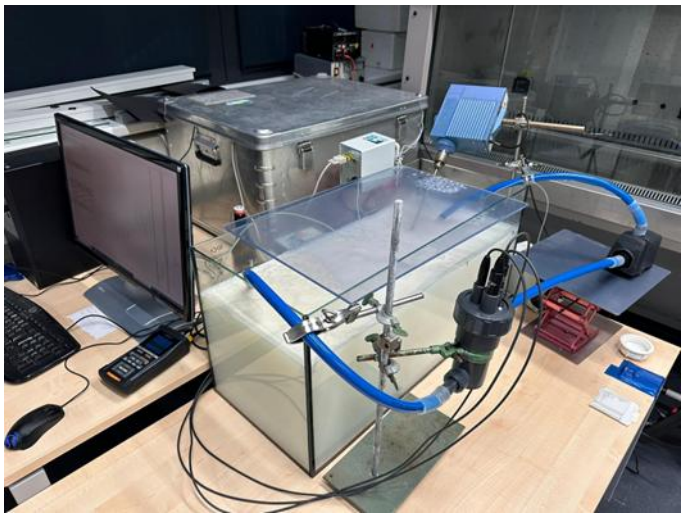

Figure 62: A setup with MWF in longtime experiments showing that measurements in highly concentrated emulsions are possible.

At the beginning of the experiment, the intensity was 2200 intensity units, and with time, it went down, making it hard to see any growth in the measurements. After several weeks, it started to grow strong, which is also seen as biofilms on the apparatus. This is analogous to the results from the previous long-time measurements. After adding chlorine dioxide, the signal went down and started to grow again. The growth phase exhibits a considerable amount of noise. This may be due to staining effects or to cells that clump together and lead to increased fluorescence. By using the amines, a higher concentration of chlorine dioxide is required here. This makes the use of chlorine dioxide difficult in this area, but by omitting the fast-reacting components, hygienization can also be achieved here (Figure 63).

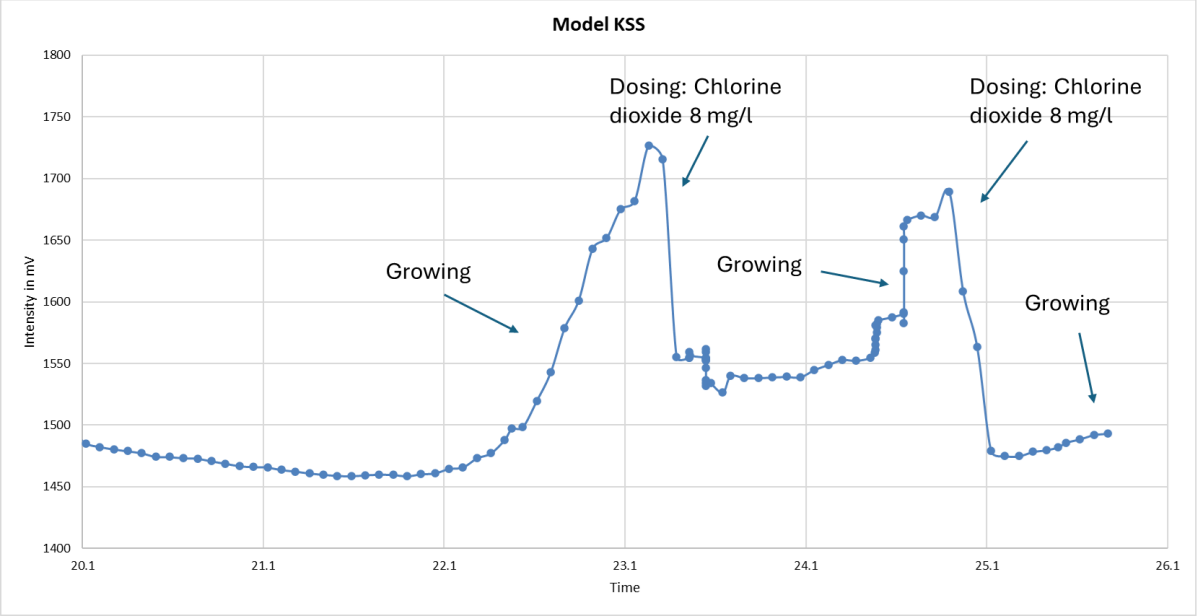

Figure 63: The growth of bacteria in a model MWF over several days and disinfection with chlorine dioxide.

This clearly shows that measurements are possible but with limitations regarding the components used. A solution approach here would be to go into the area of amine-free MWF. Measuring these solutions undiluted will also be problematic, but this problem can be solved by dilution. Since flow rates in the range of approximately 1 ml/min are more than sufficient for the measurement, the diluted solution can also be recycled.

The control of MWF is indeed feasible, though with certain limitations. It is advisable to avoid components that react quickly, such as tertiary amines and the biocide Acticide B20. However, it has been demonstrated that even challenging process waters can be effectively treated with appropriate optimizations. Consequently, the device can be utilized in most, if not all, types of process waters. This fluorescence sensor fundamentally elevates hygienization standards to a new and superior level.

6. Summary

As part of our research on microbiological contamination detection and control, we demonstrated that fluorescence can effectively detect microorganisms and monitor disinfection efficacy. In our search for a suitable target for monitoring microbial growth, we examined whether NADPH, which is essential for energy supply, could serve this purpose. Our fluorescence spectroscopy measurements on pure NADPH showed that detection is possible, achieving very low detection limits of 4,2 µg/l. However, we found that NADPH could not be detected in living cells, as its concentration in cells is too low to be an effective target (1,8 µg NADPH /gram bacteria dry weight).

Measurements of living organisms revealed fluorescence, which we thoroughly investigated to discover that this was due to autofluorescence from proteins in the cell membrane of microorganisms. We also found that chlorine dioxide can reduce or eliminate this autofluorescence. Since only a few essential amino acids fluoresce and react with chlorine dioxide, this helped us narrow down potential target compounds. We identified that tryptophan is the primary contributor to autofluorescence. Experiments with tryptophan and tryptophan-containing peptides showed a distinct degradation of the amino acid. This degradation of fluorescence was also observable in real organisms.

Given the correlation between fluorescence and living organisms, we explored whether fluorescence displays linear behaviour in living organisms. Fluorescence measurements combined with plating indicated a good linear relationship: an increase in living cells corresponds to an increase in fluorescence. We also observed that cells killed by chlorine dioxide no longer fluoresce.

To facilitate online analysis, we developed a fixed-wavelength fluorescence sensor that is both robust and sensitive. The chosen light source is a UV LED emitting at 280 nm, housed within a quartz glass tube. A bandpass filter allows transmission at 340 nm, and a photodiode capable of measuring in the range of 200 to 1100 nm is employed. The photodiode generates a current signal which is converted into a measurable current through a trans-impedance amplifier and then into a digital signal using an AD converter. Our measurements indicated that this setup can achieve detection limits as low as 2 µg Trp/L.

To assess the sensor's suitability for industrial applications, we tested it on a model cooling lubricant. The sensor effectively detected microbial contamination. Based on these preliminary

tests, we could establish a control loop that enables the detection and regulation of microbial contamination using chlorine dioxide.

7. Further Outlook

For further investigations, it would be valuable to examine the microbiological aspects of the measurements closely. Under certain conditions, low concentrations of chlorine dioxide may promote the growth of specific types of bacteria or fungi, significantly impacting the microbiome. Molds often exhibit greater chlorine dioxide resistance than bacteria, which could lead to an increased prevalence of fungi. It would be particularly interesting to analyse the microbial composition during both the dosing and growth phases.

In addition, an analytical view of the organic molecules would be unexplored. It is conceivable that such small doses retain certain molecules that can also be used for interaction between cells (quorum sensing molecules). These can also significantly influence the quality of the water.

Further optimisations could be carried out on the sensor to reduce the detection limit. The noise level would have to be reduced for this. To this end, the components used to date, such as AD converters and microcontrollers, could be optimised.

The optical filter could also be applied to the measuring cell or the photodiode to make the device more compact. This would save a component and minimise the path length of the light. This would ultimately lead to a more intense signal and thus also reduce the detection limit.

Since this device will eventually be utilised in industrial settings, testing it across various application areas and conducting pilot studies would be beneficial. For instance, the sensors could be implemented in cooling, pool, and gastronomy water, such as in dishwashers and washing machines. Water that is used in areas that have high hygiene standards is also useful, such as cutting tools in the meat and fish industry, among others. Also, the drinking water of farm animals, such as cows and pigs, is often provided in containers for the animals. However, it is essential to assess compatibility for these applications. Additionally, the optimal measurement point needs to be determined. In large water containers, the depth of measurement or whether the measurement is taken at the centre or edge can significantly impact results. As is often the case, sampling can introduce the most substantial errors in measurement.

8. References

1. Paranjape, K.; Bédard, É.; Whyte, L. G.; Ronholm, J.; Prévost, M.; Faucher, S. P. Presence of Legionella spp. in cooling towers: the role of microbial diversity, Pseudomonas, and continuous chlorine application. *Water Research* **2020,** *169*, 115252. https://www.sciencedirect.com/science/article/pii/s0043135419310267.

2. Aruliah, R.; Ting, Y.-P. Characterization of Corrosive Bacterial Consortia Isolated from Water in a Cooling Tower. *ISRN Corrosion* **2014,** *2014* (1), 1–11.

3. Di Martino, P. Ways to improve biocides for metalworking fluid. *AIMS microbiology* **2021,** *7* (1), 13–27.

4. Ma, J.-W.; Huang, B.-S.; Hsu, C.-W.; Peng, C.-W.; Cheng, M.-L.; Kao, J.-Y.; Way, T.-D.; Yin, H.-C.; Wang, S.-S. Efficacy and Safety Evaluation of a Chlorine Dioxide Solution. *International Journal of Environmental Research and Public Health* **2017,** *14* (3), 329. https://www.mdpi.com/1660-4601/14/3/329.

5. Hupperich, K.; Mutke, X. A. M.; Abdighahroudi, M. S.; Jütte, M.; Schmidt, T. C.; Lutze, H. V. Reaction of chlorine dioxide with organic matter – formation of inorganic products. *Environ. Sci.: Water Res. Technol.* **2020,** *6* (9), 2597–2606. https://pubs.rsc.org/en/content/articlehtml/2020/ew/d0ew00408a.

6. Gan, W.; Ge, Y.; Zhong, Y.; Yang, X. The reactions of chlorine dioxide with inorganic and organic compounds in water treatment: kinetics and mechanisms. *Environ. Sci.: Water Res. Technol.* **2020,** *6* (9), 2287–2312. https://pubs.rsc.org/en/content/articlehtml/2020/ew/d0ew00231c.

7. Chang, C. Y.; Hsieh, Y. H.; Shih, I. C.; Hsu, S. S.; Wang, K. H. The formation and control of disinfection by-products using chlorine dioxide. *Chemosphere* **2000,** *41* (8), 1181–1186. https://www.sciencedirect.com/science/article/pii/s0045653500000102.

8. Padhi, R. K.; Subramanian, S.; Satpathy, K. K. Formation, distribution, and speciation of DBPs (THMs, HAAs, ClO2-,andClO3-) during treatment of different source water with chlorine and chlorine dioxide. *Chemosphere* **2019,** *218*, 540–550. https://www.sciencedirect.com/science/article/pii/s0045653518322070.

9. Helmi, K.; David, F.; Di Martino, P.; Jaffrezic, M.-P.; Ingrand, V. Assessment of flow cytometry for microbial water quality monitoring in cooling tower water and oxidizing

biocide treatment efficiency. *Journal of Microbiological Methods* **2018,** *152*, 201–209. https://www.sciencedirect.com/science/article/pii/s0167701218304020.

10. Hofmann, R.; Andrews, R. C.; Ye, Q. Comparison of Spectrophotometric Methods for Measuring Chlorine Dioxide in Drinking Water. *Environmental Technology* **1998,** *19* (8), 761–773.
11. Benarde, M. A.; Snow, W. B.; Olivieri, V. P.; Davidson, B. Kinetics and mechanism of bacterial disinfection by chlorine dioxide. *Applied Microbiology* **1967,** *15* (2), 257–265.
12. Benarde, M. A.; Israel, B. M.; Olivieri, V. P.; Granstrom, M. L. Efficiency of chlorine dioxide as a bactericide. *Applied Microbiology* **1965,** *13* (5), 776–780.
13. Wen, G.; Xu, X.; Huang, T.; Zhu, H.; Ma, J. Inactivation of three genera of dominant fungal spores in groundwater using chlorine dioxide: Effectiveness, influencing factors, and mechanisms. *Water Research* **2017,** *125*, 132–140. https://www.sciencedirect.com/science/article/pii/s0043135417307005.
14. Shemesh, M.; Kolter, R.; Losick, R. The biocide chlorine dioxide stimulates biofilm formation in Bacillus subtilis by activation of the histidine kinase KinC. *Journal of Bacteriology* **2010,** *192* (24), 6352–6356.
15. Schlegel, Hans Günter, Thomas Eitinger. Allgemeine Mikrobiologie. *Aktuelle Dermatologie* **2022,** *48* (11), 26–50. https://www.thieme-connect.com/products/ejournals/html/10.1055/a-1725-0952.
16. *Escherichia coli and salmonella typhimurium, 1: cellular and molecular biology. American Soc. for Microbiology.;* Neidhardt, F. C., Ed., 1987.
17. Naresh, V.; Lee, N. A Review on Biosensors and Recent Development of Nanostructured Materials-Enabled Biosensors. *Sensors* **2021,** *21* (4), 1109. https://www.mdpi.com/1424-8220/21/4/1109.
18. McKinnon, K. M. Flow Cytometry: An Overview. *Current Protocols in Immunology* **2018,** *120* (1), 5.1.1-5.1.11.
19. Liu, S.; Zhao, J.; Guo, Y.; Ma, X.; Sun, C.; Cai, M.; Chi, Y.; Xu, K. Application of ATP-based bioluminescence technology in bacterial detection: a review. *Analyst* **2023,** *148* (15), 3452–3459. https://pubs.rsc.org/en/content/articlehtml/2023/an/d3an00576c.

20. *Principles of fluorescence spectroscopy;* Lakowicz, J. R., Ed., 3. ed.; Springer Science+Business Media LLC: Boston, MA, 2006.

21. Dartnell, L. R.; Roberts, T. A.; Moore, G.; Ward, J. M.; Muller, J.-P. Fluorescence characterization of clinically-important bacteria. *PLOS ONE* **2013,** *8* (9), e75270. https://journals.plos.org/plosone/article?id=10.1371/journal.pone.0075270.

22. *Fundamentals of bacterial physiology and metabolism*, 2021.

23. Blacker, T. S.; Duchen, M. R. Investigating mitochondrial redox state using NADH and NADPH autofluorescence. *Free radical biology & medicine* **2016,** *100*, 53–65. https://www.sciencedirect.com/science/article/pii/s0891584916303926.

24. Albrecht, C. Joseph R. Lakowicz: Principles of fluorescence spectroscopy, 3rd Edition. *Anal Bioanal Chem* **2008,** *390* (5), 1223–1224. https://link.springer.com/article/10.1007/s00216-007-1822-x.

25. Atkins, P. W.; Paula, J. de; Keeler, J. J. *Atkins' physical chemistry*, Twelfth edition; Oxford University Press: Oxford, 2023.

26. Sun, P.; Zhang, H.; Sun, Y.; Liu, J. The recent development of fluorescent probes for the detection of NADH and NADPH in living cells and in vivo. *Spectrochimica acta. Part A, Molecular and biomolecular spectroscopy* **2021,** *245*, 118919. https://www.sciencedirect.com/science/article/pii/s1386142520308982.

27. Singh, R.; Mailloux, R. J.; Puiseux-Dao, S.; Appanna, V. D. Oxidative stress evokes a metabolic adaptation that favors increased NADPH synthesis and decreased NADH production in Pseudomonas fluorescens. *Journal of Bacteriology* **2007,** *189* (18), 6665–6675.

28. Liu, Y.; Landick, R.; Raman, S. A Regulatory NADH/NAD+ Redox Biosensor for Bacteria. *ACS Synthetic Biology* **2019,** *8* (2), 264–273.

29. Walton, A. Z.; Stewart, J. D. Understanding and improving NADPH-dependent reactions by nongrowing Escherichia coli cells. *Biotechnology Progress* **2004,** *20* (2), 403–411.

30. Ruyck, J. de; Famerée, M.; Wouters, J.; Perpète, E. A.; Preat, J.; Jacquemin, D. Towards the understanding of the absorption spectra of NAD(P)H/NAD(P)+ as a common indicator of dehydrogenase enzymatic activity. *Chemical Physics Letters* **2007,** *450* (1-3), 119–122. https://www.sciencedirect.com/science/article/pii/s0009261407014790.

31. Sebastian Steigenberger, Frank Terjung, Hans-Peter Grossart, Rainer Reuter. Blue-fluorescence of NADPH as an indicator of marine primary production **2004**.

32. Yaniv Shlosberg, Benjamin Eichenbaum, Tünde N. Toth, Guy Levin, Varda Liveanu, Gadi Schuster, Noam Adir. NADPH performs mediated electron transfer in cyanobacterial-driven bio-photoelectrochemical cells **2021**.

33. Genchi, G. An overview on D-amino acids. *Amino Acids* **2017,** *49* (9), 1521–1533. https://link.springer.com/article/10.1007/s00726-017-2459-5.

34. Backman, L. *Protein Chemistry*; De Gruyter Textbook; De Gruyter: Berlin, Boston, 2020.

35. Chen, Y.; Barkley, M. D. Toward understanding tryptophan fluorescence in proteins. *Biochemistry* **1998,** *37* (28), 9976–9982.

36. Vivian, J. T.; Callis, P. R. Mechanisms of tryptophan fluorescence shifts in proteins. *Biophysical Journal* **2001,** *80* (5), 2093–2109. https://www.cell.com/fulltext/s0006-3495(01)76183-8.

37. Callis, P. R. 1La and 1Lb transitions of tryptophan: applications of theory and experimental observations to fluorescence of proteins. *Methods in enzymology* **1997,** *278*, 113–150.

38. Yang, H., Xiao, X., Zhao, X., & Wu, Y. Intrinsic fluorescence spectra of tryptophan, tyrosine and phenyloalanine **2016,** No. 10255, 1199–1206.

39. Davy, H. On a Combination of Oxymuriatic Gas and Oxygen Gas. *Proceedings of the Royal Society of London Series I* **1811,** No. 101, 155–162.

40. Aieta, E. M.; Berg, J. D. A review of chlorine dioxide in drinking water treatment. *Journal-American Water Works Association* **1986,** *78* (6), 62–72.

41. Schmidt, E.; Graumann, E. Zur Kenntnis pflanzlicher Inkrusten. I. Mitteilung: Methode zur reindarstellung pflanzlicher skelettsubstanzen (I.). *Berichte der deutschen chemischen Gesellschaft (A and B Series)* **1921,** *54* (8), 1860–1873.

42. Torén, K.; Blanc, P. D. The history of pulp and paper bleaching: respiratory-health effects. *Lancet (London, England)* **1997,** *349* (9061), 1316–1318.

43. Aston, R. N. Chlorine dioxide use in plants on the Niagara border. *Journal-American Water Works Association* **1947,** *39* (7), 687–690.

44. Myers, G. L.; Thompson, A. L. Controlling Taste and Odor with Chlorine Dioxide. *Southwest and Texas Water Works Journal* **1986,** *67* (12).

45. McGuire, L.; Dishinger, T. Chlorine Dioxide Solves Biofouling Problems in a Refinery Cooling Tower Used for Phenol Destruction. *CTI, Houston* **1984**.

46. Jonnalagadda, S. B.; Nadupalli, S. Chlorine dioxide for bleaching, industrial applications and water treatment. *Indian Chemical Engineer* **2014,** *56* (2), 123–136.

47. Gordon, G.; Rosenblatt, A. A. Chlorine dioxide: the current state of the art. *Ozone: science & engineering* **2005,** *27* (3), 203–207.

48. Gates, D. J.; Ziglio, G.; Ozekin, K. *State of the science of chlorine dioxide in drinking water;* Water Research Foundation/Fondazione AMGA, 2009.

49. *Verordnung über die Qualität von Wasser für den menschlichen Gebrauch (Trinkwasserverordnung – TrinkwV)*. *TrinkwV 2023*, 2023.

50. Rehr, A.; Jansen, M. Investigations on solid chlorine dioxide: temperature-dependent crystal structure, IR spectrum, and magnetic susceptibility. *Inorg. Chem.* **1992,** *31* (23), 4740–4742.

51. Millon, E. Ueber die Sauerstoffverbindungen des Chlors. *J. Prakt. Chem.* **1843,** *29* (46), 281–319.

52. Brandau, M. Ueber chlorige Säure. *Justus Liebigs Ann. Chem.* **1869,** *151* (3), 340–360.

53. Bray, W. Beiträge zur Kenntnis der Halogensauerstoffverbindungen: Abhandlung III. Zur Kenntnis des Chlordioxyds. *Zeitschrift für Physikalische Chemie* **1906,** No. 54, 569–608.

54. Vogt, H.; Balej, J.; Bennett, J. E.; Wintzer, P.; Sheikh, S. A.; Gallone, P. Chlorine oxides and chlorine oxygen acids. *Ullmann's Encyclopedia of Industrial Chemistry* **2000**.

55. Endrődi, B.; Stojanovic, A.; Cuartero, M.; Simic, N.; Wildlock, M.; Marco, R. de; Crespo, G. A.; Cornell, A. Selective hydrogen evolution on manganese oxide coated electrodes: new cathodes for sodium chlorate production. *ACS Sustainable Chemistry & Engineering* **2019,** *7* (14), 12170–12178.

56. Gordon, G.; Kieffer, R. G.; Rosenblatt, D. H. The chemistry of chlorine dioxide. *Progress in inorganic chemistry* **1972,** *15* (S J), 202–286.

57. Uhlmann, H. METHOD FOR PRODUCING AN AQUEOUS STABLE CHLORINE DIOXIDE SOLUTION. EP20110805787 20111222, Dec 22, 2011.

58. Gordon, G. IS ALL chlorine dioxide CREATED EQUAL? *Journal - American Water Works Association* **2001,** *93* (4), 163–174.

59. Vincenti, S.; Waure, C. de; Raponi, M.; Teleman, A. A.; Boninti, F.; Bruno, S.; Boccia, S.; Damiani, G.; Laurenti, P. Environmental surveillance of Legionella spp. colonization in the water system of a large academic hospital: Analysis of the four–year results on the effectiveness of the chlorine dioxide disinfection method. *Science of The Total Environment* **2019,** *657*, 248–253. https://www.sciencedirect.com/science/article/pii/s0048969718348769.

60. Volk, C. J.; Hofmann, R.; Chauret, C.; Gagnon, G. A.; Ranger, G.; Andrews, R. C. Implementation of chlorine dioxide disinfection: Effects of the treatment change on drinking water quality in a full-scale distribution system. *Journal of Environmental Engineering and Science* **2002,** *1* (5), 323–330.

61. Huang, J.; Wang, L.; Ren, N.; Ma, F.; Juli. Disinfection effect of chlorine dioxide on bacteria in water. *Water Research* **1997,** *31* (3), 607–613. https://www.sciencedirect.com/science/article/pii/s0043135496002758.

62. Ofori, I.; Maddila, S.; Lin, J.; Jonnalagadda, S. B. Chlorine dioxide inactivation of Pseudomonas aeruginosa and Staphylococcus aureus in water: The kinetics and mechanism. *Journal of Water Process Engineering* **2018,** *26*, 46–54. https://www.sciencedirect.com/science/article/pii/s2214714418302836.

63. Jütte, M.; Abdighahroudi, M. S.; Waldminghaus, T.; Lackner, S.; V Lutze, H. Bacterial inactivation processes in water disinfection - mechanistic aspects of primary and secondary oxidants - A critical review. *Water Research* **2023,** *231*, 119626. https://www.sciencedirect.com/science/article/pii/s0043135423000611.

64. Longley, K. E., Moore, B. E., & Sorber, C. A. Comparison of chlorine and chlorine dioxide as disinfectants. *Water Pollution Control Federation* **1980**, 2098–2105.

65. Sharma, V. K. *Oxidation of Amino Acids, Peptides, and Proteins*. *Kinetics and mechanism*; Wiley series on reactive intermediates in chemistry and biology 5; John Wiley & Sons, Inc: Hoboken, NJ, USA, 2012.

66. Young, S. B.; Setlow, P. Mechanisms of killing of Bacillus subtilis spores by hypochlorite and chlorine dioxide. *J. Appl. Microbiol.* **2003,** *95* (1), 54–67.

67. Roller, S. D.; Olivieri, V. P.; Kawata, K. Mode of bacterial inactivation by chlorine dioxide. *Water Research* **1980,** *14* (6), 635–641. https://www.sciencedirect.com/science/article/pii/0043135480901219.

68. Zhu, C.; Chen, Z.; Yu, G. Fungicidal mechanism of chlorine dioxide on Saccharomyces cerevisiae. *Ann Microbiol* **2013,** *63* (2), 495–502. https://link.springer.com/article/10.1007/s13213-012-0494-8.

69. Miller, M. B.; Bassler, B. L. Quorum sensing in bacteria. *Annual Review of Microbiology* **2001,** *55* (Volume 55, 2001), 165–199.

70. Da Cruz Nizer, W. S.; Inkovskiy, V.; Overhage, J. Surviving Reactive Chlorine Stress: Responses of Gram-Negative Bacteria to Hypochlorous Acid. *Microorganisms* **2020,** *8* (8), 1220. https://www.mdpi.com/2076-2607/8/8/1220.

71. Li Mei; Tian Shilong; Shen Jin; Wang Xizhuo; Cheng Jianxin; Li Shouqiang; Ge Xia; Tian Jiachun. Effects of chlorine dioxide on morphology and ultrastructure of Fusarium sulphureum and its virulence to potato tubers. *International Journal of Agricultural and Biological Engineering* **2017,** *10* (5), 242–250. https://www.ijabe.org/index.php/ijabe/article/view/2403.

72. Noss, C. I.; Hauchman, F. S.; Olivieri, V. P. Chlorine dioxide reactivity with proteins. *Water Research* **1986,** *20* (3), 351–356. https://www.sciencedirect.com/science/article/pii/0043135486900837.

73. TAN, H.; SEN, A. C.; WHEELER, W. B.; CORNELL, J. A.; WEI, C. I. A Kinetic Study of the Reaction of Aqueous Chlorine and Chlorine Dioxide with Amino Acids, Peptides and Proteins. *Journal of Food Science* **1987,** *52* (6), 1706–1711.

74. Byers, J. P. *Metalworking fluids;* crc Press, 2016.

75. Brinksmeier, E.; Meyer, D.; Huesmann-Cordes, A. G.; Herrmann, C. Metalworking fluids—Mechanisms and performance. *0007-8506* **2015,** *64* (2), 605–628. https://www.sciencedirect.com/science/article/pii/s0007850615001420.

76. Tang, L.; Zhang, Y.; Li, C.; Zhou, Z.; Nie, X.; Chen, Y.; Cao, H.; Liu, B.; Zhang, N.; Said, Z.; Debnath, S.; Jamil, M.; Ali, H. M.; Sharma, S. Biological Stability of Water-Based Cutting Fluids: Progress and Application. *Chin. J. Mech. Eng.* **2022,** *35* (1), 1–24. https://link.springer.com/article/10.1186/s10033-021-00667-z.

77. Afonso, I. S.; Nobrega, G.; Lima, R.; Gomes, J. R.; Ribeiro, J. E. Conventional and Recent Advances of Vegetable Oils as Metalworking Fluids (MWFs): A Review. *Lubricants* **2023,** *11* (4), 160. https://www.mdpi.com/2075-4442/11/4/160.

78. Padmanaban, V.; Anbuudayasankar, S. P.; Ashokkumar, A.; Sharan, A. Development of Bio based Semi-Synthetic Metal Working Fluid from Industrial Waste Water. *1877-7058* **2013,** *64*, 1436–1444. https://www.sciencedirect.com/science/article/pii/s1877705813017396.

79. Nune, M. M. R.; Chaganti, P. K. Development, characterization, and evaluation of novel eco-friendly metal working fluid. *Measurement* **2019,** *137*, 401–416. https://www.sciencedirect.com/science/article/pii/s0263224119300752.

80. Lodhi, A. P. S.; Kumar, D. Natural ingredients based environmental friendly metalworking fluid with superior lubricity. *Colloids and Surfaces A: Physicochemical and Engineering Aspects* **2021,** *613*, 126071. https://www.sciencedirect.com/science/article/pii/s0927775720316642.

81. Koch, T. Microbiology of Metalworking Fluids: What We Know and Lessons to be Learnt. *Acta Mechanica et Automatica* **2023,** *17* (2), 166–172.

82. VEILLETTE, M.; THORNE, P. S.; GORDON, T.; DUCHAINE, C. Six month tracking of microbial growth in a metalworking fluid after system cleaning and recharging. *Ann Occup Hyg* **2004,** *48* (6), 541–546.

83. Stolte, S.; Steudte, S.; Areitioaurtena, O.; Pagano, F.; Thöming, J.; Stepnowski, P.; Igartua, A. Ionic liquids as lubricants or lubrication additives: an ecotoxicity and biodegradability assessment. *Chemosphere* **2012,** *89* (9), 1135–1141. https://www.sciencedirect.com/science/article/pii/s0045653512007497.

84. Montgomery, R. S. Chemical effects on wear in the lubrication of aluminum. *Wear* **1965,** *8* (4), 289–302. https://www.sciencedirect.com/science/article/pii/0043164865900049.

85. Igari, S.; Mori, S.; Takikawa, Y. Effects of molecular structure of aliphatic diols and polyalkylene glycol as lubricants on the wear of aluminum. *Wear* **2000,** *244* (1-2), 180–184. https://www.sciencedirect.com/science/article/pii/s0043164800004580.

86. Rudnick, L. R. *Synthetics, mineral oils, and bio-based lubricants*. *Chemistry and technology*, Third edition; Chemical industries 135; crc Press: Boca Raton, 2020.

87. Beszterda, M.; Nogala-Kałucka, M. Current Research Developments on the Processing and Improvement of the Nutritional Quality of Rapeseed (Brassica napus L.). *Euro J Lipid Sci & Tech* **2019,** *121* (5), 1800045.

88. Rapeseed oil. *Green Sustainable Process for Chemical and Environmental Engineering and Science* **2021**, 41–55.

89. Yuan, Q.; Tu, M.; Gao, P.; Hu, C.; He, D. Comparative Analysis of Rapeseed Oils Prepared by Three Different Methods. *Journal of Oleo Science* **2020,** *69* (12), 1641–1648. https://www.jstage.jst.go.jp/article/jos/69/12/69_ess20188/_article/-char/ja/.

90. Sreenivasan, B.; Kamath, N. R.; Kane, J. G. Studies on castor oil. I. Fatty acid composition of castor oil. *J Am Oil Chem Soc* **1956,** *33* (2), 61–66. https://link.springer.com/article/10.1007/bf02612549.

91. Magee, T. V.; Zinkel, D. F. Composition of American distilled tall oils. *J Am Oil Chem Soc* **1992,** *69* (4), 321–324.

92. Council, N. R.; Agriculture, B. o.; Board, F. a. N.; Resources, Board on Agriculture and Renewable; Sciences, A. o. L.; Resources, C. o. N. *Fat content and composition of animal products*. *Proceedings of a symposium, Washington, D. C. December 12-13, 1974;* National Academy of Sciences: Washington, 1976.

93. Barbera, E.; Hirayama, K.; Maglinao, R. L.; Davis, R. W.; Kumar, S. Recent developments in synthesizing biolubricants — a review. *Biomass Conv. Bioref.* **2022**, 1–21.

94. Rudnick, L. R. *Lubricant additives*. *Chemistry and applications*, 2nd ed.; Chemical industries 124; crc Press: Boca Raton, 2009.

95. Schulz, J.; Brinksmeier, E.; Meyer, D. On the Interactions of Additives in Metalworking Fluids with Metal Surfaces. *Lubricants* **2013,** *1* (4), 75–94. https://www.mdpi.com/2075-4442/1/4/75.

96. Denkena, B. *Spanen*. *Grundlagen*, 3rd ed.; VDI-Buch Ser; Springer Berlin / Heidelberg: Berlin, Heidelberg, 2011.

97. Li, H.; Zhang, Y.; Li, C.; Zhou, Z.; Nie, X.; Chen, Y.; Cao, H.; Liu, B.; Zhang, N.; Said, Z.; Debnath, S.; Jamil, M.; Ali, H. M.; Sharma, S. Extreme pressure and antiwear additives for lubricant: academic insights and perspectives. *Int J Adv Manuf Technol* **2022,** *120* (1-2), 1–27. https://link.springer.com/article/10.1007/s00170-021-08614-x.

98. Petrushina, I.; Christensen, E.; Bergqvist, R.; Møller, P.; Bjerrum, N.; Høj, J.; Kann, G.; Chorkendorff, I. On the chemical nature of boundary lubrication of stainless steel by chlorine- and sulfur-containing EP-additives. *Wear* **2000,** *246* (1-2), 98–105. https://www.sciencedirect.com/science/article/pii/s0043164800005032.

99. Yan, L.; Yao, X.; Zhang, T.; Jiang, F.; Shui, Y.; Xie, H.; Xiang, Z.; Li, Y.; Lin, L. Passivation Effect of the Chlorinated Paraffin Added in the Cutting Fluid on the Surface Corrosion Resistance of the Stainless Steel. *Molecules (Basel, Switzerland)* **2023,** *28* (9). DOI: 10.3390/molecules28093648.

100. A. Hartwig. Komponenten von Kühlschmierstoffen, Hydraulikflüssigkeiten und anderen Schmierstoffen [MAK Value Documentation in German language, 2018]. *The MAK-Collection for Occupational Health and Safety*; John Wiley & Sons, Ltd, 2018; pp 1417–1471.

101. *Possibility of Replacing the Chorinated Paraffins in Metalworking Fluids*, 2013.

102. Gabor Zoltan Nagy; Roland Nagy. Study on Sulfurized Vegetable Oil Type Extreme Pressure Additives. *1* **2023,** *105*, 235–240. https://www.cetjournal.it/index.php/cet/article/view/cet23105040.

103. Ding, H.; Yang, X.; Xu, L.; Li, M.; Li, S.; Zhang, S.; Xia, J. Analysis and comparison of tribological performance of fatty acid-based lubricant additives with phosphorus and sulfur. *2369-9698* **2020,** *5* (2), 134–142. https://www.sciencedirect.com/science/article/pii/s2369969820300657.

104. Lotierzo, A.; Pifferi, V.; Ardizzone, S.; Pasqualin, P.; Cappelletti, G. Insight into the role of amines in Metal Working Fluids. *Corrosion Science* **2016,** *110*, 192–199. https://www.sciencedirect.com/science/article/pii/s0010938x16301792.

105. Annand, R. R.; Hurd, R. M.; Hackerman, N. Adsorption of Monomeric and Polymeric Amino Corrosion Inhibitors on Steel. *J. Electrochem. Soc.* **1965,** *112* (2), 138. https://iopscience.iop.org/article/10.1149/1.2423482/meta.

106. Tomala, A.; Naveira Suarez, A.; Rodríguez Ripoll, M. Tribological Behaviour of Corrosion Inhibitors in Metal Working Fluids under Different Contact Conditions. *AMR* **2014,** *966-967*, 347–356. https://www.scientific.net/amr.966-967.347.

107. Madanchi, N.; Thiede, S.; Herrmann, C. Functional and Environmental Evaluation of Alternative Disinfection Methods for Cutting Fluids. *2212-8271* **2017,** *61*, 558–563. https://www.sciencedirect.com/science/article/pii/s221282711631335x.

108. Saha, R.; Donofrio, R. S. The microbiology of metalworking fluids. *Appl Microbiol Biotechnol* **2012,** *94* (5), 1119–1130. https://link.springer.com/article/10.1007/s00253-012-4055-7.

109. Saha, R.; Donofrio, R. S.; Bagley, S. T. Determination of the effectiveness of UV radiation as a means of disinfection of metalworking fluids. *Ann Microbiol* **2014,** *64* (2), 831–838. https://link.springer.com/article/10.1007/s13213-013-0722-x.

110. Gerulova, K.; Buranská, E.; Tatarka, O.; Szabova, Z. Preliminary Study of Ozone Utilization in Elimination of Bacterial Contamination in Metalworking Fluids. *KEM* **2013,** *581*, 143–147. https://www.scientific.net/kem.581.143.

111. Lautenschlager, K.; Boon, N.; Wang, Y.; Egli, T.; Hammes, F. Overnight stagnation of drinking water in household taps induces microbial growth and changes in community composition. *Water Research* **2010,** *44* (17), 4868–4877. https://www.sciencedirect.com/science/article/pii/s0043135410005002.

112. Kapoor, R.; Selvaraju, S. B.; Subramanian, V.; Yadav, J. S. Microbial Community Establishment, Succession, and Temporal Dynamics in an Industrial Semi-Synthetic Metalworking Fluid Operation: A 50-Week Real-Time Tracking. *Microorganisms* **2024,** *12* (2), 267. https://www.mdpi.com/2076-2607/12/2/267.

113. Gilbert, Y.; Veillette, M.; Duchaine, C. Metalworking fluids biodiversity characterization. *Journal of applied microbiology* **2010,** *108* (2), 437–449.

114. Koch, T.; Passman, F.; Rabenstein, A. Comparative study of microbiological monitoring of water-miscible metalworking fluids. *International Biodeterioration & Biodegradation* **2015,** *98*, 19–25. https://www.sciencedirect.com/science/article/pii/s0964830514003539.

115. Mao, Y.; Chen, X.-W.; Chen, Z.; Chen, G.-Q.; Lu, Y.; Wu, Y.-H.; Hu, H.-Y. Characterization of bacterial fluorescence: insight into rapid detection of bacteria in water. *Journal of Water Reuse and Desalination* **2021,** *11* (4), 621–631.

116. Lilius, E. M.; Multanen, V. M.; Toivonen, V. Quantitative extraction and estimation of intracellular nicotinamide nucleotides of Escherichia coli. *Analytical biochemistry* **1979,** *99* (1), 22–27.

117. Simões, J.; Dong, T. Continuous and real-time detection of drinking-water pathogens with a low-cost fluorescent optofluidic sensor. *Sensors* **2018,** *18* (7), 2210.

118. Ison, A.; Odeh, I. N.; Margerum, D. W. Kinetics and mechanisms of chlorine dioxide and chlorite oxidations of cysteine and glutathione. *Inorg. Chem.* **2006,** *45* (21), 8768–8775.

119. Napolitano, M. J.; Green, B. J.; Nicoson, J. S.; Margerum, D. W. Chlorine dioxide oxidations of tyrosine, N-acetyltyrosine, and dopa. *Chemical research in toxicology* **2005,** *18* (3), 501–508.

120. Stewart, D. J.; Napolitano, M. J.; Bakhmutova-Albert, E. V.; Margerum, D. W. Kinetics and mechanisms of chlorine dioxide oxidation of tryptophan. *Inorg. Chem.* **2008,** *47* (5), 1639–1647.

121. Navalon, S.; Alvaro, M.; Garcia, H. Chlorine dioxide reaction with selected amino acids in water. *Journal of Hazardous Materials* **2009,** *164* (2-3), 1089–1097. https://www.sciencedirect.com/science/article/pii/s0304389408013368.

122. Cumberland, S.; Bridgeman, J.; Baker, A.; Sterling, M.; Ward, D. Fluorescence spectroscopy as a tool for determining microbial quality in potable water applications. *Environmental Technology* **2012,** *33* (4-6), 687–693.

123. Nakar, A.; Schmilovitch, Z.; Vaizel-Ohayon, D.; Kroupitski, Y.; Borisover, M.; Sela Saldinger, S. Quantification of bacteria in water using PLS analysis of emission spectra of fluorescence and excitation-emission matrices. *Water Research* **2020,** *169*, 115197. https://www.sciencedirect.com/science/article/pii/s0043135419309716.

124. Beal, J.; Farny, N. G.; Haddock-Angelli, T.; Selvarajah, V.; Baldwin, G. S.; Buckley-Taylor, R.; Gershater, M.; Kiga, D.; Marken, J.; Sanchania, V.; Sison, A.; Workman, C. T. Robust estimation of bacterial cell count from optical density. *Commun Biol* **2020,** *3* (1), 512. https://www.nature.com/articles/s42003-020-01127-5.

125. Deutsches Institut für Normung. *Wasserbeschaffenheit – Allgemeine Anleitung zur Zählung von Mikroorganismen durch Kulturverfahren*, 2007 (ISO 8199:2005).

126. Ayala, N.; Zamora, A.; Rinnan, Å.; Saldo, J.; Castillo, M. The effect of heat treatment on the front-face fluorescence spectrum of tryptophan in skim milk. *Journal of Food Composition and Analysis* **2020,** *92*, 103569. https://www.sciencedirect.com/science/article/pii/s0889157518313358.

127. Imtiaz, S.; Anwar, S.; Zada, L.; Ali, H.; Khurram, M. S.; Saeed, A.; Saleem, M. Fluorescence Spectroscopy for the Assessment of Microbial Load in UVC Treated Water. *J Fluoresc* **2023,** *33* (6), 2339–2347. https://link.springer.com/article/10.1007/s10895-023-03226-y.

128. Huang, X.; Wei, Z.; Zhao, G.; Gao, X.; Yang, S.; Cui, Y. Optimization of sterilization of Escherichia coli in milk by surfactin and fengycin using a response surface method. *Curr Microbiol* **2008,** *56* (4), 376–381. https://link.springer.com/article/10.1007/s00284-007-9066-8.

129. Hirayama, H.; Fujikawa, S.; Noguchi, N.; Norimatsu, J.; Takano, T.; Tsubaki, K.; Kamata, N. 222–282 nm AlGaN and InAlGaN-based deep-UV LEDs fabricated on high-quality AlN on sapphire. *physica status solidi (a)* **2009,** *206* (6), 1176–1182.

130. Liu, H.-M.; Lin, Y.-H.; Tsai, M.-Y.; Lin, W.-H. Occurrence and characterization of culturable bacteria and fungi in metalworking environments. *Aerobiologia* **2010,** *26* (4), 339–350. https://link.springer.com/article/10.1007/s10453-010-9169-8.

131. McCreath, K. J.; Specht, C. A.; Robbins, P. W. Molecular cloning and characterization of chitinase genes from Candida albicans. *Proceedings of the National Academy of Sciences of the United States of America* **1995,** *92* (7), 2544–2548.

132. Achatz, G.; Oberkofler, H.; Lechenauer, E.; Simon, B.; Unger, A.; Kandler, D.; Ebner, C.; Prillinger, H.; Kraft, D.; Breitenbach, M. Molecular cloning of major and minor allergens of Alternaria alternata and Cladosporium herbarum. *Molecular Immunology* **1995,** *32* (3), 213–227. https://www.sciencedirect.com/science/article/pii/016158909400108d.

133. GHANBARI, H. A.; WHEELER, W. B.; KIRK, J. R. Reactions of Aqueous Chlorine and Chlorine Dioxide with Lipids: Chlorine Incorporation. *J Food Science* **1982,** *47* (2), 482–485.

134. Lindgren, B. O.; Svahn, C. M. Reactions of chlorine dioxide with unsaturated compounds. II. Methyl oleate. *Acta Chem. Scand* **1966,** *20* (1).

135. Nuțiu, E.; Albu, S. Composition for Anticorrosive Cooling and Protection Emulsion. *2351-9789* **2020,** *46*, 34–37. https://www.sciencedirect.com/science/article/pii/s2351978920308775.

136. Hull, L. A.; Davis, G. T.; Rosenblatt, D. H.; Williams, H. K. R.; Weglein, R. C. Oxidations of Amines. III. Duality of Mechanism in the Reaction of Amines with Chlorine Dioxide. *J. Am. Chem. Soc.* **1967,** *89* (5), 1163–1170.

137. Rosenblatt, D. H., Hayes Jr, A. J., Harrison, B. L., Streaty, R. A., & Moore, K. A. *The Reaction of Chlorine Dioxide with Triethylamine in Aqueous Solution1*, 1963. The Journal of Organic Chemistry, 28(10), 2790-2794.

9. Appendix

9.1 List of Figures

9.2 List of Tables

9.3 Chemicals

NADPH	NADPH-Tetranatriumsalz, 100 mg ≥95 %, für die Biochemie, CAS Nr. 2646-71-1
Tryptophan	Fluca AG, pur 99%, CAS: 73-22-3
KCl	Kaliumchlorid, p.a., 1000g
NaCl	Natriumchlorid, p.a., 1000g
KH2PO4	Kaliumhydrogenphosphat Carl Roth GmbH + Co. KG ≥99%, p.a., ACS
Na2HPO4	Dinatriumhydrogenphosphat Carl Roth GmbH + Co. KG ≥99%, p.a., ACS
PO	
ClO_2	Chlorine dioxide solution 6 g/l (ClO2) a.p.f Aqua System AG
$NaClO_2$	Natriumchloritlösung 25 % (NaClO2) Brenntag GmbH
$Na_2S_2O_8$	Natriumperoxodisulfat kristallin (Na2S2O4) Brenntag GmbH
R2A-Agar	Carl Roth GmbH Ph. Eur.for microbiology (CL01.1)
H-MetPro-D-Phe-ArgD-Try-Phe-LysPro-Val-NH2	BLD Pharm, pur 97%, CAS: 158563-45- 2
Gastrin/ H-TryMet-Asp-PheNH2	Bachem AG, pur -%, CAS: H31100100
H-TryTry-Try-OH	Bachem AG, pur -%, CAS: H69700050
Try-Leu	BLD Pharm, pur 97%, CAS: 5156-22-9
(S)-2-((S)-2- Amino-3-(1Hindol-3-yl)propanamido)- 3-(1H-indol-3-yl)propanoic acid 2,2,2- trifluoroacetate	BLD Pharm, pur 95%, CAS: 1631031- 74-7
Deionized water	
Ultrapure water	

Akypo RO90	
SNS 467	
Walloxen SP20	
MTP 090	
Fosfodet CS-0606	
Lakeland PPE 1614	
Additin RC 2540	
Ilcolube 5000	
Ilcolube 7030	
Rüböl Raff	
Rizinusöl	
Tallöl Dest 25/30	
T9 (Hygold 60)	
DCHA	
TEA99	
AMP 95	
MDEA	
Acticid B20	
Diacid 1550	
Borsäure	
Isofol 16	
Phenoxyethanol	
Wallimul RFS 3085	
Crodafos T5A-LQ(RB)	
Additin RC 2526	
Rewocoros AC 101	
FOAM BAN HP 990	
Corrguard EXT	
Dicyclohexylamin	
Benzotriazol	
Irgacor L190	
Emulsogen 4617	
Rewocoros AL 200	
GL-MerGal K20	
Fungitrol L30	
Phenoxypropanol	
GL RC-Oxylat TD8	
Walloxen RO 110	
SNS 497 Na-Sulfonat	
SNS 527 Na-Sulfonat	
Moslube TFL	
Irgamet 42	

GL-MerGal K20	
Fungitrol L30	
Bodoxim AH	
Defoamer CU	
FOAM BAN MS 575	
Densil DN	
FM	
Isononansäure	
pg	
genapol	
becrosan	

9.4 Devices and Parameters

UV/Vis spectrometer	Analytik Jena Specord 205 UV-VIS Spektrophotometer Spectra: 200-500 nm, 0,1 nm step, int time 0,2 Sek. Intensity: 360 nm
Fluorescence spectrometer	Jasko FP-8300 Spectrofluorometer
HPLC fluorescence detektor	Hitachi Merck F-1080 HPLC Fluorescence Detector
Hamamatsu fluorescence detektor	Photodiode module C10439-01
GC x GC - MS	Shimadzu GCMS-QP2010 Ultra

9.5 Measurements and Data

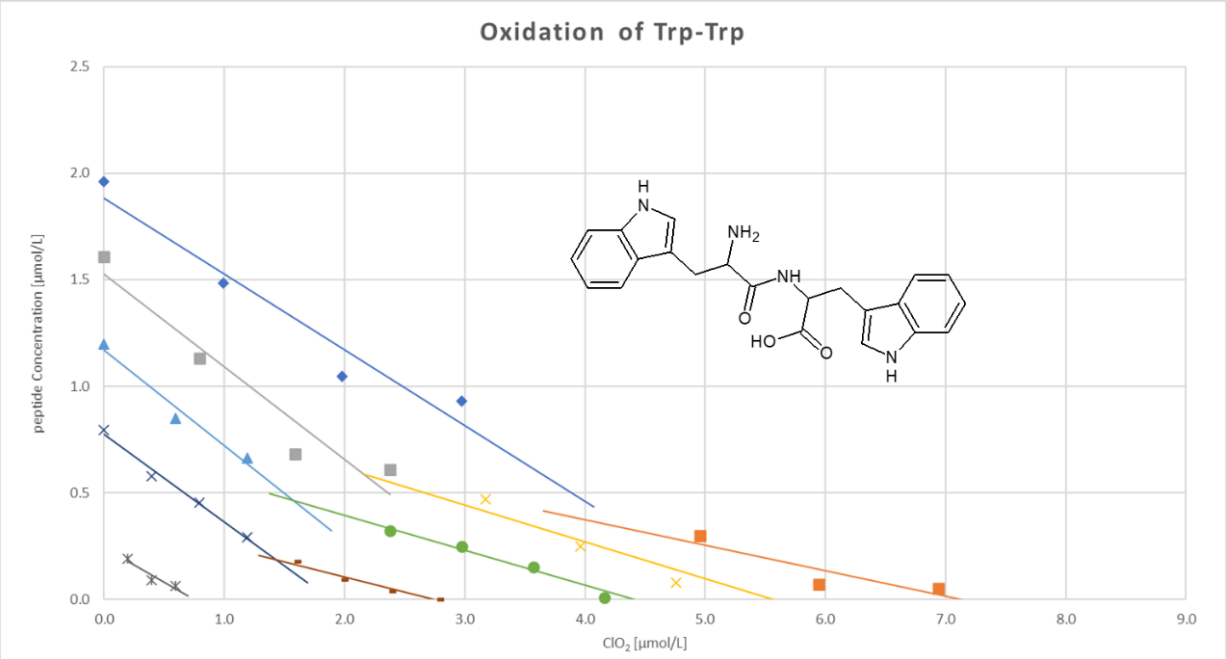

Figure 64: Measurement of Trp-Trp.

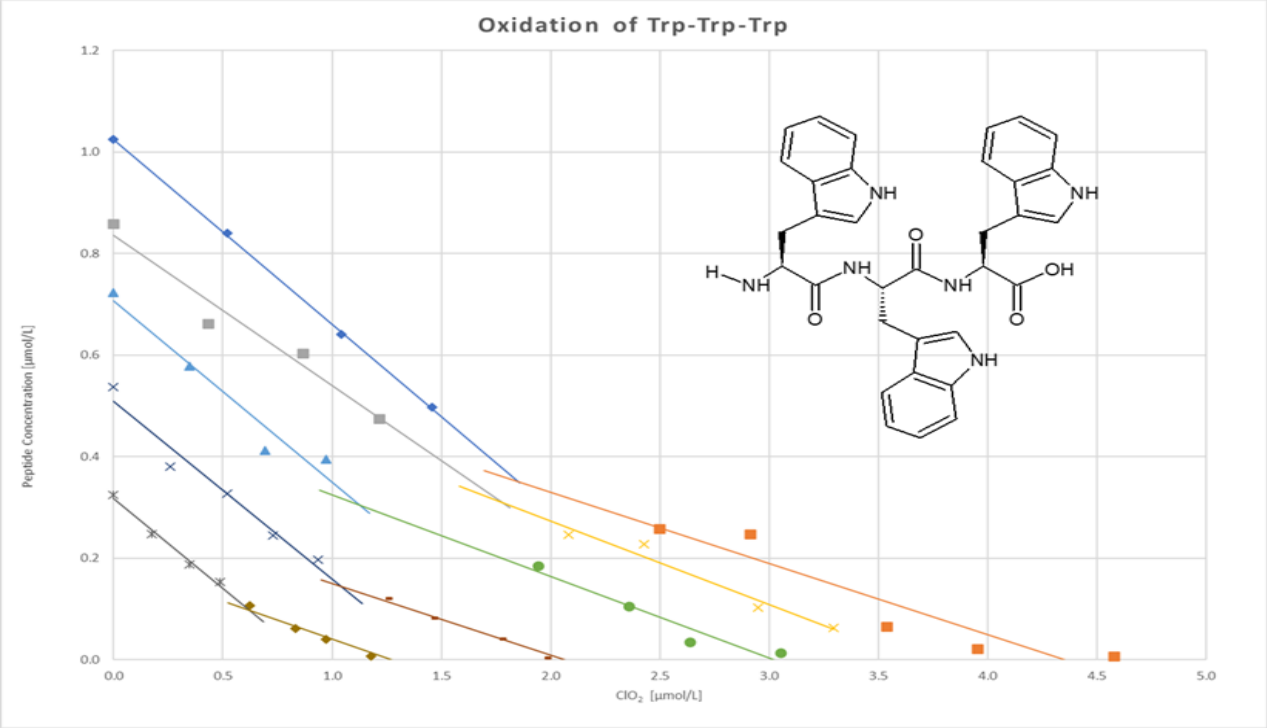

Figure 65: Measurement of Trp-Trp-Trp.

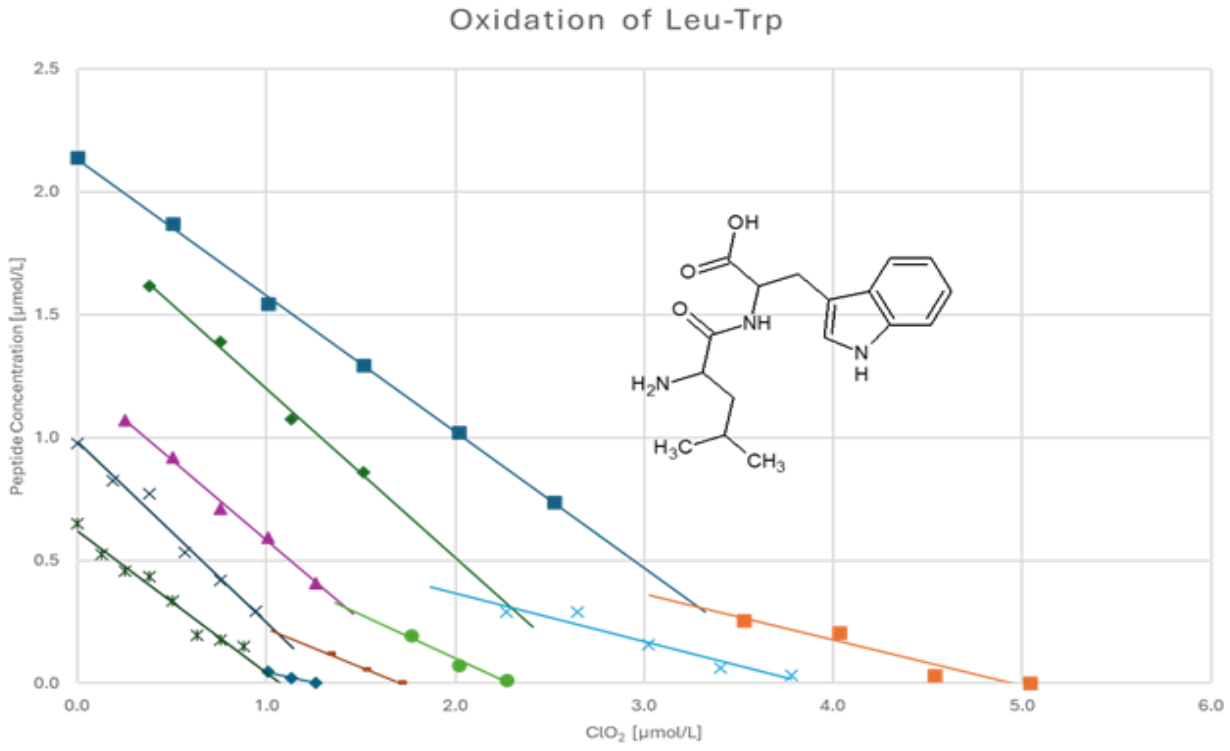

Figure 66:Measurement of Leu-Trp.

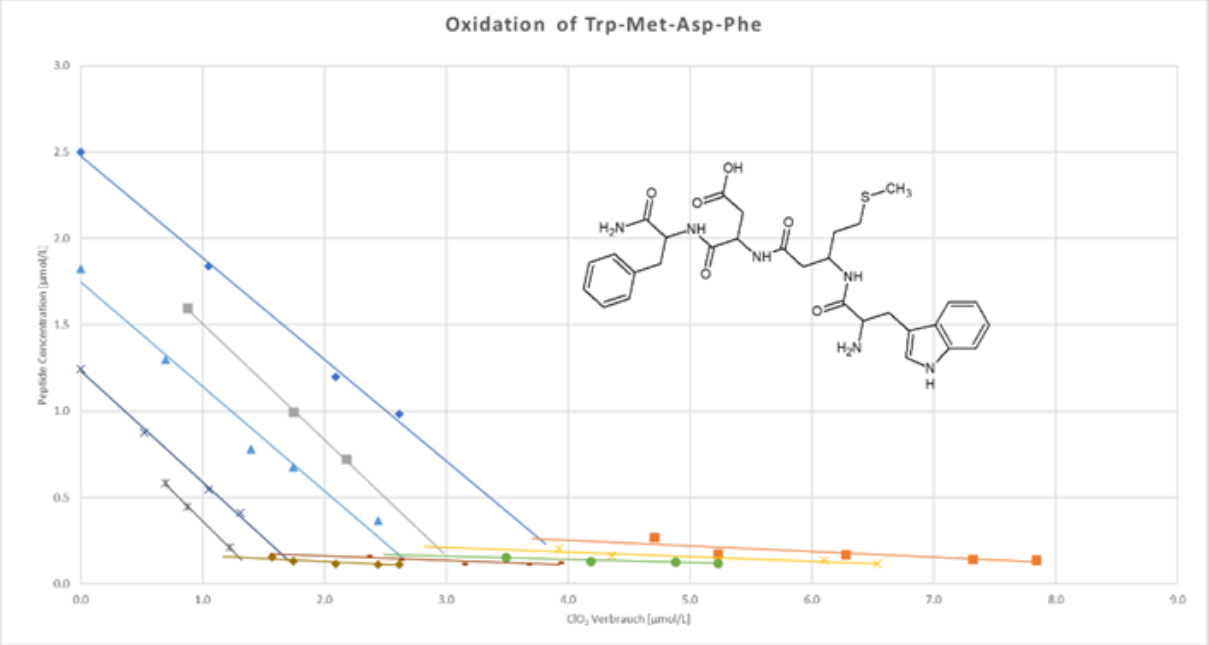

Figure 67:Measurement of Trp-Met-Asp-Phe.

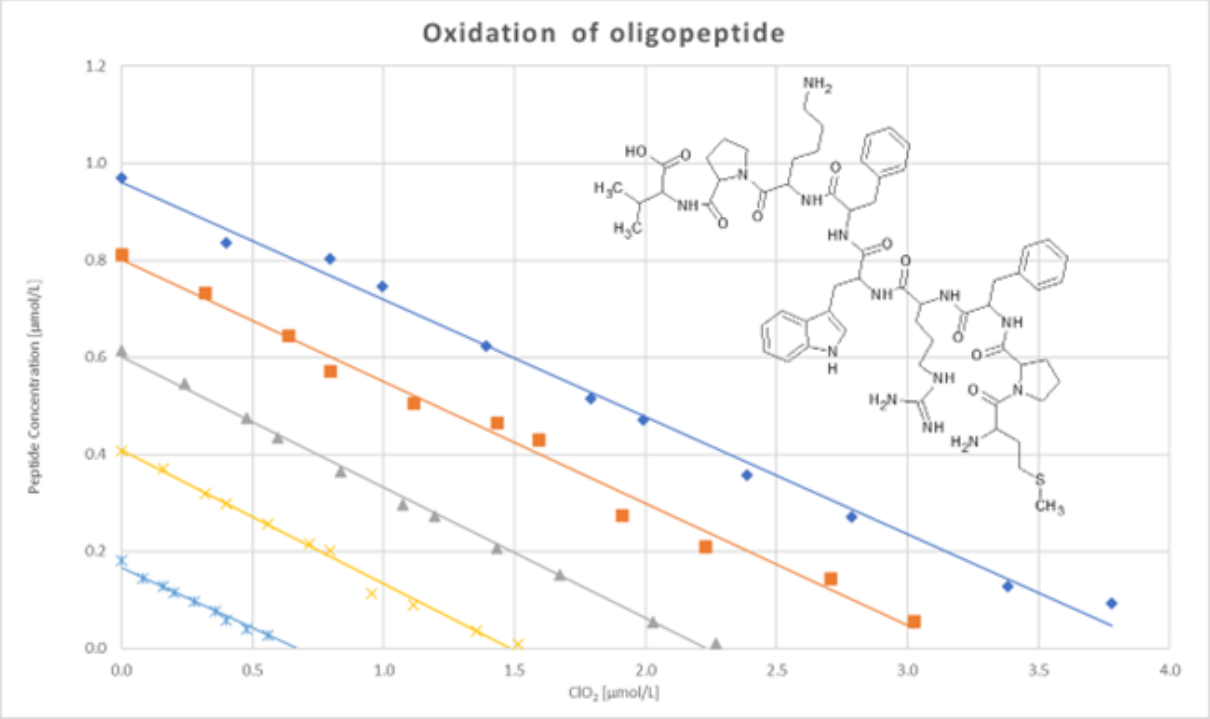

Figure 68: Measurement of the oligopeptide H-Met-Pro-D-Phe-Arg-D-Try-Phe-Lys-Pro-Val-NH_2.

Table 23: Measurement of all peptides with the two gradients.

Concentration	The gradient of the straight one	The gradient of the straight two
Trp	Middle: -0,327	Middle: -0,120
Trp-Trp	Middle: -0,395	Middle: -0,135
Trp-Trp-Trp	Middle: -0,345	Middle: -0,146
Trp-Leu	Middle: -0,642	Middle: -0,250
Gastrin	Middle: -0,658	Middle: -0,018
oligopeptide	Middle: -0,257	-

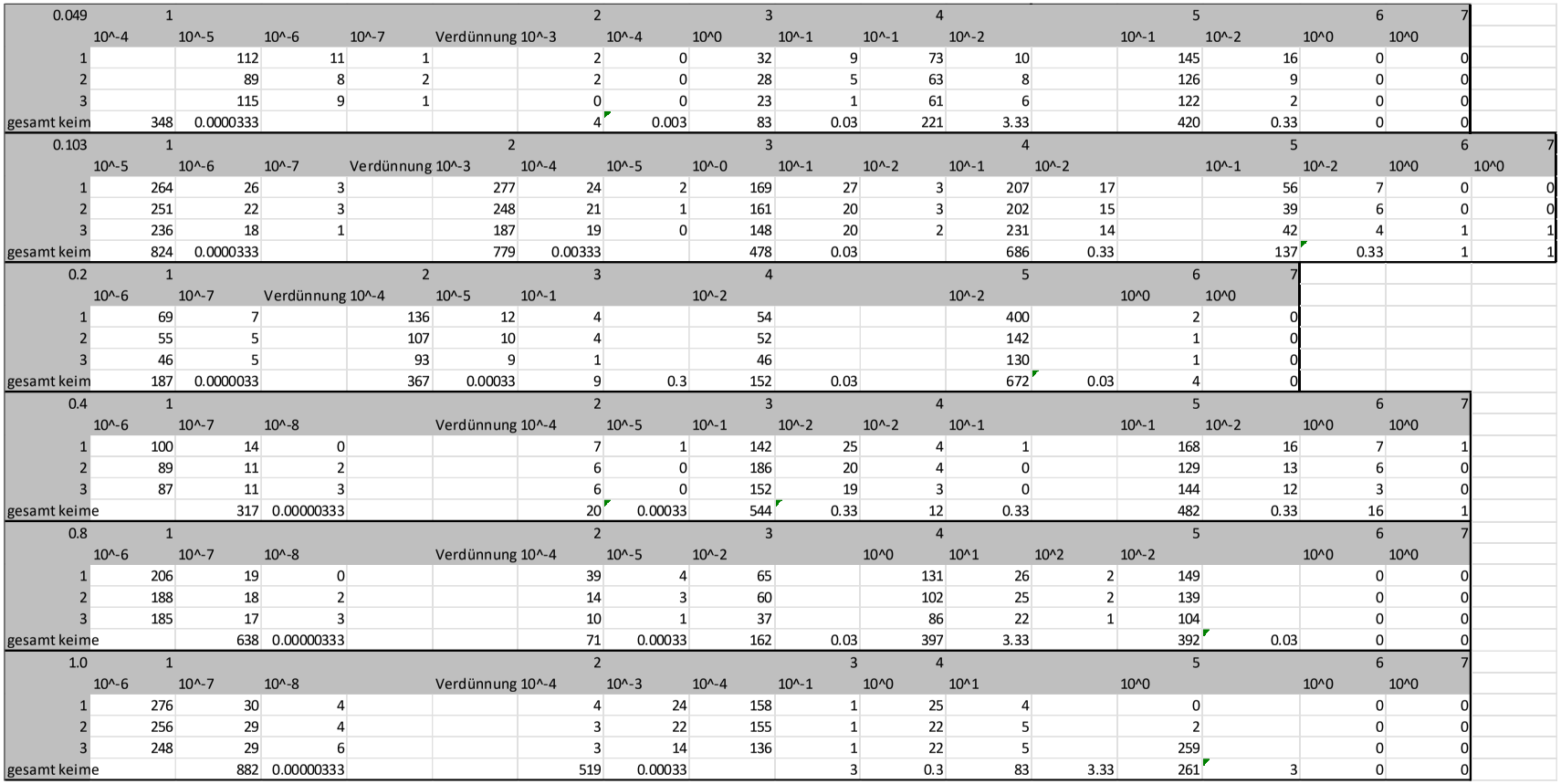

0.049	1					2		3		4			5			6	7
	10^-4	10^-5	10^-6	10^-7	Verdünnung	10^-3	10^-4	10^0	10^-1	10^-1	10^-2		10^-1	10^-2	10^0	10^0	
1		112	11	1		2	0	32	9	73	10		145	16	0	0	
2		89	8	2		2	0	28	5	63	8		126	9	0	0	
3		115	9	1		0	0	23	1	61	6		122	2	0	0	
gesamt keim	348	0.0000333				4	0.003	83	0.03	221	3.33		420	0.33	0	0	

0.103	1				2		3		4			5		6	7
	10^-5	10^-6	10^-7	Verdünnung	10^-3	10^-4	10^-5	10^-0	10^-1	10^-2	10^-1	10^-2		10^-1	10^-2	10^0	10^0
1	264	26	3		277	24	2	169	27	3	207	17		56	7	0	0
2	251	22	3		248	21	1	161	20	3	202	15		39	6	0	0
3	236	18	1		187	19	0	148	20	2	231	14		42	4	1	1
gesamt keim	824	0.0000333			779	0.00333		478	0.03		686	0.33		137	0.33	1	1

0.2	1		2		3		4		5		6	7
	10^-6	10^-7	Verdünnung	10^-4	10^-5	10^-1	10^-2		10^-2		10^0	10^0
1	69	7		136	12	4	54		400		2	0
2	55	5		107	10	4	52		142		1	0
3	46	5		93	9	1	46		130		1	0
gesamt keim	187	0.0000033		367	0.00033	9	0.3	152	0.03	672	0.03	4	0		

0.4	1				2		3		4			5		6	7
	10^-6	10^-7	10^-8	Verdünnung	10^-4	10^-5	10^-1	10^-2	10^-2	10^-1		10^-1	10^-2	10^0	10^0	
1	100	14	0		7	1	142	25	4	1		168	16	7	1	
2	89	11	2		6	0	186	20	4	0		129	13	6	0	
3	87	11	3		6	0	152	19	3	0		144	12	3	0	
gesamt keime		317	0.00000333		20	0.00033	544	0.33	12	0.33		482	0.33	16	1	

0.8	1				2		3		4			5		6	7
	10^-6	10^-7	10^-8	Verdünnung	10^-4	10^-5	10^-2		10^0	10^1	10^2	10^-2		10^0	10^0	
1	206	19	0		39	4	65		131	26	2	149		0	0	
2	188	18	2		14	3	60		102	25	2	139		0	0	
3	185	17	3		10	1	37		86	22	1	104		0	0	
gesamt keime		638	0.00000333		71	0.00033	162	0.03	397	3.33		392	0.03	0	0	

1.0	1				2		3	4			5		6	7
	10^-6	10^-7	10^-8	Verdünnung	10^-4	10^-3	10^-4	10^-1	10^0	10^1		10^0		10^0	10^0	
1	276	30	4		4	24	158	1	25	4		0		0	0	
2	256	29	4		3	22	155	1	22	5		2		0	0	
3	248	29	6		3	14	136	1	22	5		259		0	0	
gesamt keime		882	0.00000333		519	0.00033		3	0.3	83	3.33	261	3	0	0	

Figure 69: Measurement of the colony forming unit per millilitre.

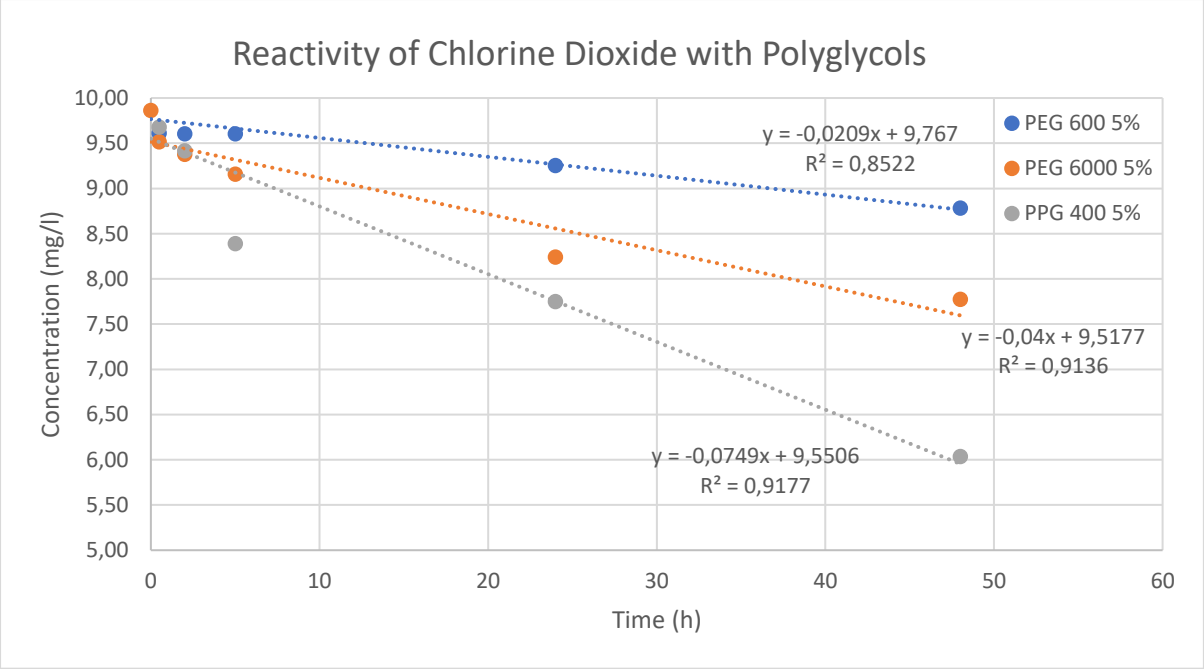

Figure 70: Determination of chlorine dioxide in the presence of polyglycols.

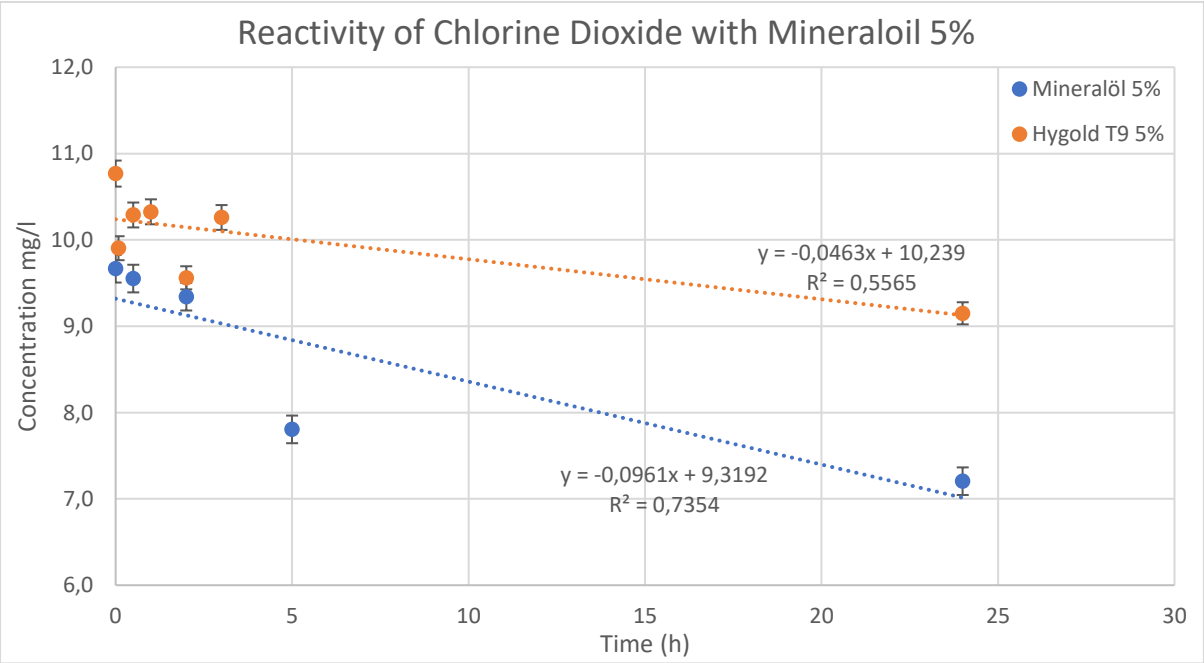

Figure 71: Determination of chlorine dioxide in the presence of mineral oils.

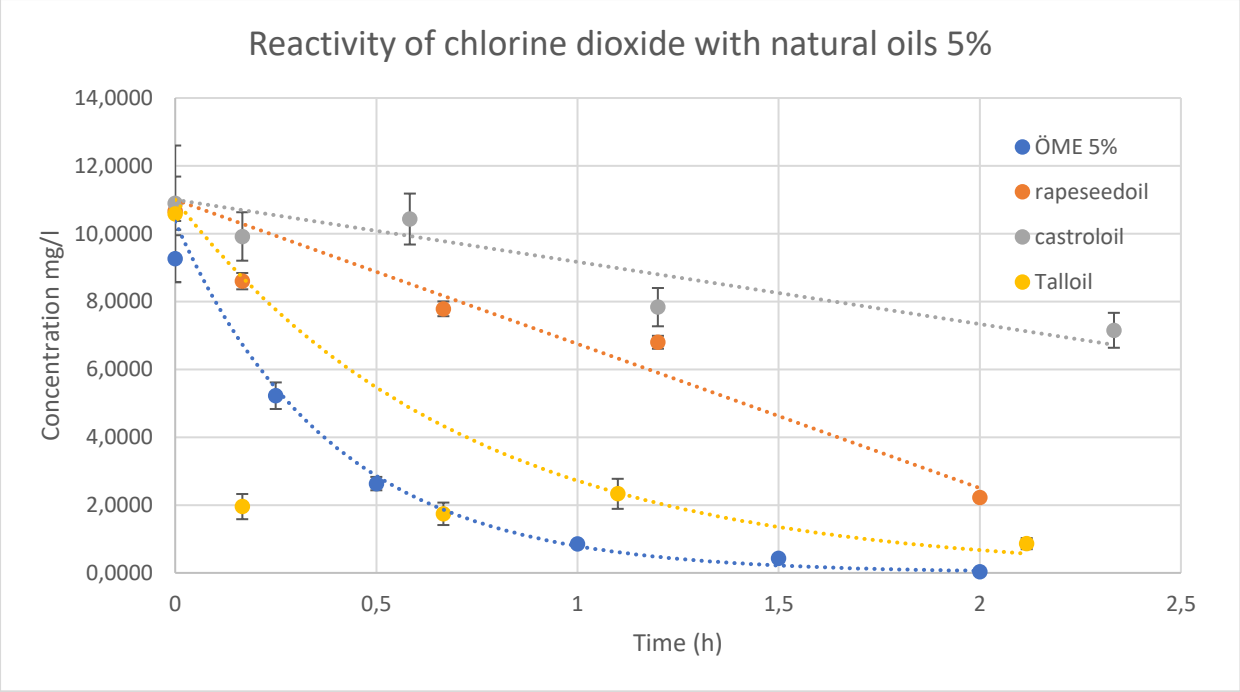

Figure 72: Determination of chlorine dioxide in the presence of natural oils.

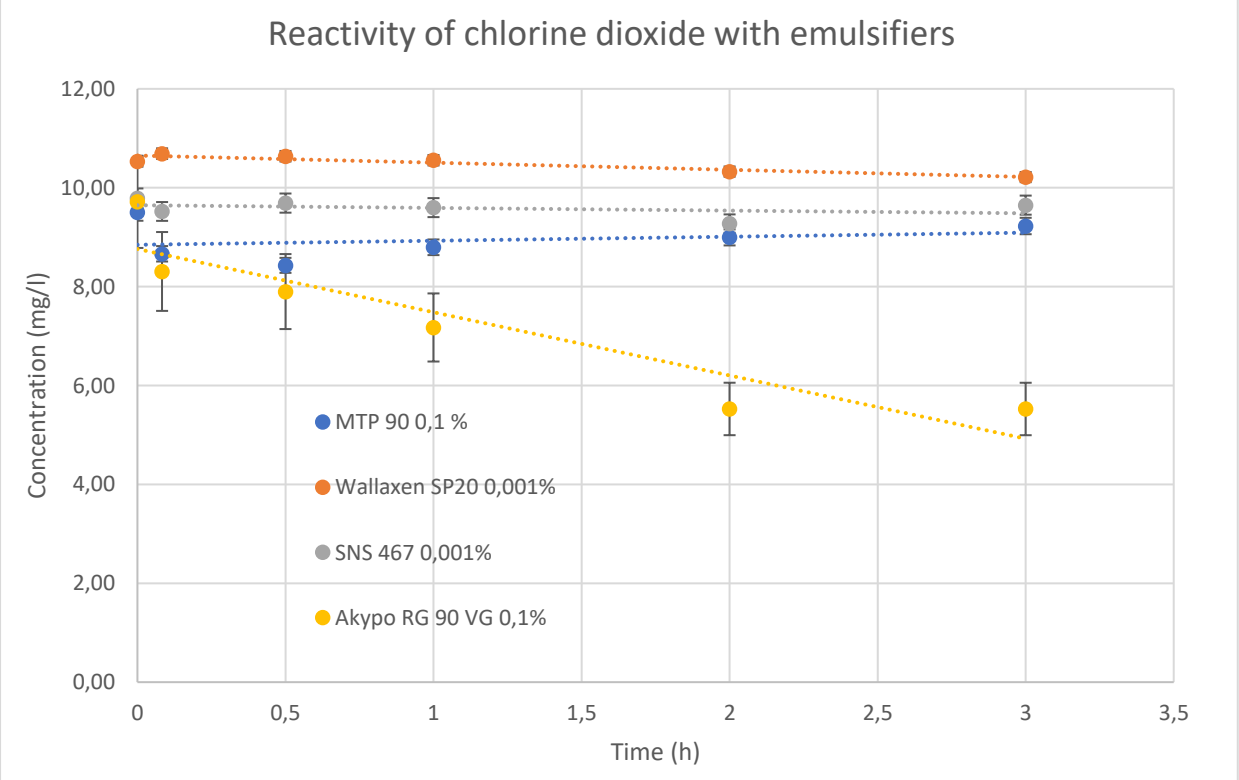

Figure 73: Determination of chlorine dioxide in the presence of emulsifiers.

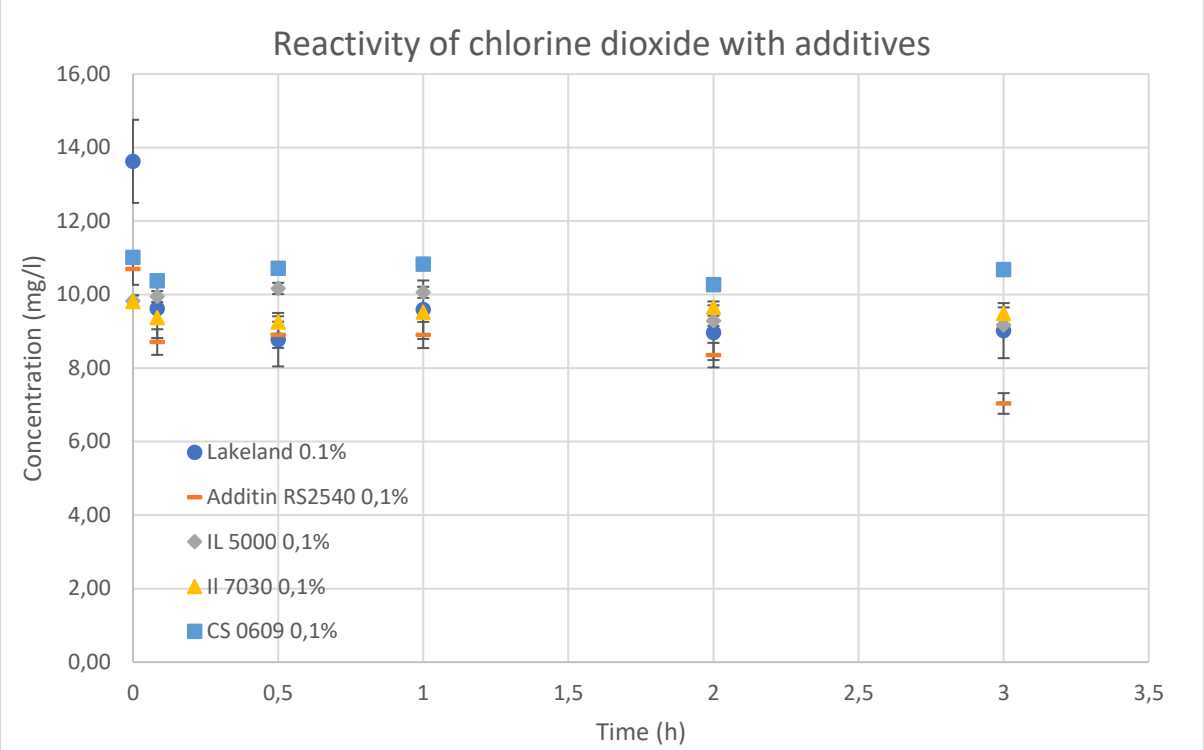

Figure 74: Determination of chlorine dioxide in the presence of additives.

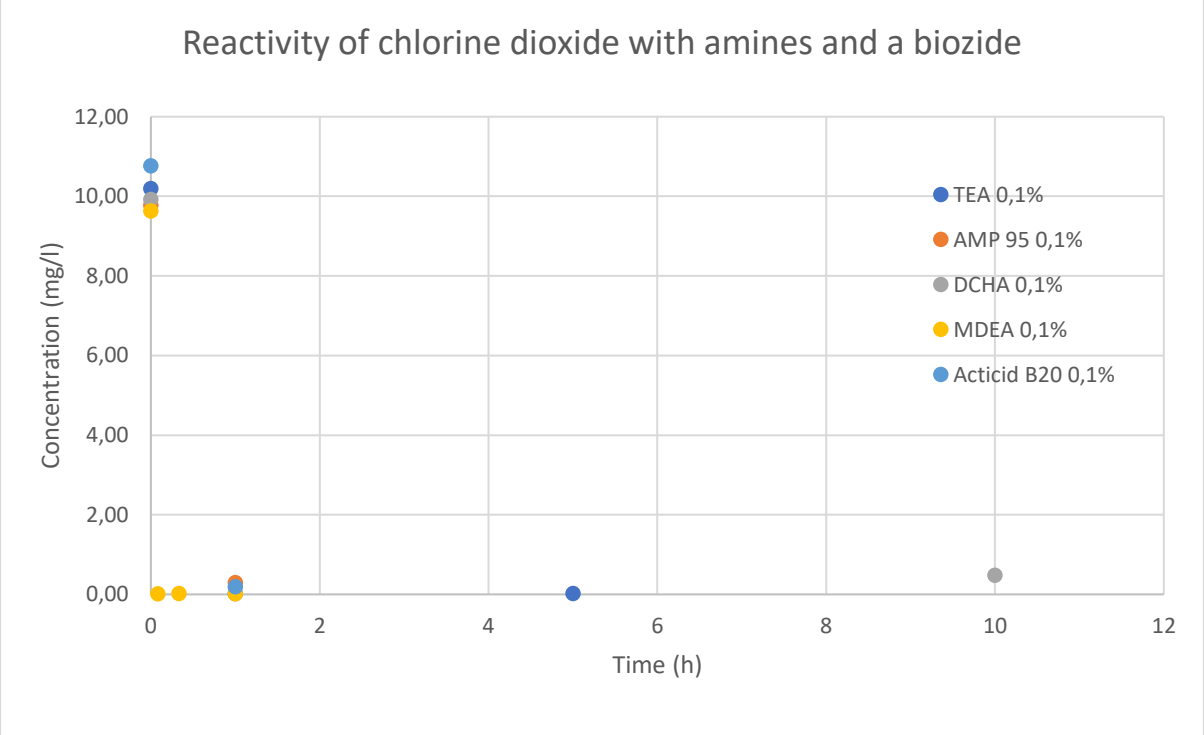

Figure 75: Determination of chlorine dioxide in the presence of amines and a biozide.

9.6 Detailed Pictures of the Sensor

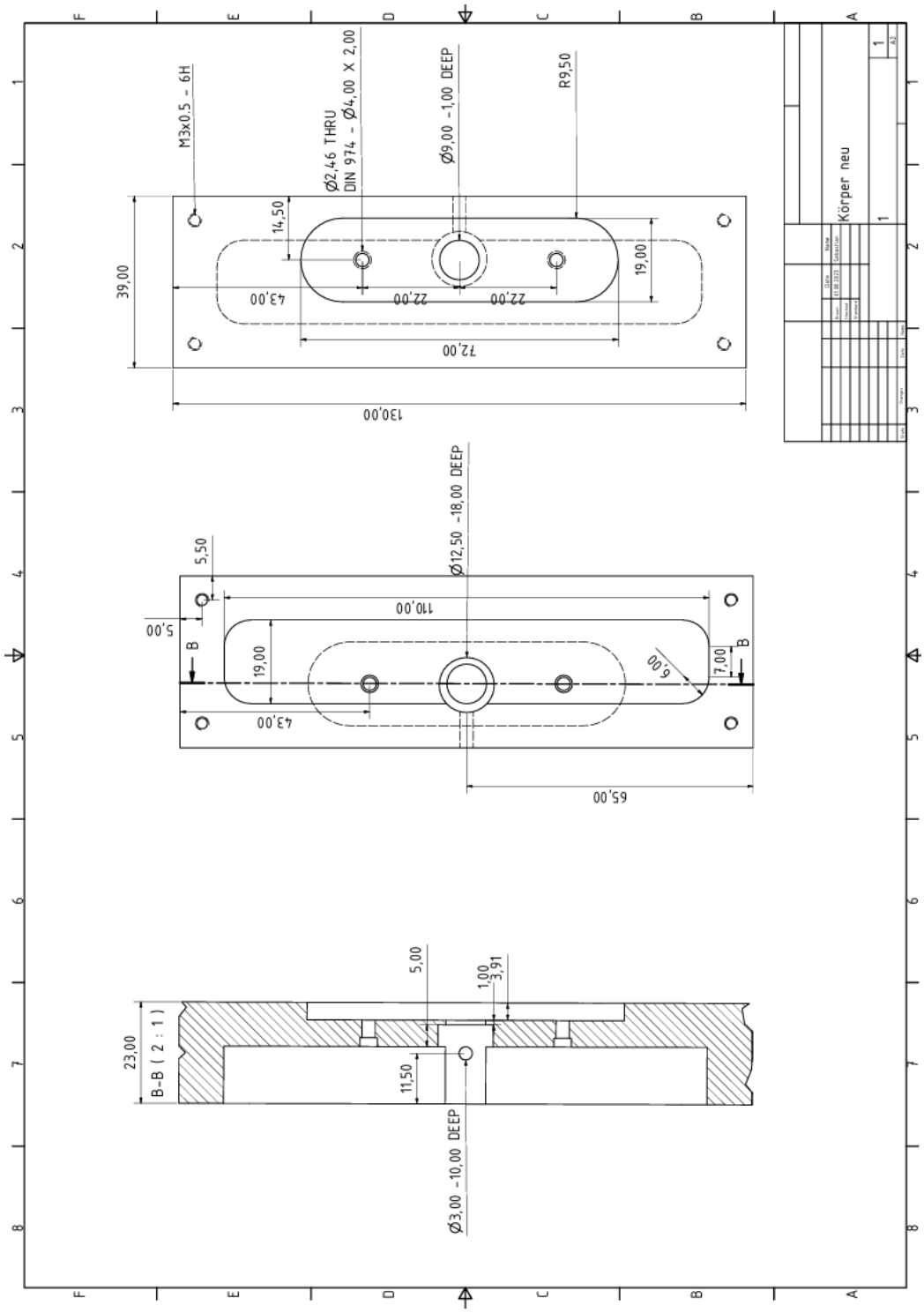

Figure 76: The detailed drawings of the aluminium housing. Dimensions are in mm. The photodetector and a bandpass filter can be installed in the housing. There are also screw connections for the lid. Made by the mechanical workshop of the University of Wuppertal.

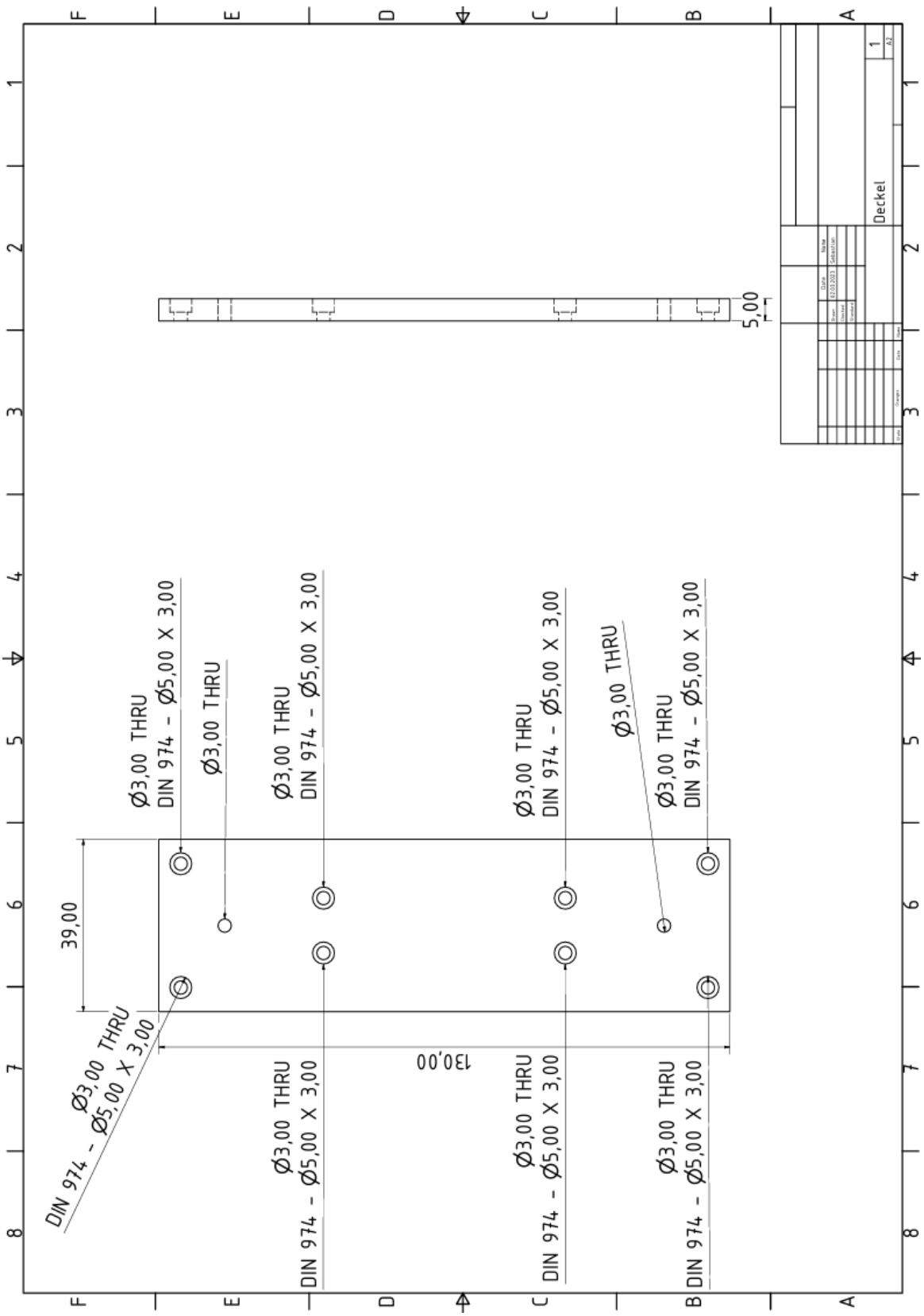

Figure 77: The detailed drawings of the aluminium lid. Here you will find drillings for the attachment to the housing as well as for the quartz tube holder. There are also outlets for the hoses. Made by the mechanical workshop of the University of Wuppertal.

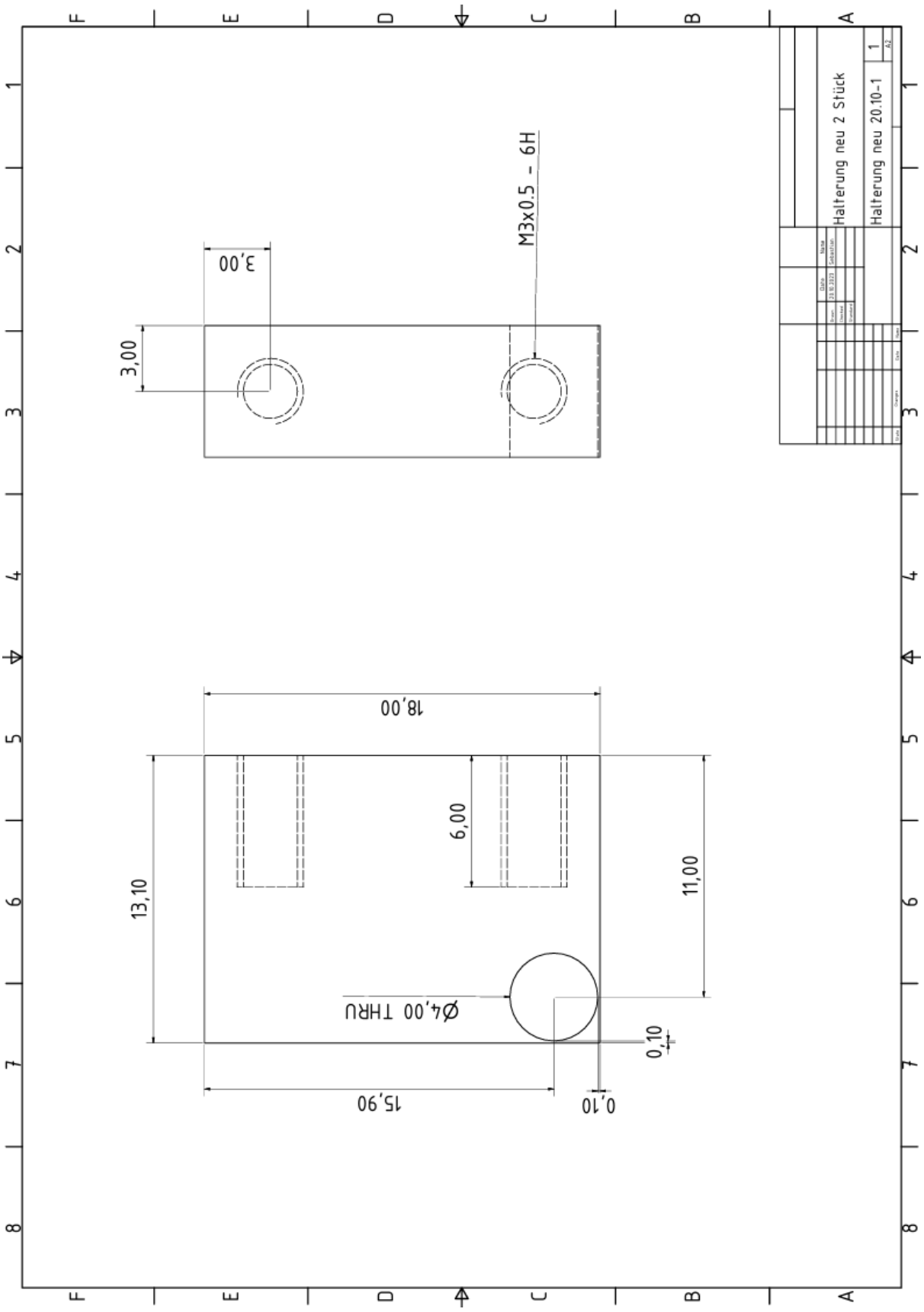

Figure 78: The detailed drawings of the holder for the flow cell. Made by the mechanical workshop of the University of Wuppertal.